INFORMATION TO USERS

This manuscript has been reproduced from the microfilm master. UMI films the text directly from the original or copy submitted. Thus, some thesis and dissertation copies are in typewriter face, while others may be from any type of computer printer.

The quality of this reproduction is dependent upon the quality of the copy submitted. Broken or indistinct print, colored or poor quality illustrations and photographs, print bleedthrough, substandard margins, and improper alignment can adversely affect reproduction.

In the unlikely event that the author did not send UMI a complete manuscript and there are missing pages, these will be noted. Also, if unauthorized copyright material had to be removed, a note will indicate the deletion.

Oversize materials (e.g., maps, drawings, charts) are reproduced by sectioning the original, beginning at the upper left-hand corner and continuing from left to right in equal sections with small overlaps.

ProQuest Information and Learning
300 North Zeeb Road, Ann Arbor, MI 48106-1346 USA
800-521-0600

Université d'Ottawa · University of Ottawa

THROMBIN INDUCES CELL SURFACE EXPOSURE OF THE PLASMINOGEN RECEPTOR ANNEXIN II: A NOVEL LINK BETWEEN COAGULATION AND FIBRINOLYSIS.

Erica A. Peterson

Thesis submitted to the Department of Biochemistry, Microbiology, and Immunology in partial fulfillment of the requirements for the degree of Master of Science.

University of Ottawa
Ottawa, Ontario, Canada
April 2002

ABSTRACT

Recent studies demonstrated a role for annexin II (A2) and its ligand p11 in fibrinolysis. Since thrombin is a potent cell modulator obligately produced at the site of clot formation, the hypothesis was addressed that thrombin regulates fibrinolysis by increasing cell surface A2 and p11. Immunofluorescence and biotinylation established that thrombin significantly increases both on human umbilical vein endothelial cell (HUVEC) and human foreskin fibroblast surfaces. Intracellular antigenic analyses revealed increased p11 but unchanged A2, suggesting that transbilayer trafficking of A2 is controlled by p11. The thrombin receptor activating peptide similarly affected cells indicating signaling through protease activated receptor 1. A direct effect on fibrinolysis was shown by observations of increased plasminogen binding to HUVEC that was inhibited by anti-p11 antibody, and activation of plasminogen by tissue plasminogen activator. These data suggest a novel link between thrombin and fibrinolysis, and other processes that may involve A2, such as cytomegalovirus infection.

DEDICATION

For my parents, Mary Ann and Eric, my grandparents, Alex and Terry, and my brother Andrew. Thank you for your love and support.

ACKNOWLEDGMENTS

First and foremost I would like to thank my supervisor, Dr. Ed Pryzdial, for his encouragement, guidance, motivation, patience, and invaluable support over the last three years.

I would also like to thank past and present members of our lab and Canadian Blood Services employees who helped make my time here much more enjoyable. In particular, I would like to thank Anita Cave, Cynthia Gilles, Laura Owen, Jade Berbari and Abed Zeibdawi for their friendship and constant encouragement. In addition, I would also like to thank Melanie Derry, Dr. Jean Grundy and Abed for their helpful discussions regarding my project.

A very special thank you goes to Michael Sutherland foe teaching me how to appreciate the arts of cell culture and immunofluorescence microscopy, not to mention allowing me to decorate his cubicle and our occasional outings to Mike's apartment.

Finally I would like to thank my family and Donny for their love and support, and for putting up with me during this difficult time.

TABLE OF CONTENTS PAGE

LIST OF FIGURES PAGE

LIST OF ABBREVIATIONS

Alphabetical List

A2	Annexin II
A2m	Monomeric form of A2
A2t	Tetrameric form of A2
anPL	Anionic Phospholipid
AP-1	Activator protein 1
APC	Activated protein C
AT	Anti-thrombin III
ATP	Adenosine Triphosphate
BME	Basal eagle media
B-Plg	S741C-biotin plasminogen
BSA	Bovine Serum Albumin
Ca^{2+}	Calcium ion
CMV	Cytomegalovirus
CREB	cAMP response element binding protein
DAPI	4',6-diamidino-2-phenylindole
DNA	Deoxyribonucleic acid
EDTA	Ethylenediaminetetraacetic acid
EGTA	Ethylene glycol-bis(β-aminoethyl ether)-N,N,N',N'-tetraacetic acid
F-Plg	S741C-fluorescein plasminogen
FITC	Fluorescein isothiocyanate
HFF	Human foreskin fibroblasts

HRP	Horse radish peroxidase
HSV-1	Herpes Simplex Virus-1
HSV-2	Herpes Simplex Virus-2
HUVEC	Human umbilical vein endothelial cells
IgG	Immunoglobulin
IMDM	Iscove's modified dulbecco's media
Kd	Dissociation constant
kDa	Kilodalton
μg	Microgram
μL	Microliter
μM	Micromolar
mM	Milimolar
mOD	Milioptical density units
mRNA	Messenger ribonucleic acid
NF-κB	Nuclear factor κB
nM	nanomolar
PA	Phosphatidic acid
PAI-1	Plasminogen activator inhibitor-1
PAR	Protease activated receptor
PC	Phosphatidylcholine
PE	Phosphatidylethanolamine
PGI_2	Prostacyclin
PI	Phosphatidylinositol

proPL	Procoagulant phospholipid
PS	Phophatidylserine
PVDF	Polyvinyl difluoride
RT	Room temperature
S2251	H-D-Val-Leu-Lys-p-Nitroaniline dihydrochloride
SDS-PAGE	Sodium dodecyl sulfate polyacrylamide gel electrophoresis
TF	Tissue factor
TFPI	Tissue factor pathway inhibitor
TM	Thrombomodulin
tPA	Tissue plasminogen activator
TRAP	Thrombin receptor activator peptide
uPA	Urokinase plasminogen activator
vWF	von Willebrand Factor

1. INTRODUCTION

1.1 OVERVIEW

Annexin II (A2) is a common cellular protein that belongs to the annexin family of calcium (Ca^{2+})-dependent anionic phospholipid (anPL) binding proteins, whose members have been implicated in membrane fusion and bridging. To date the physiological and pathological functions of A2 remain elusive. However, probable functions include roles in fibrinolysis (the biochemical pathway of blood clot dissolution), viral infection and tumor metastasis. The function of A2 in these processes are dependent on A2 being present on the cell surface, and therefore will be affected by changes in surface availability. Although A2 lacks a signal peptide and the mechanism by which it is translocated to the cell surface is unknown, a small percentage of the total cellular pool can be found on the cell surface. Since the coagulation effector thrombin can be present at each of the three functions listed above, the current project addresses the hypothesis that the potent cell modulatory capabilities of thrombin facilitate the availability of A2 by inducing its accumulation on the cell surface. In this thesis, fibrinolysis will be focused upon to test the functional regulation of A2 by thrombin.

1.2 THE ANNEXIN FAMILY

To date, 94 different annexins have been identified in over 45 species throughout the eukaryotic kingdom. Annexins are mainly intracellular proteins, which range in size from 34 to 40 kDa, with the exception of the 68 kDa annexin VI, which is a dimer (for review see (1;2)). All annexins contain two main

structural domains, an N-terminal tail and a C-terminal protein core. The later forms a 34 kDa protein structure, which makes up the bulk of each annexin (1). In contrast, the N-terminal domain is much smaller, and can contribute as little as 4 % to the total number of amino acid residues present in the protein. The C-terminal protein core regions of all annexin family members show a high degree of amino acid sequence homology. In addition, the C-terminal protein core contains the Ca^{2+}- and anPL-binding sites, thereby conferring the characteristic Ca^{2+}- and anPL-binding properties to all annexins (2). In contrast, the N-terminal domains of all annexins are unique, and confer specific properties to each protein (2).

The high degree of similarity of the amino acid sequences of the C-terminal protein core region among annexins results in a family of proteins with structurally similar three-dimensional folding patterns (2;3). This structural resemblance allows us to extrapolate the functional properties of one annexin to learn about others. Thus, the Introduction will begin with a general description of annexins, followed with a more detailed dissertation specifically on A2.

1.2.1 Structural Characteristics

1.2.1.1 Homology and Structure of the C-terminal Protein Core

All annexins contain a similar motif, the annexin repeat, which confers the characteristic structural properties of the protein core domain to all family members (1;4). The annexin repeat is a highly conserved 70 amino acid domain, repeated either four or eight (in the case of annexin VI) times in the protein (see

Figure 1: Annexin Family Protein Structure. A schematic of the structural organization of annexin family members is shown in Panel A. All annexins are separated into two main structural domains, the N-terminal domain (blue region), and the C-terminal protein core (black region). The protein core is composed of 4 copies of the annexin repeat, a highly homologous 70 amino acid domain. Each repeat contains 5 α-helices (denoted a to e) and a 17 amino acid consensus sequence termed the endonexin fold (purple highlighting). In panel B, the ribbon and wireframe depictions of the x-ray crystal structure of annexin V (red: repeat 1, blue: repeat 2, green: repeat 3, yellow: repeat 4) are shown from the top (Panel B: a,a') and the side (Panel B: b,b'). The side view allows us to observe the disc shaped orientation of the protein. The hydrophilic center channel (turquoise arrow), along with the tight association of helices 1 and 4, and 2 and 3 is observed in the top view. The calcium ions bound to the protein are shown as purple spheres (taken from (5)).

A

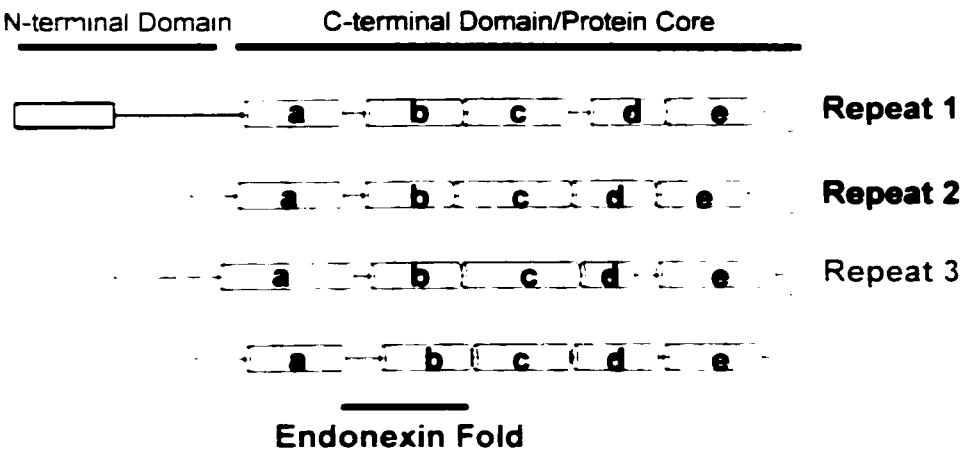
N-terminal Domain
C-terminal Domain/Protein Core
a
b
c
d
e
Repeat 1
Repeat 2
Repeat 3
Endonexin Fold

B

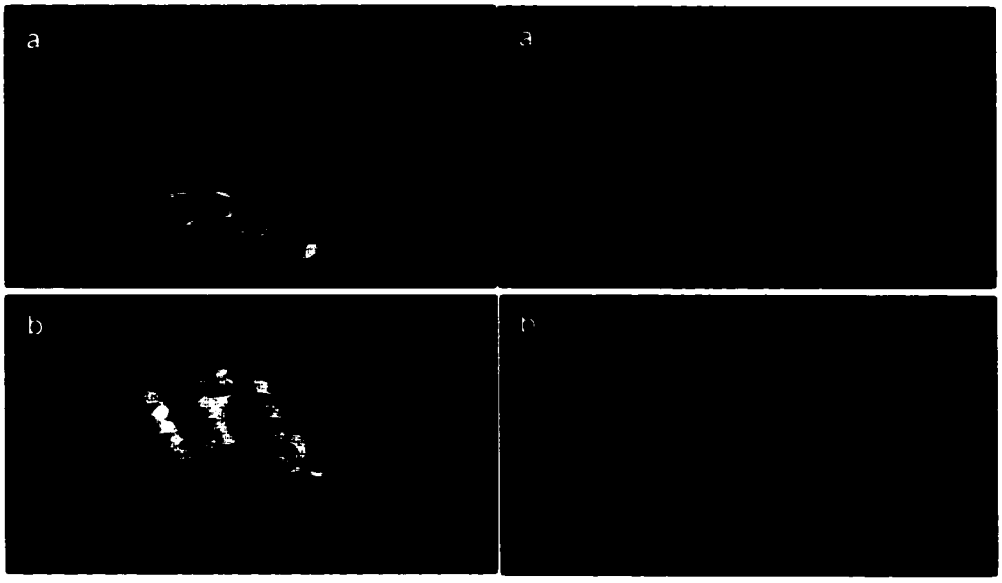
a
a
b
b

Figure1, Panel A) (4;5). These four annexin repeats fold together to form a 34 kDa protein core that is highly resistant to proteolysis. Most amino acid variations that are found in the annexin repeats are conservative substitutions (1).

The high degree of homology between the four annexin repeats in different family members derived from the same species, and between repeats found in the same protein, can be observed by comparison of the amino acid sequences (1). This is exemplified by a comparison of the sequences of human annexin I and A2, which revealed a 51% identity in amino acid residues (6). A comparison of the four repeats within A2 revealed only a 30% identity (6). However, it was noted that all annexins contain a conserved 17 amino acid consensus sequence (Lys-Gly-X-Gly-Thr-Asp-Glu-X-X-Leu-Ile-X-Ile-Leu-Ala-X-Arg), termed the endonexin fold, in each repeat (see Figure1, Panel A) (5). The high degree of identity observed in the region encompassing the endonexin fold, suggests that this region may play an important role in annexin function.

Sequence homology is also observed between annexins found in different species. Indeed, analysis of the human, bovine, porcine, and murine amino acid sequences of A2 demonstrated a 98% identity between the various species (6). Similarly, analysis of annexin V from different species demonstrated a 92 to 96% identity (7). Further examination of these annexin V sequences predicts that the evolutionary mutation rate of the protein is approximately a 1 % difference in amino acid sequence per 8 million years (7). This low mutation rate combined

with the high degree on inter-species homology, implies that annexins play an important physiological role within the cell.

The three-dimensional structure of certain annexins, including human annexin I (8), N-terminally truncated A2 (9), annexin III (10), annexin V (11), and annexin VI (12) have been solved by X-ray crystallography. As predicted by the high homology between family members, the crystal structures of the protein core region had similar topology (3). Therefore the crystal structure of annexin V (13), shown in Figure 1, will be used to discuss the secondary and tertiary structure of the annexin family protein core, as well as the location of the Ca^{2+}- and anPL-binding sites.

Examination of ribbon and wireframe depictions of the crystal structure of annexin V after refinement (Figure 1, Panel B) revealed that each annexin repeat (numbered 1 to 4) is composed of five α-helices (denoted a to e), which wind around each other in a right-handed superhelix (11;13). Hydrophobic inter-repeat contacts between repeats 1 and 4, and repeats 2 and 3, result in the formation of two tightly associated modules. These two modules are loosely held together by hydrophobic interactions between various side chains of the superhelices (11;13). The resulting structure is a parallelogram-like arrangement with a hydrophilic center channel (see Figure 1, Panel B: a,a') (11;13). The center channel, which is formed by helices a and b of repeat 2, and helix b of repeat 4, contains numerous conserved polar and charged molecules as well as buried water molecules (3). When the ribbon and wireframe plots are viewed from the

side, the annexin C-terminal protein core appears as a disc-shaped structure with convex and concave faces (11;13) (see Figure 1, Panel B: b,b').

1.2.1.2 Calcium-binding Sites

Annexins contain two types of Ca^{2+}-binding sites, type II (or AB) and type III (or DE) sites, which differ in the number of protein and water ligands complexed to the Ca^{2+} ion (1). The Ca^{2+}-binding sites found in annexins are distinct in structure and affinity from the EF-hand (or type I) Ca^{2+}-binding sites found in proteins such as calmodulin (14). EF-hand Ca^{2+}-binding sites have more carboxylate and fewer water ligands, along with a longer Ca^{2+}-binding loop (15). The structural differences between EF hand and type II or III Ca^{2+}-binding sites are responsible for the higher affinity and lower Kd (dissociation constant) of EF-hand Ca^{2+}-binding sites, which are typically orders of magnitude lower than those of the type II and type III annexin Ca^{2+}-binding sites (16).

Analysis of the amino acid sequences of annexin repeats was carried out to determine which regions of the protein were involved in Ca^{2+}-binding. This analysis identified the endonexin fold (5), which encompasses the loop between helices a and b (AB loop) and the majority of helix b in each repeat, as the structure responsible for high affinity Ca^{2+}-binding (3) (Figure 1, Panel A). Mutational analysis of the endonexin fold (17) and examination of the crystal structure of Ca^{2+}-saturated annexin V (11;13), were employed to determine which amino acid residues contributed ligands for Ca^{2+} coordination. This investigation demonstrated that conserved amino acid residues from the AB loop

in the endonexin fold, along with a glutamic or aspartic acid residue located approximately 40 amino acids downstream in helix d of the same repeat, provide the ligands for type II Ca^{2+}-binding sites (17) (Figure 2, Panel A: b). Thus, the consensus sequence of type II sites was established to be Gly-X-Gly-Thr-X_{48}-Asp/Glu (3). The two glycine and the threonine residues located in the AB loop donate 3 peptide carbonyl oxygen ligands while the acidic residue provides 2 carboxylate oxygen ligands. Consequently, in type II sites the Ca^{2+} ion is coordinated to 5 protein ligands and 2 water molecules in a pentagonal bipyramidal formation (3) (Figure 2, Panel A: b). Superimposition of the phospholipase A_2 binding loop with the structure of the Ca^{2+}-binding site found in repeat 1 on annexin V demonstrated a direct match in both structure and sequence (18;19). The Ca^{2+}-binding site of phospholipase A_2 is formed from a loop of sequence X-X-G^{30}-X-G^{32} and an aspartic acid (D^{49}) located 17 amino acids downstream. Thus, the Ca^{2+} ion is coordinated by 3 main chain carbonyl oxygens ligands (from the X-X-G^{30}-X-G^{32} loop) and 2 carboxylate oxygens ligands (provided by D^{49}) (18). The superimposition analysis demonstrated that G^{30} and G^{32} of phospholipase A_2 are equivalent to G^{102} and G^{104} residues of the endonexin fold of annexin V, while D^{49} is equivalent to the aspartic acid residue located in helix d (D^{144}). This similarity is also seen with the type II Ca^{2+}-binding sites found in repeats 2 and 4. Therefore, the structure of annexin type II sites are structurally related to the phospholipase A_2 Ca^{2+}-binding sites (18).

A second type of Ca^{2+}-binding site, which binds Ca^{2+} with low affinity, has also been identified in annexin family members. These sites, termed type III

sites, occur in the loop between helices d and e (DE loop), with an additional protein ligand supplied by helix e (13). Examination of the molecular structure of type III sites revealed that the Ca^{2+} ion is coordinated to 3 protein ligands, 2 main chain carbonyl oxygens from amino acids in the DE loop and a carboxylate group from a side chain of an acidic amino acid residue located in helix e, and 3 water molecules (3).

Studies involving different types of Ca^{2+}-binding sites have demonstrated that the Ca^{2+}-binding affinity is inversely correlated with the number of water molecules present in the binding site (15), thereby suggesting that type II sites have a higher affinity for Ca^{2+} than type III sites. This has been experimentally determined by site-directed mutagenisis of the endonexin fold, which eradicated high affinity Ca^{2+}-binding (20-22). In addition, mutation of the type II and type III sites in A2 has confirmed that A2 deficient in type III sites bound to phosphatidylserine liposomes at 5 to 10 μM Ca^{2+}, while A2 mutants lacking type II sites required 200 to 300 μM Ca^{2+} for anPL-binding (22). Accordingly, the type II sites are responsible for the high affinity Ca^{2+}-binding displayed by annexins. Nonetheless, while annexin type III sites bind Ca^{2+} with low affinity, they have been identified as high affinity lanthanum-binding sites (13). The significance of lanthanum-binding has not been unequivocally established, but it has been proposed to be involved in ion channel activity displayed by certain annexins (19).

Although the secondary and tertiary structure of the annexin repeats are highly conserved among family members, the location of the Ca^{2+}-binding sites

Figure 2: Location of Ca^{2+}-Binding Sites in a Typical Annexin. The location of the annexin V Ca^{2+}-biding sites are shown in relation to the backbone of the protein. The position of the type II Ca^{2+}-binding sites on a depiction of the backbone of annexin V are shown in Panel A (a: side view, b: top view). The three type II sites in annexin V are located in the endonexin folds of repeats 1, 2, and 4, which extend from the convex face of the protein (Panel A: a). Panel B shows the position of the type III sites of annexin V (a: side view, b: top view). Both type III sites in annexin V are located in repeat 1 of the protein. In Panels A and B the protein ligands are shown in yellow, the Ca^{2+} ions are depicted in purple and the water ligands are in red (taken from (5)).

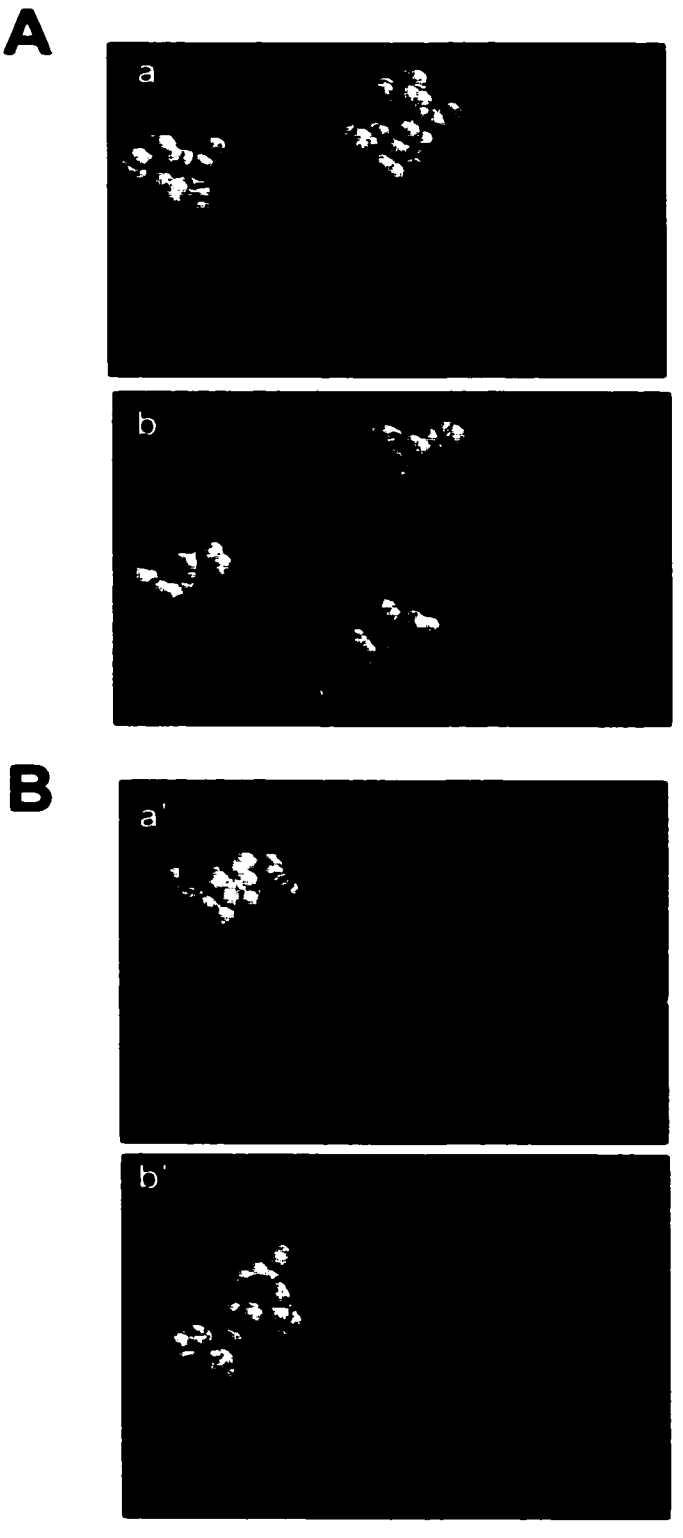
A
a
b
B
a'
b'

may vary slightly from one annexin to another. However, they are always found on the convex side of the protein, as seen for annexin V (8-12). The location of the type II and type III Ca^{2+}-binding sites of annexin V is shown in Figure 2 (13;17). Annexin V contains 3 type II sites located in repeats 1, 2, and 4 (Panel A: a), and 2 type III sites in repeat 1 of the protein (Panel B) (13;17). These Ca^{2+}-binding sites are situated on the loops between helices, which extend from the convex face of annexin V (13;17). It has been determined that annexins usually contain 3 type II Ca^{2+}-binding sites, two of which are located in repeats 2 and 4 of the proteins (3). All annexins, with the exceptions of annexin I and A2, contain a third high affinity site in repeat 1 (3). Site directed mutagenisis studied have determined that the third high affinity site in annexin I (8) and A2 (9;22) is located in repeat 3.

1.2.1.3 Anionic Phospholipid-binding Sites

anPL-binding by the annexin protein core is facilitated by the existence of hydrophobic residues on the convex face of the disc. It has been shown that annexin V contains hydrophobic residues in the loop between helices a and b of the annexin repeats, which are predicted to stabilize interactions between the protein and phospholipid membranes (13). Furthermore, certain hydrophobic amino acid residues, such as the tryptophan residue located in the AB loop of repeat 3 in A2 (23;24) and annexin V (25), shift from a concealed location in the hydrophobic protein core to an exposed position upon Ca^{2+}-binding. These shifts, which can be followed by fluorescence spectroscopy, are proposed to

allow the solvent exposed tryptophan residue to insert into the membrane upon phospholipid binding, thereby facilitating annexin-membrane association (26-28).

The Ca^{2+}-dependence of the anPL-binding of annexins may indicate the direct involvement of Ca^{2+}-binding sites in phospholipid binding. This hypothesis has been supported by several observations. Studies using electron microcopy demonstrated that annexin V bound to phospholipid bilayers showed no significant structural rearrangements, demonstrating that the association with anPL did not required major conformational changes (29;30). In addition, both the eradication of the type II Ca^{2+}-binding site located in repeat 3 of A2 by site directed mutagenisis, and peptides corresponding to the sequence of the high affinity Ca^{2+}-binding sites of A2 prevented the association of the protein with phospholipid membranes. As a result, the putative involvement of the Ca^{2+}-binding sites in anPL-binding, indicates that the anPL-binding sites are located on the convex face of the annexin protein core. This has been experimentally demonstrated for annexin V (31). The mechanism by which annexins bind to anPL has not yet been experimentally determined. However, studies involving Ca^{2+}-dependent anPL binding by phospholipase A_2 may provide additional insight due to the high structural similarity between the Ca^{2+}-binding sites of phospholipase A_2 and type II sites in annexins (2;18). Experiments involving phospholipase A_2 have shown that the two water ligands in the Ca^{2+}-binding site are displaced by phosphoryl and acyl backbone carbonyl oxygens of phospholipids upon association with membranes, demonstrating that the Ca^{2+}-binding sites are involved in phospholipid binding (32). The data suggest that

displacement of water ligands by phospholipids may be involved in the Ca^{2+}-coordination in type II sites upon association with phospholipid membranes. The finding that sulfate ions are located in close proximity to the Ca^{2+} ions in annexin x-ray crystal structures supports the putative involvement of annexin Ca^{2+}-binding sites in anPL binding (13;25).

1.2.1.4 N-terminal Domain

Unlike the protein core, the N-terminal domain or tail of annexins is highly variable in both length (from 11 to over 100 amino acids) and amino acid composition, and unlike the protein core, is sensitive to proteolysis (1). This high degree of variability confers unique physical and biochemical properties to each annexin. Therefore, this region determines the specific functions of each annexin. In addition, the presence of phosphorylation and ligand binding sites in the N-terminal domains of certain annexins suggests the N-terminal tail may play a role in functional regulation. (1).

1.2.2 Membrane and Calcium Binding Properties of Annexins

1.2.2.1 Membrane Binding and Fusion

A characteristic biochemical property possessed by all annexins is the ability to bind phospholipid in a Ca^{2+}-dependent manner. Examining the phospholipid binding specificity of various annexins revealed that they preferentially bind anPL, specifically phosphatidic acid (PA), phosphatidylserine (PS), and phosphatidylinositol (PI) (2). Binding to non-charged phospholipids, such as phosphatidylethanolamine (PE) and phosphatidylcholine (PC), has also

been demonstrated, but requires high Ca^{2+} concentrations or low pH (33). Certain annexins, including A2 (34;35), have also been shown to associate with phospholipid in the absence of Ca^{2+}, which is believed to be mediated through the Ca^{2+}-indendent association of annexins with membrane proteins (1;2).

Once the Ca^{2+}-dependent association of annexins with phospholipid membranes has taken place, certain annexins are then capable of mediating membrane-bridging (1). While the mechanism of membrane bridging has not been fully elucidated, two possible scenarios have been explored. The first scenario, which has been experimentally demonstrated for annexin I (36), proposes that each annexin contains two spatially distinct phospholipid binding sites, thus allowing the protein to bind two separate phospholipid membranes. Recently, a second scenario has suggested that membrane aggregation may be facilitated by Ca^{2+}-dependent self-association of annexins bound to separate membranes (37;38).

Annexin-mediated fusion of phospholipid membranes has also been observed for certain family members. The rate of annexin-mediated membrane fusion is generally very slow and therefore is probably not physiologically relevant (1). However when certain components are included in the membrane, such as cis-unsaturated fatty acids, the rate of fusion is dramatically enhanced. Thus membrane fusion may be physiologically relevant when membranes contain high cis-unsaturated fatty acids concentrations (38).

1.2.2.2 Calcium-binding

Although each annexin requires Ca^{2+} to bind phospholipid, the Ca^{2+} requirements to reach half-maximal binding vary widely among family members. These Ca^{2+} thresholds range from the sub-micromolar to micromolar (μM) range for annexin I and A2, to in excess of 100 μM for annexin V (2). These differences in Ca^{2+} affinities may be due to variations in the locations and positions of the Ca^{2+} binding sites in different annexins.

1.2.3 Function

As described previously, all family members display certain biological properties, such as Ca^{2+}, anPL, and membrane binding, as well as the ability to aggregate anPL-containing membranes, described previously (1;2). In addition, certain family members have been shown to interact with both cytoskeletal and extracellular matrix proteins. Indeed, *in vitro* studies have demonstrated binding to the cytoskeletal microfilament actin by A2 and annexins I and VI (39;40;40;41;41), and binding of A2 and annexin VI to members of the non-erythroid spectrum family (42;42). A2 also exhibited *in vitro* binding to an intermediate filament of the cytoskeleton, the glial fibrillary acid protein (43). Binding of the extracellular matrix proteins, collagen and tenascin C, have been observed for annexin V (44) and A2 (45) respectively.

Although the *in vivo* functions of most annexins have not yet been determined, the biochemical properties described above suggest that annexins may be involved in membrane-related processes such as membrane

organization, membrane trafficking, and linkages between membranes and cytoskeletal elements (1). For instance, the ability of certain annexins to bind to cytoskeletal elements and extracellular matrix components as well as anPL suggests a role for the proteins in both membrane organization, links between the plasma membrane and the underlying cytoskeleton, and cellular migration (46). In addition, numerous family members have also been implicated in membrane trafficking events such as endocytosis (47) and exocytosis (48;49;49). The mechanisms by which annexins mediated membrane trafficking events would likely involve the phospholipid membrane aggregation and fusion abilities displayed by certain family members.

Additional biochemical properties identified for certain annexin family members include anticoagulant activity (50) and phospholipase A2 inhibition (51). *In vitro* anticoagulant activity was observed for several annexins, including A2, and annexins II, V, and IV (52;53). The inhibition of coagulation *in vitro* is mediated by competition with coagulation factors X, Xa and Va for anPL-binding sites. This competitive inhibition prevents factor X activation and Factor Xa and Va activity, thereby averting thrombin generation (52-54). *In vivo* anticoagulant activity, has been proposed for annexin V, and is hypothesized to occur through the development of annexin V networks, which restrict the movement of clotting factors on the membrane surface (55).

Another biochemical property displayed by numerous annexin family members is the ability to inhibit phospholipase A_2 activity-*in vitro* (51;56-58). When these assays were performed with non-ionic phospholipids or in the

absence of Ca^{2+}, phospholipase A_2 inhibition was eliminated. This result suggested that the *in vitro* mechanism of phospholipase A_2 inhibition by annexins, like their anticoagulant activity, was most likely due to competition for phospholipid binding (59). However, annexin phospholipase A2 inhibition by phospholipid sequestration was believed to be an unlikely mechanism of phospholipase inhibition *in vivo*. More recent studies favor a protein-protein interaction model. The ability of peptides specific to residues located in the third repeat of annexin I to inhibit phospholipase A_2 directly (60;61;61-63), suggested that annexin I may interact directly with phospholipase A_2. Studies of cytoplasmic phospholipase A_2 inhibition by annexin I, N-terminally deleted annexin I, A2, A2t, annexin III, and annexin V, demonstrated inhibition only by annexin I, N-terminally deleted annexin I, and A2, and to a lesser extent annexin V (64). Direct interactions between phospholipase A_2 and annexin I, N-terminally deleted annexin I, and A2 were later demonstrated by immunoprecipitation (64). Thus, certain annexins appear to non-specifically inhibit phospholipase A_2 *in vitro* by a phospholipid sequestration mechanism, but specific inhibition through protein-protein interactions is a property displayed only by select family members.

Because phospholipase A_2 activation is one of the first steps in the inflammatory response, the anti-inflammatory inhibition displayed by certain annexins is directly related to phospholipase A_2 inhibition (62). Indeed, preliminary in vivo experiments using intravenous or topically applied annexins

have demonstrated an inhibition of the formation of pro-inflammatory compounds mediated by the activation of phospholipase A_2 (65;65;66).

Other biochemical functions displayed by annexin family members include ion channel activity (67;68). Early experiments involving purified bovine annexin VII revealed that the protein could form capacitative gating currents in acidic phospholipid bilayers (69). Further analysis with purified bovine and human and annexin VII, as well as recombinant annexin VII established that annexin VII could form voltage sensitive ion channels in artificial membranes in the presence of Ca^{2+} (68;68;70;71;71). These experiments were later repeated with purified human and recombinant annexin V (72-74). However, while annexin VII forms Ca^{2+} selective channels, native and recombinant human annexin V can conduct numerous divalent cations including Ca^{2+}, Ba^{2+}, Sr^{2+}, Mg^{2+}, and monovalent cations such as Li^+, Cs^+, Na^+ and K^+ (73;75;75). The three-dimensional structure of the annexin core, determined by x-ray crystallography of annexin V, corroborates the electrophysiological data obtained. The annexin V structure contains a centrally located pore perpendicular to the membrane-binding surface, which is wider on the membrane side. In addition, the amino acid side chains that protrude into the pore all belong to acidic amino acids (3;3;11;13;13). Thus, another proposed function is a role for certain annexins in ion conductance across membranes (67). To date it has been established that annexins II, V, VII, and XII can form ion channels (3).

1.3 Annexin II

1.3.1 Structure

1.3.1.1 C-terminal Protein Core

The three-dimensional structure of the C-terminal core has been identified by x-ray crystallography analysis of an N-terminally shortened form of A2 (9). Like all annexins A2, a 36kDa ubiquitously expressed annexin family member, contains the four annexin repeats and the highly conserved 34 kDa protein core described previously (for review see (76)) (see Figure 2, Panel A).

Analysis of the Ca^{2+}-binding sites of A2 has determined that the protein contains three type II and two type II Ca^{2+} binding sites (22). The type II sites are located in repeats 2, 3, and 4, while the type III binding sites have been identified in repeat 1 (described in Figure 3, Panel A). The type II Ca^{2+}-binding sites involve residues Met^{117}, Gly^{119}, Gly^{121}, and Asp^{161} in repeat 2, and Met^{277}, Gly^{279}, Gly^{280}, and Asp^{321} in repeat 4 (9). These two type II sites are similar to the ones found in repeats 2 and 4 of annexin V (Figure 2). The structure of the type II site in repeat 3, which involves residues Gly^{201}, Arg^{205}, Gly^{206}, Thr^{207}, and Glu^{246} of A2 (9), is distinct from the sites located in repeats 2 and 4 due to differences in the amino acid sequences of helix a and the AB loop of repeat 3 (20;21). However, site directed mutagenisis of the amino acids located within the AB loop of repeat 3, demonstrated that repeat 3 was in fact able to bind Ca^{2+} (21;22).

The type III Ca^{2+}-binding sites have been shown to involve Gly^{49}, Val^{51}, Glu^{52} and Lys^{87}, Leu^{90}, and Glu^{95} in repeat 1 (9;22). The increased number of water ligands in type III sites lead to a 30-fold reduction in affinity when compared to type II sites (2).

1.3.1.2 N-terminal Domain

The N-terminal domain of A2, is a 30 amino acid structure, which distinguishes the architectural and functional properties of A2 from those displayed by other family members. In addition, the N-terminus of A2 is proposed to be the regulatory domain of the protein. This hypothesis is based on the fact that the N-terminus contains serine and tyrosine residues that can be modified by phosphorylation. Tyrosine phosphorylation of A2 can be accomplished *in vitro* by $pp60^{src}$ (77), fps encoded tyrosine kinase (78), insulin receptor tyrosine kinase (79), and the epidermal growth factor receptor kinase (EGFR kinase) (80). Both $pp60^{src}$ and the EGFR kinase have been shown to phosphorylate A2 *in vivo* (80). The tyrosine phosphorylation site has been mapped to the Tyr^{23} residue of A2 (77). Two serine phosphorylation sites, Ser^{11} and Ser^{25}, exist in the N-terminal tail of A2. Protein kinase C has been shown to phosphorylate both Ser^{11} and Ser^{25} (81) *in vitro* and *in vivo* (82-84), while phosphorylation at Ser^{11} has been observed by cAMP- and calmodulin-dependent kinases *in vitro* (83) (Figure 2, Panel A).

In addition, the N-terminus of A2 contains a binding site for p11, an 11 kDa member of the S-100 family of EF-hand type Ca^{2+}-binding proteins (85). Binding of p11 to the N-terminus of the protein allows A2 to exist as two different forms inside the cell, a monomeric form (A2m), or a heterotetrameric form (A2t) (see Figure 3, Panel B). A2t results from the non-covalent association of two A2 monomers with a p11 dimer (see Figure 3, Panel B) (40;86;87). The relative proportion of A2m to A2t has been determined in various cell types. In

Figure 3: Structure of Annexin II. In Panel A, the key features of the A2 protein structure are shown. The regulatory domain of the protein, the N-terminal domain (block letters), contains a binding site for p11 (pink amino acid residues), and serine and tyrosine phosphorylation sites (green amino acid residues). The C-terminal protein core contains the annexin repeats and the endonexin fold (purple regions). The 3 type II Ca^{2+}-binding sites (blue stars) are located in repeats 2, 3, and 4, while the 2 type III Ca^{2+}-binding sites (black stars) are found in repeat 1. A2 can exist as two different configurations inside the cell, a monomeric form (A2m), and a heterotetrameric form (A2t), resulting from the non-covalent association of two A2m subunits with a p11 dimer (Panel B). The structures of A2m (Panel B: a) and A2t (Panel B: b) bound to anPL (blue circles) are shown in Panel B.

A

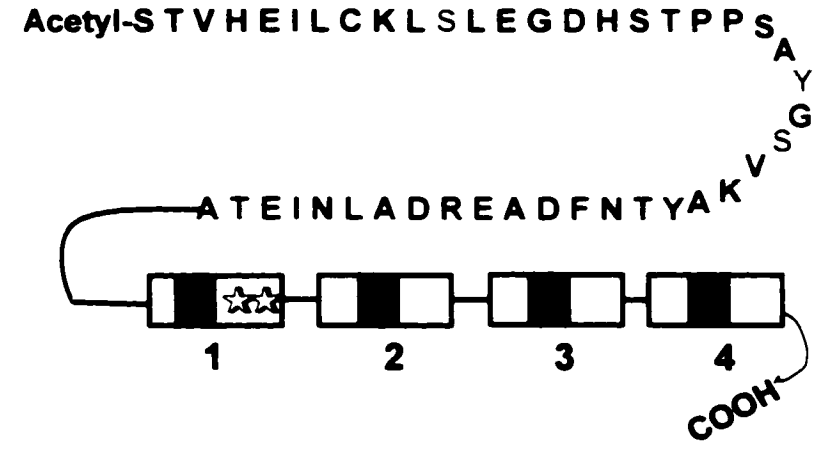
Acetyl-STVHEILCKLSLEGDHSTPPSAYGSVKATEINLADREADFNTYAK
1
2
3
4
COOH

B

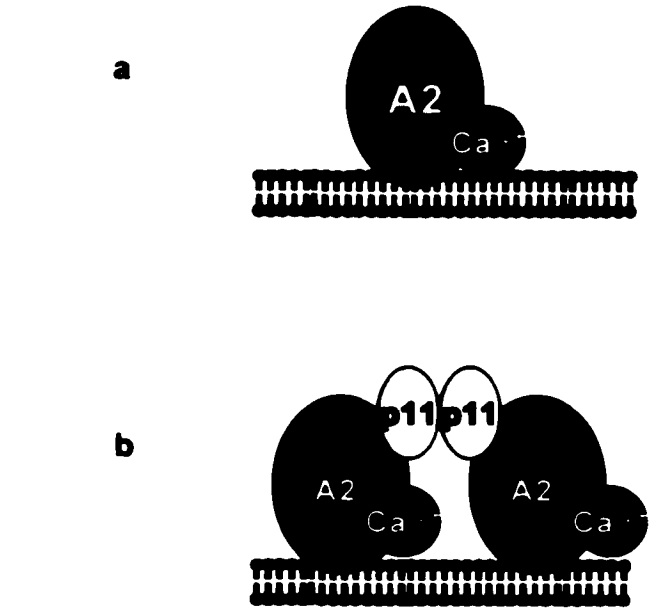
a
A2
Ca
b
p11
p11
A2
Ca
A2
Ca

endothelial and epithelial cells 90 to 95% of total A2 exists as A2t, while in fibroblasts A2t makes up only 50% of the total cellular pool (76). Therefore, the ratio of A2m to A2t exhibits significant differences according to the origin of the cell type. A2 can also be found as a dimer, resulting from the association of one A2 monomer with 3-phosphoglycerate kinase, which accounts for only a small portion of the total cellular A2 pool (76).

The location of the p11-binding site of A2 was first elucidated by protease digestion of the protein. Treatment with chymotrypsin removes the first 29 amino acids, and yields a protein core unable to bind p11 (85). Further insight was gained by V8 protease digestion of A2, which truncates the protein at residue 14 (85). This truncated form of A2 was also unable to bind p11 (85), indicating that the first 14 amino acids were likely involved in the p11-binding site. The structure of the p11-binding site of A2 was studied using secondary structure prediction and circular dichroism spectroscopy. Circular dichroism spectroscopy demonstrated that while the first 18 amino acids of the N-terminus have a random conformation in the presence of buffer, in the presence of trifluoroethanol or when complexed to p11 the first 12 amino acids adopt an α-helical configuration (88). This α-helix is an amphipathic helix with residues Val^3, Ile^6, Leu^7, and Leu^{10} found on the hydrophobic side (88). Identification of the residues of the α-helix involved in binding was carried out competitive binding assays performed with peptides encompassing the first 12 amino acids of the A2 N-terminus containing single amino acid mutations. These analyses revealed that the hydrophobic side chains of residues Val^3, Ile^6, Leu^7, and Leu^{10} are the p11

contact sites (89). Thus the interaction between A2 and p11 appears to be governed by hydrophobic interactions.

The position of the A2-binding site on p11 was delineated by progressive recombinant truncation of p11, which demonstrated that residues 85 to 95 were necessary for A2 binding (90). This region contains numerous hydrophobic amino acid residues, corroborating the suggestion that hydrophobic interactions are responsible for the association of A2 and p11. Further analysis of the region that mutation of Thr^{85} and Phe^{86} to Ala inhibited the association of p11 and A2 (90).

Recently, the x-ray crystal structure of a complex of p11 and the N-terminus of A2 has been solved (Figure 4, Panel A) (91-93). Analysis of a ribbon depiction derived from the crystal structure demonstrated that the hydrophobic portion of the α-helix of A2 becomes buried in a hydrophobic groove of the p11 dimer, indicating that hydrophobic interactions are involved (Figure 4, Panel B) (91). Furthermore, studies of the structure determined that the contact sites on A2 determined by mutagenisis studies, residues Val^3, Ile^6, Leu^7, and Leu^{10} of the N-terminus, are involved in p11 binding (Figure 4, Panel B) (91;93).

1.3.2 Biochemical Properties

1.3.2.1 Anionic Phospholipid- and Calcium-binding

Like all annexins, A2 displays the general biochemical and physical characteristics conferred by the presence of the annexin repeats and the highly conserved protein core (76). Thus, A2 can bind anPL in a Ca^{2+} dependent

Figure 4: Interaction Between p11 and the N-terminus of A2. A ribbon plot depiction of the x-ray crystal structure corresponding to the N-terminus of A2 (yellow and green helices) complexed with a p11 dimer (p11 subunit 1: blue, p11 subunit 2: red) is shown in Panel A. In Panel B, the hydrophobic amino acid side chains of A2 (Val^3, Ile^6, Leu^7, Leu^{10}) and p11 (Thr^{85}, Phe^{86}) involved in the association of A2 with p11 have been shown in stick and ball format (taken from (91)).

A

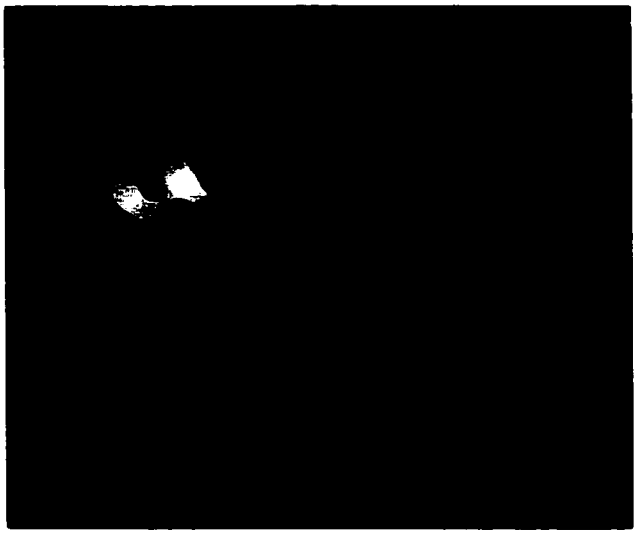

B

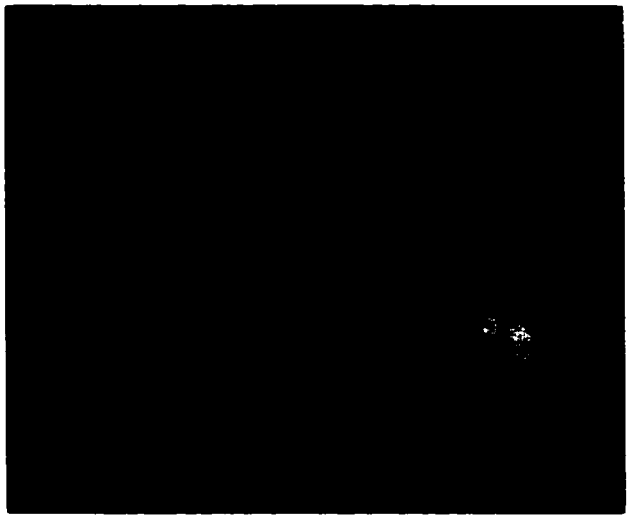

manner, with a preference for PA, PI, and PS (76). Additionally, A2 has been shown to bind to membranes of A549 cells (34) and early endosomes (35) in the absence of Ca^{2+}. This Ca^{2+}-independent phospholipid binding has been proposed to occur through the association of A2 with unidentified membrane proteins, and has been shown to require residues 15 to 24 of A2. Interestingly, recent observations have demonstrated that the presence of cholesterol in phospholipid membranes can enhance the ability of A2 to bind and aggregate anPL-containing membranes in the presence and absence of Ca^{2+} (94;95).

The unique ability of A2 to bind p11, and to exist as two different forms inside the cell, allows the protein to exhibit different functional properties depending on the form in which the protein is found (76). The A2 calcium requirements for phospholipid binding differ with respect to A2m and A2t. A2t has the lowest Ca^{2+} requirement to reach half-maximal binding to anPL of all annexin family members, and is the only annexin able to bind phospholipid at intracellular or nanomolar (nM) Ca^{2+} concentrations (76). In contrast, A2m necessitates extracellular or μM Ca^{2+} concentrations for anPL binding. Indeed, studies involving PS liposomes demonstrated that the Kd (Ca^{2+}) for binding of A2t was less than 10 nM, while the Kd for A2m is close to 2 μM (96).

The membrane aggregation properties of A2t are also distinct from those displayed by A2m. A2t has been shown to aggregate chromaffin granules and phospholipid liposomes at sub-μM to μM Ca^{2+} concentrations, whereas milimolar (mM) Ca^{2+} concentrations are required for aggregation to occur in the presence of A2m (96-98). Like membrane aggregation, membrane fusion by A2 is also

controlled by the configuration in which it is found. Although both A2m and A2t can facilitate membrane aggregation, only A2t can subsequently mediate membrane fusion (47;99;100).

1.3.2.2 Binding and Bundling of F-actin.

In addition to the ability to aggregate anPL-containing membranes A2 has been shown to bind to F-actin, and induce F-actin bundling (40). Site-directed mutagenisis of A2 was employed to determine the location of the of the F-actin binding site. A2 mutants lacking the 16, 13 or 9 C-terminal amino acids were unable to bind or bundle F-actin (101). These experiments established that the 9 C-terminal amino acid residues, LLYLCGGDD, are involved in the F-actin binding of A2 (101). The loss of actin bundling activity was attributed to the loss of actin binding. The region of A2 involved in bundling was identified as residues 286 to 294 of the protein, due to the ability of a synthetic peptide with an identical amino acid sequence to fully eradicate F-actin bundling (102).

The effect of A2m and A2t of binding and bundling of F-actin were also evaluated. The F-actin binding abilities of A2m and A2t are identical (76). However, although A2m and A2t exhibit F-actin bundling at mM Ca^{2+} concentrations, only A2t can bundle F-actin at physiological μM Ca^{2+} concentrations (103-105).

Hence, at intracellular Ca^{2+} concentrations only A2t can bind phospholipid, aggregate anPL-containing membranes, induce membrane fusion, and bundle F-

actin. Therefore, A2t appears to be the physiologically active form of A2 inside the cell.

1.3.2.3 N-terminal Domain Regulatory Effects

The N-terminus of A2 exhibits an inhibitory role on the phospholipid binding, membrane aggregation, and F-actin bundling activities of the protein (76). It has been shown that removal of the first 27 or 43 residues of the N-terminus of A2 reduces the Kd (Ca^{2+}) for chromaffin granule aggregation from 1 mM to 29-141 μM (76). Binding of p11 to the N-terminus of A2m and subsequent formation of A2t further reduces this Kd to 2 μM (97). Thus, p11 binding to the N-terminus of A2 and the subsequent formation of A2t appears to counteract the inhibitory effect of the N-terminus. It has been proposed that the reversal of the inhibitory effect of the N-terminus in A2t results from a conformational change in the N-terminal region during tetramer formation (76).

The N-terminal domain of A2 also contains serine and tyrosine phosphorylation sites that have a further regulatory effect on the protein. Phosphorylation of the protein has been shown to occur upon membrane binding (106), or cell stimulation with agonists such as nicotine (107) or platelet derived growth factor (108). Phosphorylation of the Tyr-23 residue by pp60src decreases the lipid binding affinity of the protein, prevents chromaffin granule aggregation, and inhibits binding and bundling of F-actin (109). Protein kinase C phosphorylation of the Ser^{25} residue of A2 prevents lipid vesicle aggregation without affecting phospholipid binding activity (98;110). While protein kinase C

phosphorylation of A2 has been shown to diminish the vesicle aggregation activity, A2 phosphorylation mediated by treatment with protein kinase C, MgATP, and 12-O-tetradecanoylphorbol-13-acetate revealed that phosphorylated A2 induced chromaffin granule membrane fusion (111). These results suggest that phosphorylation may be involved in the mechanism by which A2 mediates phospholipid membrane fusion. Phosphorylation of Ser^{11} by protein kinase C (84;85;110), or calmodulin- or cAMP-dependent kinases inactivates the p11 binding site, and prevents the association of A2 with p11 (85). Thus, phosphorylation of A2 at Ser^{11} may be employed to control the A2t/A2m ratio inside the cell.

1.3.3 Cellular Localization

1.3.3.1 Sub-cellular Localization

The biochemical properties of A2m and A2t dictate their cellular localization; thus the cellular distribution of A2 inside the cell is dependent on the form in which it is found. Because A2m cannot bind anPL at intracellular Ca^{2+} concentrations (usually 0.01 to 0.1 μM for resting cells (112)), the monomeric form is located in the cytosol of the cell (113). However, A2t can bind anPL at intracellular Ca^{2+} concentrations, resulting in its localization to the inner leaflet of the plasma membrane (114;115). The dimeric form of A2 resides in the nucleus of the cell (76).

Although A2 lacks a secretory signal and therefore cannot be secreted via the typical endoplasmic reticulum dependent pathway, the protein has been

identified extracellularly. A2 has been identified on the surface of a variety of cell types, including endothelial, keranocyte, and glioma cells (45). Studies performed in endothelial cells have demonstrated that A2 is constituitively translocated to the cell surface within 16 hours of biosynthesis, and that this surface A2 pool corresponds to approximately 5% of the total cellular A2 (116-119). Immunofluorescence microscopy studies have colocalized A2 and p11 on the cell surface (120), inferring that cell surface A2 is most likely present as A2t. In addition, A2 has been identified as a soluble protein in the extracellular fluid (121).

1.3.3.2 Cell Type Distribution of Annexin II.

Although annexins and A2 are ubiquitously expressed throughout the eukaryotic kingdom, their distribution within each organism can vary from one cell type to another (1). Thus, certain organs and tissues may express high levels of A2, while others do not (1).

Analysis of various tissues has reported that A2 is present in the lung, intestine, placenta, brain, spleen, kidney, and adrenal gland. A2 is absent in the heart, smooth muscle, skeletal muscle, liver, platelets, and erythrocytes. Numerous cell types, including epithelial, and endothelial, fibroblasts, macrophages, and spleenocytes also express high levels of A2 (76).

1.3.4 Functions

The function of A2, much like the cellular localization, is dependent on the form in which the protein is found. The dimeric form has been shown to regulate the action of DNA polymerase α (122;123). The roles for A2m and A2t have not yet been unequivocally established *in vivo*, but their *in vitro* biochemical properties suggest roles in membrane trafficking events, such as exocytosis (48), and cell-cell adhesion (1;37). Recent data have implicated A2 in fibrinolysis (124), viral infection (125) and tumor invasion (126).

1.3.4.1 Annexin II-Mediated Plasminogen Activation

A2 has been implicated in fibrinolysis, the biochemical pathway of blood clot lysis. This pathway is initiated by the activation of plasminogen to plasmin by tissue plasminogen activator (tPA). Activated plasmin will then cleave the fibrin clot resulting in blood clot dissolution (for review see (127)).

Early studies identified A2 as an endothelial cell surface co-receptor for t-PA and plasminogen (119;128). Binding and kinetic analysis of plasminogen activation by tPA demonstrated that A2 also accelerated plasmin generation 60 fold, thereby acting as a cofactor in the t-PA dependent conversion of plasminogen to plasmin ((129) for review see (124)) (see Figure 4). Both plasminogen binding to A2 and A2-mediated plasmin generation were inhibited by a C-terminal Lys analog, ε-aminocaproic acid (εACA), and by removal of C-terminal Lys residues with carboxypeptidase B (119;129). The ability of εACA and carboxypeptidase B treatment to eradicate plasminogen binding indicates a

Figure 5: Role of A2 in Plasmin Generation. A2 has been identified as an endothelial cell surface coreceptor for plasminogen (Plg) and tissue plasminogen activator (tPA) (Panel A). Furthermore, A2 can act as a cofactor in the tPA-dependent conversion of Plg to plasmin (Pn) (Panel B).

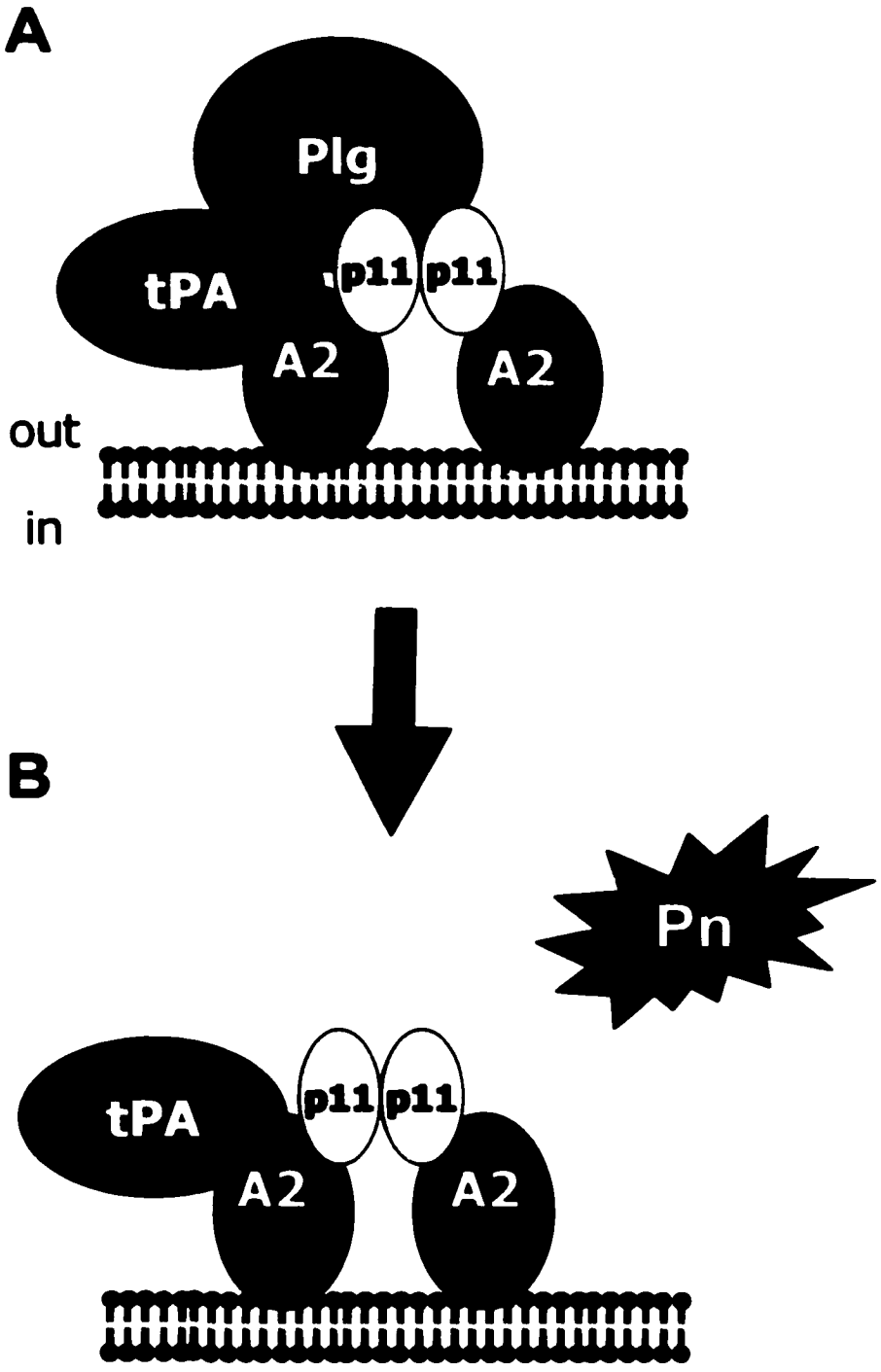
A
Plg
tPA
p11
p11
A2
A2
out
in
B
Pn
tPA
p11
p11
A2
A2

requirement for C-terminal Lys residues for plasminogen binding to A2. The authors proposed that plasminogen binds to Lys^{307} residue of A2 after proteolytic processing of the Lys^{307}-Arg^{308} bond an unknown serine protease (119).

The tPA binding site was identified as residues 7-12 of the A2 tail domain (130). In addition, it was observed that the addition of homocysteine, a thiol-containing amino acid formed from the removal of a methyl group from methionine, inhibited the interaction between A2 and tPA (108;130). Further analysis of the tPA binding site revealed that mutation of the Cys^9 residue to Gly reduced the ability of the mutant A2 to bind tPA, indicating that Cys^9 appears to contribute to tPA binding (130). It was later determined that the ability of homocysteine to prevent tPA binding to A2 results from its complexation with the Cys^9 residue (130). These results suggested that the atherothrombotic phenotype displayed in individuals with elevated plasma homocysteine levels may be due to the inhibition of tPA binding and activity by homocysteine (131;132).

More recent experiments have focused on determining whether A2t is involved in plasminogen and t-PA binding (for review see (133)). A2t was shown to enhance the rate of activation Glu-plasminogen 341-fold compared to a 6-fold enhancement observed in the presence of A2m (120). These data indicate that the p11 subunit may play a crucial role in tPA acceleration by A2. Studies involving recombinant proteins demonstrated that t-PA-dependent Glu-plasminogen activation was stimulated 77 fold by recombinant A2t, and 46-fold by recombinant p11, compared to only 2 fold by recombinant A2m (120). The

ability of p11 alone to stimulate plasminogen activation suggested that p11 may contain a binding site for plasminogen. Binding of Glu-plasminogen to a p11 affinity column and acceleration of Glu-plasminogen activation by p11 were inhibited by εACA and carboxypeptidase B treatment (134). Together these data demonstrate that plasminogen binding site on A2 may be located on the C-terminal Lys residues of the p11 subunit (residues 85-96) (120).

While these observations correlate A2 with a putative role as a regulator of fibrinolytic activation *in vitro*, more *in vivo* data is needed. Recently, the discovery of annexinopathies (135), diseases caused by the deregulated expression of various annexins, including A2, has provided *in vivo* evidence of the involvement of A2 in fibrinolysis (135). Overexpression of A2 has been correlated with accelerated fibrinolysis and bleeding in acute promyelocytic leukemia (136). Furthermore, A2 has been implicated in plasminogen-mediated matrix invasion by macrophages (137). Finally, studies involving the rat carotid artery thrombus model demonstrated that injections of recombinant A2 were able to reduce thrombus formation (138). These observations demonstrate the ability of A2 to act as a fibrinolytic activator *in vivo*.

1.3.4.2 Regulation of Plasmin Activity by Annexin II.

To further investigate the role of A2 in fibrinolysis, its effect on plasmin activity was studied. It was observed that the presence of A2t in a fibrin polymer inhibited plasmin-dependent polymer lysis, while A2m and annexins I, V, and VI had no effect (139;140). This inhibition was latter shown to result from a loss of

plasmin activity due to enhanced A2t-mediated plasmin autodegradation (141). These data have identified A2t as an *in vitro* regulator of plasmin activity, however more physiological data was needed to correlate A2t to plasmin regulation *in vivo*. Recent immunohistochemical studies of A2 and p11 have localized the presence of A2t in a pathological blood clot (141). Although further investigation is required, the presence of A2t in a pathological blood clot suggests that it may play a physiological role in plasmin regulation on the fibrin clot surface.

1.3.4.3 Proposed Role of Annexin II in Cytomegalovirus Infection.

Numerous observations show a correlation between A2 and CMV infection. Early studies demonstrated that cell surface A2 binds human CMV (142), that high levels of A2 are present in cells that are productively infected by CMV (143), and that A2 has been observed on the surface of CMV grown in fibroblasts (142;144;145).

Direct evidence for a role for A2 in CMV infection was obtained from preliminary experiments involving antibody interference of A2, or the addition of exogenous purified A2. These experiments determined that antibodies specific for A2 were observed to prevent both CMV infection of human fibroblast cells (144), and synsitia formation of cells transfected with the CMV encoded fusogenic protein glycoprotein B (146). It was also observed that exogenous A2m could enhance CMV binding to anPL-containing membranes, while A2t could mediate CMV binding and fusion to phospholipid membranes (125).

Recent studies performed in our laboratory further characterized the roles of A2m, A2t and p11 in CMV infection. Exogenous purified p11 and A2t caused a 4-fold enhancement in CMV entry (147). The enhancement in CMV entry was reflected in the production of infectious viral progeny, which was enhanced 10-fold by A2t and 3-fold by p11 (147). Interference with endogenous p11 and A2 present on the surface of human foreskin fibroblasts with anti-p11 and anti-A2 antibodies caused an 80% reduction CMV entry and productive infection (147). These observations allow us to propose a role for A2 as a cell surface receptor for the CMV.

1.3.4.3 Role of Annexin II in Extracellular Matrix Remodeling

Several recent observations have identified A2 as a potential mediator of cell-cell, cell-matrix interactions, and matrix remodeling. A2 has been shown to bind extracellular matrix proteins including tenascin C (45), collagen I (148), and fibrin (140). In addition, binding of A2 with these matrix proteins has been shown to modulate their activities. Indeed, association of tenascin C with A2 resulted in mitogenisis, cell migration, and a loss of focal adhesions (46).

Furthermore, A2 has been shown to act as a binding site for plasminogen and tissue plasminogen activator, as well as an accelerator of plasmin activation (119;149). Plasmin activation is an important mediator of migration, debris removal, and fibrin clearance by macrophages at a site of injury inflammation. Moreover, antibody interference with A2 prevented Lys-plasminogen and plasmin binding, plasmin activation on the macrophage surface, and inhibited the ability

of macrophages to degrade and migrate through extracellular matrices (137). Thus A2 is involved in plasmin-mediated extracellular matrix remodeling by macrophages (137). It has been proposed that the ability of A2 to interact with serine proteases, such as tPA and plasmin, and matrix proteins, including tenascin C, provides a structural link between cell surface proteases and matrix proteins. This link would facilitate degradation of the extracellular matrix by cell surface proteases, thereby enabling extracellular matrix remodeling. Together these data provide a basis for the role of A2 in cell-matrix interactions, as well as a role in remodeling of the extracellular matrix.

1.3.4.4 Annexin II and Tumor Invasion

Deregulated expression of A2 has been associated with various types of cancer. A2 protein and mRNA levels have been shown to be up-regulated in human pancreatic cancer (150;151), multidrug resistant small cell lung cancer (152), high grade gliomas (153), and hepatocellular carcinomas (154). Likewise, A2 levels are also enhanced in cancerous cell lines, including pancreatic cancer derived cell lines (150), B-cell lymphoma cells (155), PC12 rat adrenal pheochromocytoma cells (156), and F9 murine teratocarcinoma cell lines (157). Furthermore A2 levels are up-regulated on the surface of metastatic cancer cells, such as metastatic human breast carcinoma BT20 cells (126), human glioma U87 cells (126), as well as RAW117 and KM12 cell lines, compared to non-metastatic cancer cell lines (117;158).

In addition, A2 has been shown to interact with cathepsin B, a cysteine protease whose expression is up-regulated in cancerous cells, particularly at the invasive edge (159). Thus, the observation that A2 is a cell surface receptor for procathepsin B, the cathepsin B proenzyme, provides an additional link between A2 and neoplasia (159).

The observation that the location of the S100 gene cluster colocalizes with a region that is frequently rearranged in different tumor types (160), combined with the demonstration that certain S100 family members are up-regulated in melanomas (161) and murine metastatic mammary epithelial cells (162), have suggested a link between the deregulated expression of S100 proteins and cancer. The fact that the p11 subunit of A2t belongs to the S100 family (163) lends further credence to the hypothesized link between A2 and cancer.

Tumor metastasis and invasion is a two step process. First, neoplastic cells must degrade the extracellular matrix adhesion proteins holding them in place. Once the adhesive forces have been broken, the metastatic cells are free to migrate to new locations. Degradation of the extracellular matrix is achieved by the action of cell surface proteases such as urokinase plasminogen activator (uPA), tPA, and cathepsin B (126). Activation of proteolysis occurs via an enzymatic cascade, tPA activates cathepsin B, cathepsin B activates uPA, which in turn activates plasmin (126). The observation that cell surface A2, tPA, and cathepsin B are associated with tumors with invasive potential, along with the fact that A2 colocalizes cell surface proteases with matrix proteins has lead scientists to propose a link between A2 and tumor invasion (126). It has been

hypothesized that the ability of A2 to facilitate extracellular matrix degradation may be exploited by metastatic cells to migrate to different areas in the body.

1.4 THROMBIN

The main focus of this thesis was to study the consequences of thrombin-mediated cell stimulation on the sub-cellular distribution of A2. Therefore, a brief overview on the structure (164), generation (165), as well as the cell modulatory functions (166) of the enzyme will be presented.

1.4.1 Structure

Thrombin belongs to the serine protease family, a family of enzymes that cleave peptide bonds using a common mechanism that involving a Ser, His, and Asp residues in their active sites (164). Thrombin is a 36.7 kDa heterodimer, composed of a 6 kDa A chain and a 31 kDa B chain, which are linked by a disulfide bridge which occurs between residue 22 on the A chain and residue 168 on the B chain. Active thrombin exists as three different isoforms, α-thrombin, β-thrombin, and γ-thrombin (164). The α form is generated directly from its zymogen prothrombin, while the β and γ forms are derived from the α form by autoproteolysis. β-thrombin results from cleavage of the Arg^{70} or Arg^{73} bond in the B chain (164). γ-thrombin is produced from β-thrombin by an additional cleavage at Arg^{154} (164). The peptides released remain non-covalently associated with the β- and γ-thrombin (164). The β and γ forms are enzymatically

active, and have been shown to cleave small synthetic substrates (167) and proteins substrates such as the anticoagulant antithrombin III (168). However they are no longer able to efficiently cleave certain physiological substrates, including fibrinogen (168) and thrombospondin (169), or activate protein C (168). Therefore β-thrombin and γ-thrombin cannot participate in blood clotting, and are not considered physiologically significant, but could be found to have altered substrate recognition of importance in the future.

Like other members of the serine protease family, thrombin contains a highly conserved active site with a serine residue. The catalytic triad involved in peptide bond cleavage includes amino acid residues Ser^{254}, His^{92}, and Asp^{146} (164;170). Although the mechanism used by all serine proteases is similar, their distinct peptide bond cleavage specificity is achieved from unique substrate binding pocket composition. The conformation of the thrombin substrate-binding pocket is designed to specifically cleave peptide bonds on the C-terminal side of Arg residues that fit the X-Pro-Arg motif (164). The Asp^{148} residue is what renders the molecule partial to cleaving Arg-X peptide bonds (170).

Crystal structures of α-thrombin and certain substrates and inhibitors, including hirudin, fibrinopeptide A, and thrombin receptor peptides, have been solved (171). These structures demonstrated that thrombin contains secondary binding sites or exosites, distinct from the active site and substrate binding pocket, which confer an additional degree of specificity to the peptide bond cleavage activity of the protein (for review see (171)). Therefore, unlike other serine proteases, such as trypsin, which have a broad substrate range, thrombin

cleaves only specific Arg-X bonds. This is particularly evident when the cleavage of fibrinogen by thrombin is investigated. Of the 376 potential thrombin cleavage sites in fibrinogen, only 4 are actually cleaved by thrombin (171). Studies of the crystal structures of α-thrombin with hirudin and fibrinopeptide A lead to the discovery of the fibrinogen- or hirudin-recognition exosite (171). This exosite promotes high affinity binding of fibrinogen to thrombin, and contributes to the high substrate specificity demonstrated by the enzyme (171).

1.4.2 Generation

Thrombin is generated from its zymogen prothrombin, a vitamin K dependant 71.6 kDa single chain protein synthesized in hepatic parenchymal cells, by factor Xa, in a reaction that requires factor Va, Ca^{2+}, and anPL as cofactors (165). A detailed dissertation on the mechanism of thrombin generation and the coagulation cascade is beyond the scope of this thesis. However, the localization of thrombin production on the cell surface, or on the surface of certain herpesviruses, is of importance to this project. Therefore, the discussion will be limited to thrombin generation on the surface of the cell or virus.

1.4.2.1 Thrombin Generation on the Endothelial Cell Surface

All the components necessary for the initiation and maintenance of the blood coagulation cascade are found circulating in plasma except for the triggering mechanism. This triggering mechanism involves the exposure of

tissue factor (TF) and anPL to the coagulation zymogens present in the blood stream (165). In resting endothelial cells, the plasma membrane phospholipid distribution is asymmetrical, with the anPL confined to the inner leaflet of the plasma membrane (172;173). Likewise, the TF factor distribution in the resting endothelium is confined to the interior of the endothelial cells and the sub-endothelium (127). Hence, under resting conditions the anPL and TF are inaccessible to the coagulation factors present in plasma. Therefore, in order for the anPL and tissue factor to come into contact with the clotting factors, the both triggers must be exposed on the cell surface. This stimulus only occurs at the site of vascular injury or at the formation of a platelet clot (127). Once anPL and TF are presented on the endothelial cell surface, the coagulation cascade is activated, and thrombin generation occurs.

1.4.2.2 Thrombin Generation on the Cytomegalovirus Surface.

Recently, it has been discovered that thrombin generation can occur directly on the surface of certain herpesviruses, including herpes simplex virus-1 (HSV-1) and –2 (HSV-2), as well as CMV (174). This ability results from the fact that the viral envelope contains the triggers required for the initiation of coagulation. It has been shown that the envelopes of HSV-1, HSV-2, and CMV contain host cell derived tissue factor and anPL (174). Therefore, once the viral tissue factor and anPL interact with the circulating zymogens present in plasma, cellular regulation is bypassed and coagulation is initiated on the virus surface.

1.4.3 Function

The two main physiological functions of thrombin are blood clot formation and cellular modulation. Other functions include feedback modulation of hemostasis. However, this introduction will focus solely on the cell modulatory function of thrombin.

1.4.3.1 Cellular Modulation

Thrombin can elicit many diverse biochemical responses through interactions with its cell surface receptors. Generally, thrombin stimulation of its receptors has been found to activate various second messenger systems including phospholipase C, A_2, and D, activate kinases such as protein kinase C, MAP kinase, and tyrosine kinases, increase the cytosolic Ca^{2+} concentration, induce mitosis and control the movement of ions in and out of cells (166). In endothelial cells, one of the cell types utilized for this project, thrombin has been found to activate phospholipase C, A_2 and D, elevate cytosolic Ca^{2+} levels, and increase plasma membrane permeability (166).

Thrombin also elicits endothelial-specific effects including the release of von Willebrand factor, endothelin, nitric oxide, prostaglandin I_2 and increases in intracellular cyclic AMP (175-183). These biochemical effects result from the interaction of thrombin with thrombin receptors located on the cell surface.

1.4.3.2 Thrombin Receptors

Thrombin receptors belong to the protease activated receptor or PAR family. PARs are seven transmembrane domain, G-protein linked, cell surface receptors ((166;184). To date, three family members, PAR-1 (185;186), PAR-3 (187), and PAR-4 (188;189) have been identified as thrombin receptors. These three receptors differ in their thrombin requirements for activation. In platelets thrombin can activate PAR-1 at concentrations of 1 nM (190). However, at thrombin concentrations below 1 nM platelet PAR-4 is believed to remain inactive (189;191). The differences in thrombin requirements for activation between PAR-1 and PAR-4 are due to structural differences. PAR-1 has been shown to possess a high affinity-binding site for thrombin that interacts with the hirudin-recognition exosite (192), while PAR-4 lacks a high affinity-binding site (189).

Although these receptors differ in their requirements for thrombin for activation, their mechanism of activation is similar (166). In order to activate PAR-1, thrombin must first bind to the anion binding exosite of the receptor located on the extracellular N-terminal domain (see Figure 5). Thrombin then cleaves the N-terminus of the receptor between residues 41 and 42 (185). This generates a new N-terminus that subsequently binds to the second extracellular loop of the receptor, thereby acting as a tethered ligand. The binding of the tethered ligand to the receptor causes a conformational change in the receptor allowing it to allosterically activate G proteins inside the cell leading to second messenger generation (185). It has been shown that peptides that mimic the first six amino acids of the tethered ligand can activate the receptor (193-195).

Figure 6: Mechanism of Activation of Cell Surface Thrombin Receptors. Activation of PAR-1 occurs by a two step process. Thrombin must first bind to the N-terminus of the receptor, cleaving it to reveal a new N-terminus (Panel A). The newly revealed N-terminus (red box) then acts as a tethered ligand and activates the receptor resulting to G protein mediated signal transduction (Panel B).

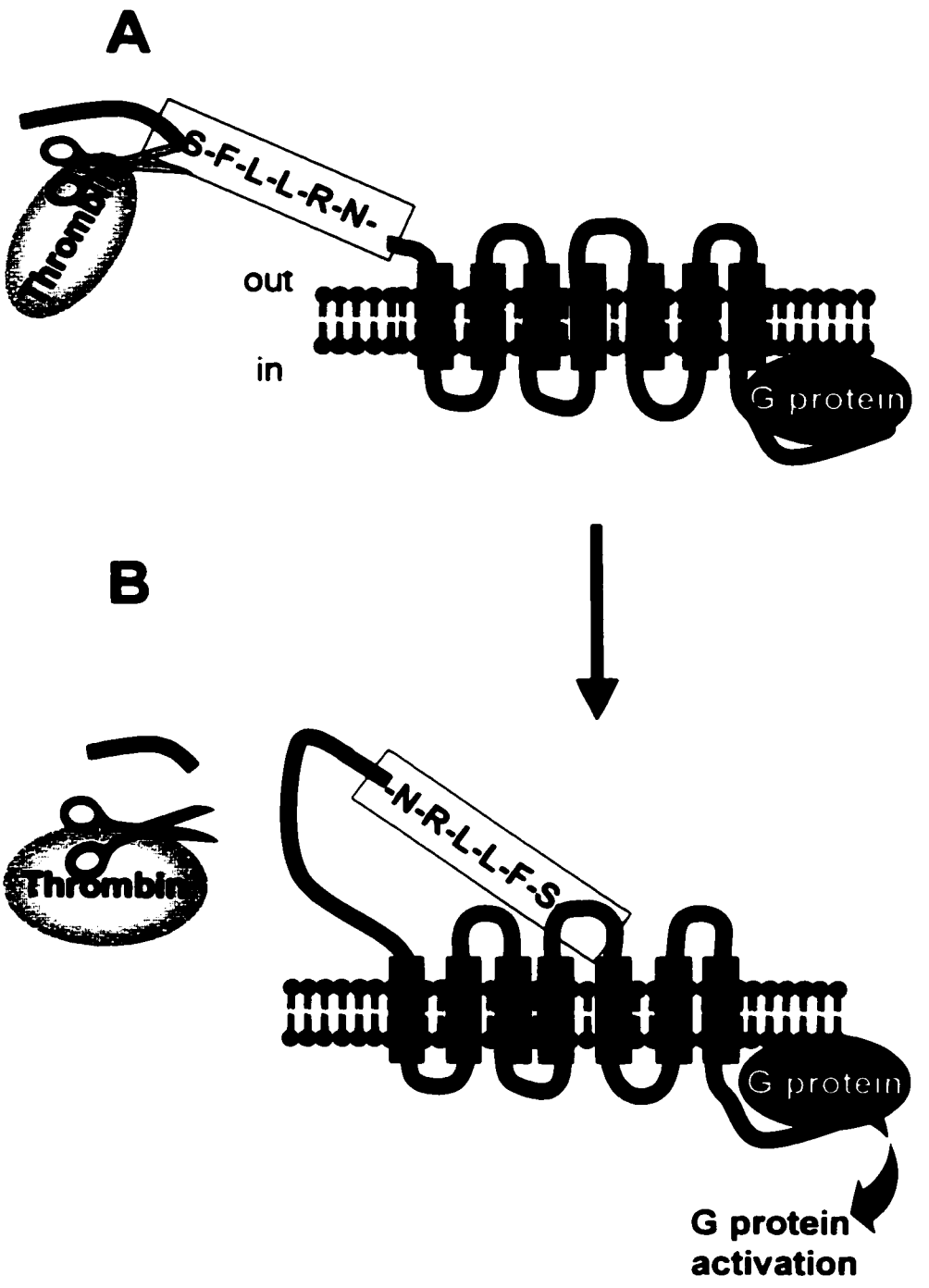
A
S-F-L-L-R-N-
Thrombin
out
in
G protein
B
-N-R-L-L-F-S
Thrombin
G protein
G protein
activation

Studies performed on platelets demonstrated that although these peptides can activate PARs, they are not as potent agonists as thrombin. While thrombin in the nM range can activate PAR-1 and PAR-4, SFLLRN the PAR-1 activating peptide can activate platelet PAR-1 at concentrations of 10 μM (190), and GYPGQV the PAR-4 peptide requires concentrations of 500 μM to activate its receptor (191). Interestingly, the PAR-3-activating peptide, TFRGAP is unable to activate its receptor at concentrations of 100 μM (189).

1.5 ENDOTHELIAL CELLS

The endothelium plays a key role in the regulation of hemostasis (127). The initiation of coagulation and thrombin generation, as well as fibrinolytic activation and plasmin formation, can occur on the surface of endothelial cells (127). In addition, the endothelium is the first site of infectious contact between various viruses and the organism. The ability of the endothelium to participate in coagulation, fibrinolysis, and viral infection, makes endothelial cells a relevant cell type for the examination of the role of A2 in fibrinolysis and CMV infection. Therefore, I will begin by discussing the morphology of cultured and native endothelial cells, followed by the role of the endothelium in coagulation and fibrinolysis.

1.5.1 Endothelial Cell Morphology

1.5.1.1 Morphology of Native Endothelial Cells

Early examination of arterial, venular, and microvascular endothelial cells determined that they exhibited similar basic morphological characteristics *in vivo*. However, recent studies have established that endothelial cells display a large degree of heterogeneity. Indeed, the morphology and surface antigens of endothelial cells derived from different tissues, and from the microvascular and large vessel endothelium can be quite different (196). In fact, the large vessel endothelium, which is believed to control physiological parameters such as vascular tone, blood pressure, displays cobblestone monolayer morphology both *in vitro* and *in vivo* (196).

In contrast, the microvasular endothelium, whose main functions include neovascularization and the exchange of oxygen and nutrients, can form tube like structures when grown on extracellular matrix preparations mimicking basement membranes (196). The microvascular endothelium can be further divided into 3 subtypes, continuous, discontinuous, and fenestrated, which vary in morphology and tissue expression (196-198). Continuous endothelial cells form tight junctions between one another, and are located in the brain, retina, lung, muscle and adipose tissue (196-198). The discontinuous endothelium on the other hand is found in the liver, spleen and bone marrow, and contains gaps between neighboring endothelial cells (196-198). Fenestrated endothelial cells contain a unique structural feature, fenestrae, which localize them to endocrine glands, glomeruli, renal tubules, and intestinal villi (197).

Endothelial cells isolated from large vessel and microvascular endothelium also differ in surface antigenisity and in their responses to growth factors. Examples include the effects of interleukin 4 and fibroblast growth factor on these two types of endothelial cells. Large vessel endothelium responds only weakly to interleukin 4, whereas the microvasculature exhibits a strong response (196). The addition of fibroblast growth factor to cultures of microvascular endothelial cells induces morphological changes to a fibroblast-like morphology, while having no effect on large vessel-derived endothelial cells (196).

Protein antigens, as well as the microvascular morphology of endothelial cells have been shown to differ in response to the tissue of origin (127). Surface receptors, glycoproteins, and cytoskeletal proteins have also been shown to vary in capillaries obtained from different tissues. This variation of surface glycoproteins supplies each different type of endothelial cell with its own surface glycoprotein fingerprint. Intracellular protein expression also varies between endothelial cells originating from different tissues. A typical example of the variation of protein expression is the presence of von Willebrand factor (vWF) (196). Although vWF is used as an endothelial cell marker for cells derived from large vessels, such a human umbilical vein endothelial cells, it is not observed in numerous microvascular endothelial cells such as glomerular capillaries, and the lymphatic and liver sinusoidal endothelium (196). Further examination of vWF expression has deemed it an unsuitable endothelial cell marker for microvascular endothelial cells (196).

Thus, when choosing an endothelial cell type as a cell model for the study of a particular problem the origin of the particular endothelial cell, both tissue type and species must be taken into account.

1.5.1.2 Morphology of Cultured Endothelial Cells

Studies of endothelial cell derived from numerous tissues have demonstrated that isolation procedures and cell culture conditions may alter the cellular phenotype (127). Certain tissue and vessel-associated physiological functions are lost in cultured cells. Along with the loss of specific functions, cultured endothelial cells appear to be activated. In vivo, cultured endothelial cells are quiescent, and only replicate at a rate of 0.1 % per day (127). However, cultured endothelial cells have been shown to replicate at rates between 1 and 10 % per day (127).

Thus, cultured endothelial cells do not generate a perfect cell model of the endothelium. However, no technique to date has been able to isolate and culture endothelial cells in their quiescent, unaltered, natural state. Therefore, while the cultured endothelial cell models are imperfect, they may still generate important information about various endothelial cells functions (199).

1.5.2 Function of the Endothelium in Coagulation

The main function of the vascular endothelium is the regulation of the hemostatic system (for review see (170)). Other roles which will not be discussed in detail, include the control of blood flow by means of vasoactive

substance secretion, and directing the movement of nutrients, plasma proteins, and blood cells through the organism via interactions with endothelial cell surface receptors (127).

1.5.2.1 Anticoagulant Properties of the Endothelium

Under normal conditions the unperturbed endothelium adopts an anti-coagulant state. Transformation of the endothelium from an anticoagulant to a procoagulant state occurs only once a stimulus, such as tissue injury, induces the exposure of tissue factor (TF) and anPL on the endothelial cell surface (127). *In vitro*, tissue factor expression in endothelial cells can be induced by treatment with thrombin, certain cytokines, and oxidized lipoproteins (127). The functions of TF and anPL in the coagulation cascade have been well defined. TF has been shown to greatly accelerate the factor VIIa-dependent conversion of factor X to Xa (127). anPL serves as a binding site for various coagulation factors, localizing the enzymes to a common surface and facilitating their interactions (170). Thus, TF and anPL exposure initiates the coagulation cascade, whose end product, thrombin, causes fibrin clot formation.

Other factors, such as platelet activating factor (PAF), heparin neutralizing components, and endothelial cell surface PARs, help maintain the procoagulant environment once coagulation has been initiated (127). This is exemplified by the ability of thrombin-mediated PAR-1 stimulation to induce the expression of prothrombotic molecules such as TF, plasminogen activator inhibitor, and PAF (127).

Because blood clot formation in the absence of tissue injury is disadvantageous to the organism, several anticoagulant pathways have evolved to control the initiation and the extent of activation of coagulation. The normal anticogulant state of the vascular endothelium is maintained three different ways. First by providing a physical barrier to prevent an interaction between the clotting activators located inside endothelial cells and in the sub-endothelium, and the circulating plasma zymogens (127). The second method involves the presentation of an anticoagulant surface that prevents platelet adhesion and blood clot formation (127). The control of the extent thrombin generation and activity by the activation of various anticoagulant pathways is the final step used to control unwanted coagulation (127;200). The main endothelial cell mediated anticoagulant substances that control thrombin activity and coagulation include prostacyclin, thrombomodulin, anti-thrombin III, heparan sulfates, dermatan sulfates and tissue factor pathway inhibitor (127;200). The role of the endothelium in coagulation is summarized in Figure 7.

Prostacyclin (PGI_2) is a lipid-derived compound formed from arachidonic acid, which is produced and secreted into plasma by endothelial cells. Interaction of plasma PGI_2 with cell surface receptors on platelets causes a calcium overload, resulting in stiff platelets unable to perform secretory functions (127;170;200). In addition, PGI_2 also prevents platelet adhesion by preventing von Willebrand factor and fibrin binding to platelets. Low plasma levels of PGI_2 are found at all times, but pulsatile sheer stress, thrombin interaction with endothelial cell surface receptors, and platelet activation stimulate its production

Figure 7: Regulatory Functions of Endothelial Cells in Coagulation and Fibrinolysis. The function of endothelial cells in the initiation of the coagulation (Panel A) and fibrinolysis (Panel B) pathways have been outlined. Proteins secreted by endothelial cells are shown in blue, while proteins present on the endothelial cell surface are shown in red (+ indicates an activator, while – indicates an inhibitor).

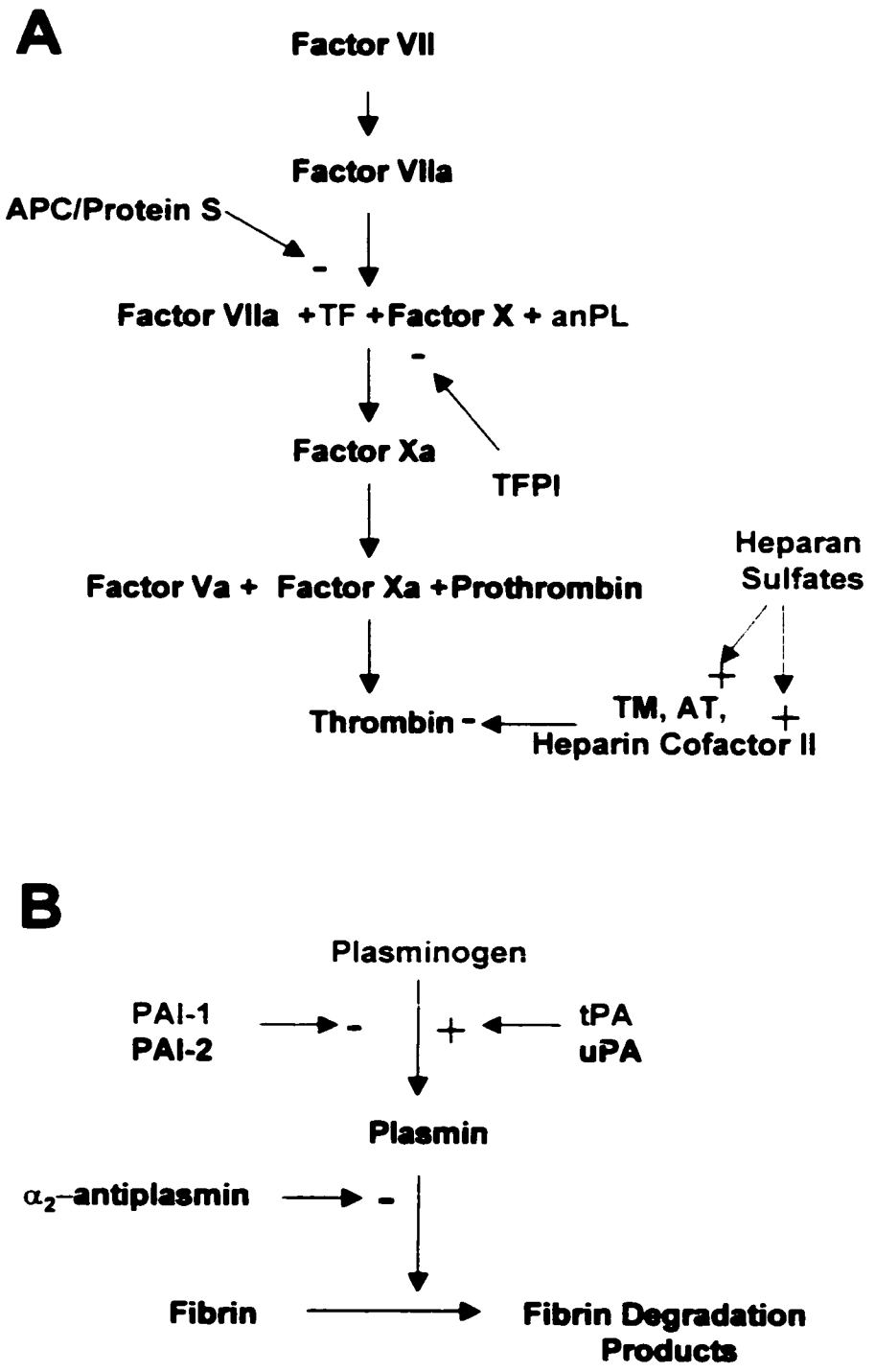
A
Factor VII
Factor VIIa
APC/Protein S
-
Factor VIIa +TF +Factor X + anPL
-
Factor Xa
TFPI
Heparan
Sulfates
Factor Va + Factor Xa +Prothrombin
+
TM, AT,
Heparin Cofactor II
+
Thrombin -
B
Plasminogen
PAI-1
PAI-2
-
+
tPA
uPA
Plasmin
α_2-antiplasmin
-
Fibrin
Fibrin Degradation
Products

and secretion (127;170;200). Thus, PGI_2 contributes to the constitutive and active anticoagulant activities.

Thrombomodulin (TM) is a 60 kDa membrane glycoprotein present on the surface vascular endothelial cells of arteries, veins, capillaries and lymphatics located throughout the body except in the central nervous system (127;170;200). Its main role is to enhance thrombin-mediated protein C activation. Along with its role in activated protein C formation, TM has been shown to reduce the ability of thrombin to activate platelets, fibrinogen, and clotting factors V and XIII (127;170;200). In addition, binding of thrombin to TM induces rapid endocytosis and degradation of the protein. Interestingly, TM is expressed at 1000 fold higher concentrations in the microvasculature than in major blood vessels (170). Thus, any active thrombin circulating in major blood vessels will be bound and inactivated by TM once it reaches the capillaries (170). Therefore, the presence of TM on endothelial cells is another mechanism by which endothelial cell maintain their anticoagulant surfaces.

Heparan sulfates found on the endothelial cell surface, and dermatan sulfates located in the sub-endothelium can function to enhance the activity of various anticoagulant compounds, such as anti-thrombin III and heparin cofactor II (170;200). Anti-thrombin III (AT), a 58 kDa plasma protein synthesized in the liver, megakaryocytes, and the endothelium, is another potent thrombin inhibitor. Futhermore, AT has been shown to inhibit a variety of clotting factors including thrombin XIIa, XIa, Xa, IXa, plasma kallikrien, and plasmin (170). Although AT is a slow acting inhibitor, binding of soluble heparin, or heparan sulfate bound to the

endothelial cell surface can accelerate its activity 1000 fold (170). Similarly, heparin has also been shown to enhance the activity of another anticoagulant, heparin cofactor II. Once heparin cofactor II binding to heparan sulfates or dermatan sulfates has occurred, the protein functions to inhibit thrombin activity (170).

The final anticoagulant associated with endothelial cells is tissue factor pathway inhibitor (TFPI). TFPI is a 42 kDa glycosylated lipoprotein which functions to inhibit thrombin generation by binding and inactivating factor Xa within the tissue factor, VIIa, Xa complex, forming a ternary complex (127;170). TFPI, which is synthesized and stored in endothelial cells, is released into plasma by heparin (127;170).

1.5.3 Fibrinolytic Functions of Endothelial Cells

In addition to their function in coagulation and anticoagulation, endothelial cells also play an important role in fibrinolysis. The central reaction of the fibrinolytic pathway is the conversion of the inactive zymogen plasminogen to plasmin by various plasminogen activators (127). Activated plasmin is then able to mediate blood clot lysis through the degradation of the fibrin polymer (127). The plasminogen activators identified to date include tPA and uPA (urokinase plasminogen activator) (170). The 54 kDa uPA, is synthesized in connective tissue, fibroblasts, macrophages, and epithelial cells (170). However, the inability of endothelial cells to produce uPA suggests that it is not important in fibrinolysis. Functional studies of uPA have demonstrated that the protein is most probably

involved in tissue repair and wound healing. tPA on the other hand, is a single chain, 68 kDa serine protease that is produced in endothelial cells (170). Furthermore, stimulation of endothelial cell with agonists such as thrombin induces tPA expression on the endothelial cell surface (170). The endogenous expression of tPA by endothelial cells, combined with the thrombin mediated-induction of its cell surface expression, suggest a functional role for tPA in fibrinolysis.

Unrestrained fibrinolytic activation can lead to bleeding disorders, which like uncontrolled clotting, is undesirable for the organism in question. Thus, pathways to control the initiation and extent of fibrinolysis have evolved in endothelial cells (170;201;202). Inhibition of the initiation of fibrinolysis is achieved through the action of plasminogen activator inhibitors. Endothelial cells secrete a plasminogen activator inhibitor, PAI-1, which inhibits the activity of both tPA and uPA (170). Binding of this 52 kDa single chain glycoprotein to vitronectin results in its stabilization, and facilitates its interaction with tPA (170). Once fibrinolysis has been initiated, the extent of plasmin activity is controlled by α_2-antiplasmin. α_2-antiplasmin, a 70 kDa plasma protein, is a direct inhibitor of plasmin activity (170). Additional functions include enhanced plasmin degradation, and inhibition of fibrin clot lysis by inhibition of plasminogen binding to fibrin (170). The role of endothelial cells in fibrinolysis is summarized in Figure 7 (Panel B).

1.5.3.1 Plasminogen Receptors Located on Endothelial Cells.

Interestingly, studies comparing plasmin generation on the cell surface and in solution phase have revealed that tPA and plasminogen bound to the endothelial cell surface had accelerated plasmin generation (203). It was also noted that plasmin bound to the surface of endothelial cells was protected from inactivation by inhibitors such as α_2-antiplasmin (201). Thus, identification of the endothelial cell surface plasminogen and tPA receptors was carried out (for review see (201;202)).

Early experiments identified approximately 10^7 mol/cell of plasminogen binding sites (203;204), a number of cell surface receptors that cannot be accounted for by a single surface protein. Therefore, it was proposed that several cell surface proteins might contribute to plasminogen binding. Further investigation has identified two different types of plasminogen receptors, proteins that express C-terminal Lys and non-proteins (202). The former category was identified on the basis that C-terminal Lys residues were responsible for the interaction between plasminogen and the putative receptors. Indeed, both A2 (119) and the p11 subunit of A2t (205) were identified as plasminogen receptors which interact via a C-terminal Lys dependent mechanism, as described previously.

Another candidate receptor, α-enolase, was identified by labeling cell surface proteins, running them on a plasminogen-sepharose column, and eluting the plasminogen binding proteins with a C-terminal Lys analog (206). Characterization of the interaction between α-enolase and plasminogen

demonstrated that removal of C-terminal Lys residues by carboxypeptidase B treatment and the addition of excess C-terminal Lys containing peptides, eradicated the plasminogen/α-enolase interaction, thereby confirming the C-terminal Lys-dependence of the interaction (206). Further investigation into the importance of α-enolase as a plasminogen receptor revealed that the protein accounts for approximately 10 % of cell surface plasminogen binding sites on U837 cells (207).

A third plasminogen receptor, a 45 kDa endothelial cell surface protein, was also identified using a plasminogen-sepharose column (208;209). To gain more insight on the identity of this protein, two-dimensional SDS-PAGE of HUVEC lysates, followed by ligand blotting with I^{125} plasminogen was undertaken. Observation of the ligand blot determined that the 45 kDa band was composed of two proteins of similar molecular weight, one of which was later identified as actin (210). Additional experiments revealed that cell surface actin bound both plasminogen and tPA, and that these interactions were inhibited by competition with C-terminal Lys analogs (210).

Thus, to date A2 (119), the p11 subunit of A2t (205), α-enolase (206), actin (210), and an unidentified 45 kDa cell surface protein (208;209) have all been identified as protenacious cell surface plasminogen receptors.

Non-protenacious compounds, such as gangliosides, have also been identified as cell surface plasminogen receptors (211). Gangliosides are glycosphingolipids composed of hexoses, hexosamines, sialic acid, G_{M1} pentasaccharide, ceramides, and glucocerebrosides, which are found on the

surface of most cell types (212). The ability of gangliosides to interact with plasminogen was first demonstrated *in vitro* by I^{125} plasminogen binding to insoluble gangliosides (211). The individual components of gangliosides listed above were unable to inhibit the interaction, indicating the interaction was structurally specific to intact gangliosides (211). An *in vivo* role for gangliosides in plasminogen binding was evaluated by following plasminogen binding to the surface of various cell types, including endothelial cells, in the presence of gangliosides. The observation that gangliosides were capable of inhibiting plasminogen binding to the cell surface indicated that they may act as plasminogen receptor *in vivo* (211).

1.5.3.2 Endothelial Cell Surface Tissue Plasminogen Activator Receptors.

Several possible receptors for tPA have also been identified. As described previously both A2 (130) and actin (210) have been identified as cell surface plasminogen and tPA receptors. In addition, competition studies using I^{125} labeled recombinant tPA and plasminogen have demonstrated that tPA can also interact with α-enolase and gangliosides (213). The ability of these receptors to bind both tPA and plasminogen with either common or distinct regions, may function to colocalize the proteins on the endothelial cell surface, resulting in an enhancement in plasminogen activation.

Furthermore, a novel 20 kDa endothelial cell surface tPA binding protein was identified by chemical crosslinking of I^{125} tPA with a HUVEC monolayer

(214). Additional experiments demonstrated that the 20 kDa tPA receptor enhanced tPA activity 90 fold, and was unable to bind plasminogen (214).

1.5.4 Endothelial Cell Surface Protease Activated Receptors.

1.5.3.1 Protease Activated Receptors Expressed by Endothelial Cells.

The ability of thrombin to cause significant activation of vascular endothelial cells has led to the study and identification of endothelial thrombin receptors. As stated previously, thrombin receptors belong to the protease activated receptor family of which 4 members, PAR-1, PAR-2, PAR-3 and PAR-4 have been discovered (215). PAR-1, PAR-3 and PAR-4 are activated by thrombin, while PAR-2 is activated by trypsin (215). Studies of the tissue distribution of these 4 PARs have determined that only PAR-1, PAR-2 and PAR-3 are expressed by endothelial cells (184;216).

Since the activation of PARs requires their cleavage, after stimulation by thrombin or trypsin the receptors are non-functional and must be replaced. It has been demonstrated that in endothelial cells, PAR-1 receptors are found both on the cell surface as well as in unidentified membrane systems within the cell (217;218). This intracellular pool may be used to replenish thrombin receptors inactivated by thrombin cleavage thereby diminishing the refractory period after stimulation. Such mechanisms may exist for other members of the PAR family.

1.5.3.2 Protease Activated Receptor Stimulation by Other Coagulation Proteases.

Coagulation proteases factor Xa and factor VIIa have been shown to activate cells and provoke cellular responses such as gene induction and signal transduction (219). In addition, it was observed that the factor Xa and VIIa-mediated cellular stimulation required proteolytic activity (219), suggesting that the involvement of protease activated receptors. This hypothesis was addressed by testing whether Xa or VIIa could activate PAR-1, PAR-2, PAR-3, or PAR-4. Experiments have determined that both PAR-1 and PAR-2 are activated after stimulation of cells with factor Xa (220-222). PAR-2 activation was also observed by factor VIIa, although the presence of tissue factor and Xa were necessary for stimulation to occur (223). Thus, upstream coagulation proteases can activate thrombin and trypsin receptors, indicating that thrombin may not be the only physiologically important trigger of PAR-1 activation.

1.6 SPECIFIC GOALS

The hypothesis driving the current work is that thrombin-mediated cellular modulation results in an up-regulation of A2 on the cell surface for use as a fibrinolytic activator or a CMV receptor, as shown in Figure 8.

Thus, my first goal was to study the effect of thrombin and an analogous thrombin signaling peptide specific for PAR-1, on the cellular distribution of A2 and p11. I commenced by examining their effect on the surface A2 and p11 distribution. Next I determined whether thrombin- or TRAP-mediated cellular activation resulted in the synthesis of intracellular A2 or p11 or the redistribution of intracellular protein stores.

The ability of CMV to generate thrombin on its surface combined with the suggestion that A2 is a putative CMV receptor lead us to test whether CMV stimulation of cells could induce surface A2 exposure. Therefore, my second goal was to provide initial data on the effect of CMV stimulation on the sub-cellular distribution of A2.

The ability of A2t to function as a cell surface co-receptor for tPA and plasminogen has been well documented in the literature. Hence my third goal was to evaluate if the thrombin-mediated increases in cell surface A2t could play a functional role in fibrinolysis, by enhancing the plasminogen and tPA binding, as well as the tPA acceleration on the cell surface.

Figure 8: Proposed Mechanism of Thrombin Induced Surface A2 Exposure. We hypothesize that thrombin, generated either by tissue injury and initiation of coagulation or directly on the CMV surface, can interact with its receptors leading to a G protein-linked induction of intracellular signaling. The end result of this cellular modulation is enhanced A2 and p11 on the cell surface, which can then act either as a virus receptor, or a fibrinolytic cofactor.

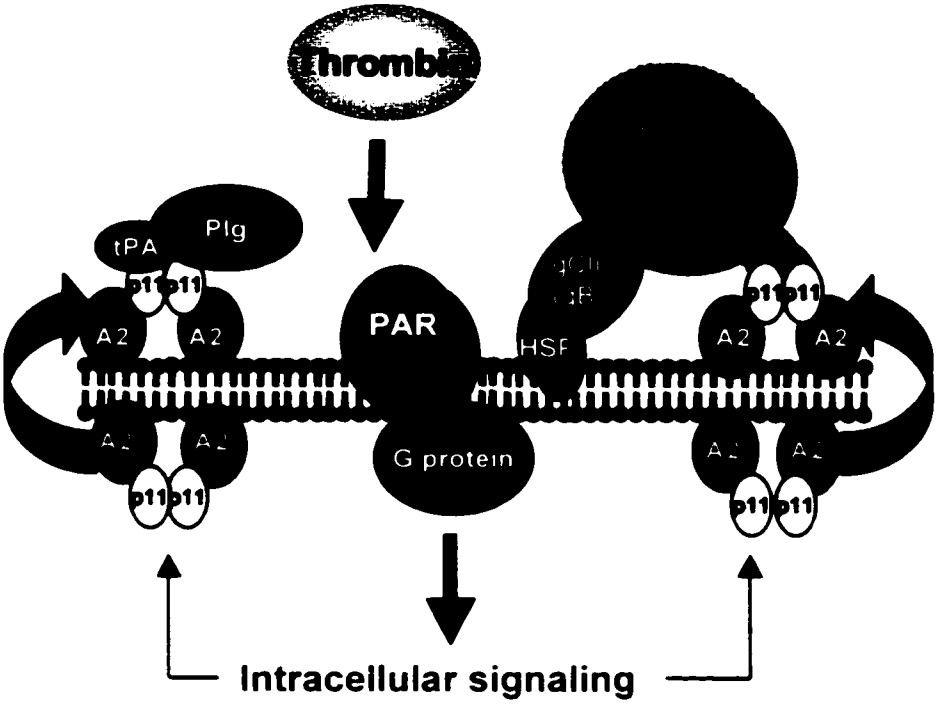
Plg
tPA
p11
p11
A2
A2
PAR
HSP
G protein
Intracellular signaling

2. MATERIALS AND METHODS

2.1 GENERAL

2.1.1 Reagents

All experiments were conducted in PBS (Na_2HPO_4 10.14 mM, KH_2PO_4 1.47 mM, NaCl 136.89 mM, KCl 2.68 mM), HBS (11 mM N-2-hydroxyethylpiperazine-N-2-ethanesulfonic acid (Hepes), 137 mM NaCl, 3 mM $CaCl_2$, 4 mM KCl, 1 mM $MgCl_2$, 1 mM glucose), or HBS/BSA (HBS supplemented with 1 mg/mL bovine serum albumin) as indicated. Recombinant S741C-Fluorescein plasminogen, and S741C-Biotin plasminogen, kind gifts from Dr Michael Nesheim were produced as described previously (224). Chromogenic substrate S2251 (H-D-Val-Leu-Lys-p-Nitroaniline dihydrochloride) was obtained from Chromogenix. Ethylene glycol-bis(β-aminoethyl ether)-N,N,N',N'-tetraacetic acid (EGTA) and ethylenediaminetetraacetic acid (EDTA) were from Sigma. Polyclonal rabbit anti-p11 IgG was raised to a synthetic peptide corresponding to residues 21-38 of p11 linked to keyhole limpet and affinity-purified using this same p11 peptide linked to Sepharose. This polyclonal anti-p11 was used in plasminogen binding experiments. Along with purified A2m and p11, used as western blotting controls, the purified polyclonal anti-p11 were kind gifts from Dr David Waisman.

The primary antibodies used in immunofluorescence microscopy experiments included monoclonal anti-A2 IgG1 (Transduction Laboratories, for intracellular A2 staining), monoclonal anti-A2 IgG2a (Calbiochem, for surface A2 staining), monoclonal anti-p11 IgG1 (Transduction Laboratories), monoclonal

anti-vimentin IgG1 (Sigma, for intracellular vimentin), polyclonal goat anti-vimentin (Sigma, for surface vimentin staining) and polyclonal rabbit anti-von Willebrand factor IgG (Dakopatts a/s). Isotype controls included non-immune mouse IgG1 (Sigma, for intracellular staining), mouse IgG2a (Sigma, for surface staining), and goat serum (Sigma, for surface staining). The secondary antibodies utilized in immunofluorescence microscopy experiments were fluorescein isothiocyanate (FITC)-conjugated rabbit anti-goat IgG (Sigma), FITC-conjugated goat anti-rabbit IgG (Sigma) and Cy^3-conjugated donkey anti-mouse IgG (Jackson ImmunoResearch).

Western blotting experiments were performed with monoclonal antibodies directed against A2 (Zymed), p11 (Transduction Laboratories) or β-actin (Sigma). Horse raddish peroxidase (HRP)-conjugated goat anti-mouse IgG (Jackson ImmunoResearch) was used as the secondary antibody in all western blotting experiments.

2.1.2 Isolation and Identification of Human Umbilical Vein Endothelial Cells.

2.1.2.1 Isolation of Human Umbilical Vein Endothelial Cells.

HUVEC were isolated from umbilical cords by the method of Jaffe et al. as described in (208;225). Briefly, intact placentas with attached umbilical cords were obtained from the General Campus of the Ottawa Hospital (Ottawa, Ontario). The umbilical cords were removed from the placentas, and washed with PBS under sterile conditions. To remove the HUVEC, the cord was incubated with 20 mL of collagenase (2 mg/mL) at 37°C for 15 minutes. The cells were collected by rinsing the cord with 30 mL of Iscove's Modified

Dulbecco's Media (IMDM) (GibcoBRL), followed by centrifuging the flow through for 10 minutes at 1500 rpm at 25°C. The pellet was resuspended in 15 mL of IMDM supplemented with 5% fetal bovine serum (GibcoBRL), 2 mM L-glutamine (GibcoBRL), 20 μg/mL gentamycin (GibcoBRL), 59 μg/mL heparin (Sigma), and 10 μg/mL endothelial cell growth supplement (Calbiochem) (complete IMDM), and seeded in cell culture flasks coated with gelatin (1 mg/mL). HUVEC were cultured at 37°C in 5% CO_2.

2.1.2.2 Characterization of Human Umbilical Vein Endothelial Cells.

To ascertain whether the cells isolated from the umbilical cords were endothelial cells, staining for von Willebrand factor (vWF) and phase-contrast observation were undertaken. Isolated cells grown to confluence on gelatin coated glass coverslips, were simultaneously fixed and permeabilized with 4% paraformaldehyde, 0.25% gluteraldehyde, and 0.2% TritonX-100 in HBS. vWF was detected by incubating the cells with rabbit anti-vWF IgG (Dakopatts a/s) for 1 hour at room temperature (RT) in a moist chamber. After 3 PBS washes, the primary antibody was detected by incubation with FITC-conjugated goat anti-rabbit IgG (Sigma) for 1 hour at RT. The nuclear DNA was then stained with 25 ng/mL 4',6-diamidino-2-phenylindole (DAPI, Sigma) for 5 minutes. The cells were washed three times with PBS and once with double distilled water before being mounted on glass slides with 5 μL of mounting media (0.1% p-phenylene diamine, and 50% glycerol in PBS). To determine whether the observed staining

was specific, the staining procedure described above was repeated omitting the primary antibody.

Unless otherwise indicated, all photographs were obtained using a Zeiss Axioplan2 epifluorescent microscope and a Sony 3 CCD color video camera (model DXC-950P). Fluorescence images were acquired using 40x Plan-NEOFLUAR or 63x Plan-APOCHROMAT objectives, and phase contrast micrographs were obtained with 10x Plan-NEOFLUAR or 100x Plan-NEOFLUAR objectives. In all experiments, the exposure time and light intensity were controlled using Northern Eclipse software (Empix), thereby ensuring all photomicrographs were taken under identical conditions.

2.1.3 Isolation of Human Foreskin Fibroblasts

Human foreskin fibroblasts (HFF) cells were isolated from human foreskins obtained from the Ottawa Hospital (Civic Campus) by an in house protocol. Briefly, the foreskins were washed 3 times with sterile PBS supplemented with 40 μg/mL gentamycin, homogenized with scissors, and washed again. The slurry obtained was incubated for 5 minutes with trypsin/EDTA at 37°C. The supernatant was discarded, and the slurry was then incubated with trypsin/EDTA for 30 minutes at 37°C. The supernatant was then removed, mixed 1 to 1 with basal eagle media (BME; GibcoBRL) supplemented with 15% bovine calf serum calf (GibcoBRL), 2 mM L-glutamine, and 20 μg/mL gentamycin (complete BME), and centrifuged for 12 minutes at 1200 rpm. The

pellet obtained was resuspended in complete BME, and the cells were seeded in T175 tissue culture flasks and grown at 37°C in 5% CO_2.

2.1.4 Cell Culture

The HUVEC isolated, were passaged by detaching the cells with trypsin/EDTA and splitting them in a 1 to 4 ratio. The subcultures were propagated in complete IMDM until passage 5. All experiments were performed on cells of passage 5 or lower.

Human foreskin fibroblasts (HFF) were passaged by detaching the cells with trypsin/EDTA, and sub-culturing at a 1 to 5 ration in BME supplemented with 5% bovine calf serum, 2 mM L-glutamine, 20 μg/mL gentamycin. All HFF experiments were performed on cells of passage 15 or lower.

2.1.5 Thrombin and TRAP Treatment of Cells.

2.1.5.1 Human Umbilical Vein Endothelial Cells

HUVEC were grown to confluence on gelatin coated 22 x 22 mm glass coverslips or cell culture plates. Monolayers were washed once with IMDM/BSA (IMDM supplemented with 1mg/mL BSA and 2 mM L-glutamine), and treated with 0.4 to 8 nM human α-thrombin (Haematologic Technologies) or 0.1 to 10 μM thrombin receptor activator peptide (TRAP; Sigma) in IMDM/BSA for 5 minutes at 37°C. The cells were then washed once with complete IMDM supplemented with 2mM Ca^{2+} (IMDM/Ca^{2+}), and allowed to recover in IMDM/$Ca^{2+}$for 1 hour at 37°C.

2.1.5.2 Human Foreskin Fibroblasts

HFF grown to confluence on 22x22 mm glass coverslips or in cell culture plates were washed once with incomplete BME (BME supplemented with 1mg/mL BSA and 2mM L-glutamine), and treated with human α-thrombin (0.4 to 8nM) or TRAP (0.1 to 10 μM) in incomplete BME for 5 minutes at 37°C. Cells were washed once with complete BME supplemented with 2 mM Ca^{2+} (BME/Ca^{2+}), and placed in BME/Ca^{2+} for 1 hour at 37°C.

2.1.6 Cytomegalovirus Preparation and Treatment of Cells.

2.1.6.1 Cytomegalovirus Preparation

Human CMV strain AD169 was grown in HFF cells, purified by tartrate-glycerol ultracentrifugation, and quantified by electron microscopy as described in (125). Quantification of the CMV preparation used in our experiments demonstrated that the virus concentration was 7.35 x 10^{11} virus particles/mL, while the protein concentration was 4.44 mg/mL.

2.1.6.2 Cytomegalovirus Treatment of Cells

HUVEC and HFF grown to confluence on 22 x 22 mm glass coverslips or in tissue culture plates were washed once with heparin free complete IMDM (IMDM*), treated with CMV (7.14 x 10^4 virus particles/cell) in IMDM* for 5 to 45 minutes at 37°C. The cells were then washed once with complete IMDM and placed in complete IMDM for 15 to 105 minutes at 37°C.

2.1.7 Quantification and Statistical Analysis of Data

Microscopy experiments were quantified by first calculating the total fluorescence intensity of A2 or p11 staining in each photomicrograph using Northern Eclipse software. The total fluorescence intensity of each photomicrograph was then divided by the number of nuclei present in each field, as determined by nuclear staining with DAPI, in order to generate the total fluorescence intensity/cell. The average total fluorescence intensity/cell for each experimental condition was compared to the values obtained for mock treated cells in order to obtain the fold-enhancement of the levels of A2 or p11. For all microscopy experiments, a total of a least 5 fields of view were quantified for each experimental condition.

Quantification of A2 and p11 western blotting experiments was undertaken by scanning the A2 and p11 lanes on film exposures of the western blots to determine the intensity of each band. The levels obtained for the various experimental conditions were then relativized to the level that was obtained for mock treated cells, thereby generating the fold-enhancement in A2 or p11 levels. In the case of total A2 and p11 levels, the intensity of each band was normalized to the levels of β-actin present in each sample, prior to the comparison with mock treated cells.

To determine if the results obtained for thrombin or TRAP treated cells were significantly different from mock treated cells, statistical analysis of our results was undertaken by first performing an analysis of variance, followed by Dunnett's test using MyNova version 2.21 (written by S. Brooks). For each

separate procedure the average of at least 3 different experiments were evaluated.

2.2 EFFECT OF THROMBIN OR TRAP ON INTRACELLULAR ANNEXIN II AND P11

2.2.1 Immunofluorescence Microscopy of Permeabilized Cells.

HUVEC treated with thrombin or TRAP as described previously, were washed once with HBS, and simultaneously fixed and permeabilized by treatment with 4% paraformaldehyde, 0.25 % gluteraldehyde and 0.2 % Triton X-100 for 10 minutes at RT. Fixed cells were washed 3 times with PBS, and stained for vimentin, A2 or p11 by incubating the cells with monoclonal antibodies directed against p11 (2.5 μg/mL for HUVEC, and 1.25 μg/mL for HFF; Transduction Laboratories), A2 (2.5 μg/mL for HUVEC, and 1.25 μg/mL for HFF; Transduction Laboratories) or vimentin (2.5 μg/mL for HFF and HUVEC; Sigma) for 1 hour at RT. Isotype controls were treated with a non-immune antibody solution containing equivalent amounts of mouse IgG1 (Sigma). After 3 PBS washes, the cells were placed in a secondary antibody solution, containing Cy^3-conjugated donkey anti-mouse IgG (1.25 μg/mL; Jackson ImmunoResearch), at RT for 1 hour. The nuclear DNA was then stained with 25 ng/mL DAPI for 5 minutes. The washing was repeated, and the cells were mounted and visualized as described in section 2.1.2.

HUVEC treated with CMV as described in Section 2.1.6, were fixed and permeabilized as described above. The cells were then double stained for A2

and vimentin with monoclonal mouse anti-A2 IgG (0.8 μg/mL; Oncogene) and polyclonal goat anti-vimentin IgG ([protein]= 156.4 μg/mL; Sigma) in a moist chamber for 45 minutes. The isotype controls were treated with mIgG2a (0.16 μg/mL; Sigma) and goat serum ([protein] = 284 μg/mL). The primary antibodies were detected by incubation with a secondary antibody solution containing rabbit IgG (Sigma), donkey serum (Sigma), Cy^3-conjugated donkey anti-mouse IgG (2.8 μg/mL), and FITC-conjugated rabbit anti-goat IgG ([Ab]= 2 μg/mL; Sigma) for 45 minutes in a moist chamber. Photographs were taken at a magnification of 1260x using a Zeiss epifluorescent microscope, with an exposure time of 1 minute for vimentin and 30 seconds for A2.

2.2.2 Western Blotting of Cellular Lysates.

After treatment with thrombin, TRAP or CMV as described previously, HUVEC and HFF cells were washed twice with HBS, lysed with Laemmli sample buffer containing dithioerithrol (DTT) (12.5 mg/mL for thrombin or TRAP treated cells) or 2% β-mercaptoethanol (for CMV treated cells) and heated at 95°C for 2 minutes. Samples were separated by SDS-PAGE on 15% polyacrylamide gels (acrylamide/bis ratio of 37.5:1), transferred to polyvinyl difluoride (PVDF) membranes, and probed with monoclonal antibodies directed against A2 (0.05 ng/mL) or p11 (0.05 ng/mL). After washing the membranes were incubated with HRP-conjugated goat anti-mouse IgG, and the bands were detected by chemiluminescence (ECL, Pierce) on X-OMATOR scientific imaging film (Kodak). To ascertain that equivalent amounts of cellular lysates were loaded in each

lane, the membranes were re-probed with monoclonal anti-β-actin IgG (0.085 ng/mL) followed by HRP-conjugated goat anti-mouse IgG and visualization by chemiluminescence (ECL).

2.3 EFFECT OF THROMBIN OR TRAP ON CELL SURFACE ANNEXIN II AND p11.

2.3.1 Observation of Cell Surface Annexin II by Immunocytology

HUVEC and HFF cells were stimulated with thrombin and TRAP as described previously. After treatment, the cells were washed once with complete IMDM, and coincubated with monoclonal anti-A2 (1.33 μg/mL; Oncogene) and polyclonal goat anti-vimentin ([protein]=0.195 mg/mL) for 30 minutes at RT. Isotype controls were treated by substituting the primary antibodies with mIgG2a (1.33 μg/mL; Sigma) and goat serum ([protein]=0.71 mg/mL). After washing in complete IMDM, the cells were incubated with Cy^3-conjugated donkey anti-mouse (1.25 μg/mL) and FITC-conjugated rabbit anti-goat (Sigma; 1.66 μg/mL) antibodies at RT for 30 minutes. Stained cells were washed extensively, and fixed with 4% paraformaldehyde in HBS. After fixation the genetic material in the nuclei was stained with DAPI (25 ng/mL), and the cells were mounted and visualized as described in section 2.1.2.

2.3.2 Examination of Extracellular Annexin II and p11 by Cell Surface Labeling with Biotin.

The surface of thrombin or TRAP treated cells were chemically labeled with biotin by incubating the cells with sulfo-NHS-Biotin (0.5mg/mL in HBS;

Pierce) for 30 minutes at RT. After 3 washes with cold HBS, the cellular proteins were solubilized using Triton X-100 lysis buffer (40 mM TRIS, 150 mM NaCl, 3% Triton X-100, 1 mM EGTA, and 0.2 mM phenylmethylsulfonyl fluoride).

Surface proteins were isolated by incubation with avidin-conjugated Sepharose beads (Sigma) overnight at 4°C. After 3 washes with Triton X-100 lysis buffer, the surface proteins bound to the beads were released by the addition of Laemmli sample buffer containing 12.5 mg/mL DTT, and boiling for 2 minutes at 95°C. The affinity-depleted surface proteins were separated by SDS-PAGE on 15% polyacrylamide gels, and A2 was detected by western blotting.

To identify biotinylated p11, solubilized cells were pre-incubated overnight at 4°C with non-immune mouse IgG1 (6.66 μg/mL), followed by a 2 hour incubation with protein A/G Sepharose at RT. After centrifugation, p11 was depleted from clarified supernatants by incubation with anti-p11 (Transduction Laboratories) for 2 hours at RT followed by 2 hours with protein A/G beads. Isotype controls were performed by substituting the anti-p11 antibody with non-immune mIgG1 (6.66 μg/mL). After 3 washes with Triton X-100 lysis buffer, proteins were released from the beads with Laemmli sample buffer containing 12.5 mg/mL DTT, and boiled for 2 minutes at 95°C. The samples were subjected to 15% polyacrylamide SDS-PAGE, transferred to PVDF, and the biotinylated proteins were visualized by probing the membrane with HRP-conjugated avidin (Sigma), followed by ECL chemiluminescent detection. To confirm the identity of the observed bands, the blot was re-probed with anti-p11 IgG1.

2.3.3 Elution of Surface Ca^{2+}-dependent Annexin II.

After treatment with thrombin or TRAP as previously described, HFF and HUVEC were washed twice with HBS, and the calcium dependent surface proteins were eluted by incubation with 20 mM EGTA in HBS for 20 minutes at 37°C. Supernatants were removed, and centrifuged at 13 000 rpm for 2 minutes. 150 μL of the eluted proteins were removed, and denatured by the addition of 4x Laemmli sample buffer with DTT (50 mg/mL), followed by boiling at 95°C for 2 minutes. The samples were then separated by SDS-PAGE on 15% polyacrylamide gels, and the A2 was visualized by western blotting as described previously.

2.3.4 Evaluation of Sub-membranous Annexin II.

HUVEC and HFF were treated with thrombin, TRAP or CMV (as previously described), washed with HBS, and fixed with 4% paraformaldehyde and 0.25% gluteraldehyde. Simultaneous staining for A2 and vimentin was undertaken by incubation with a primary antibody solution containing monoclonal mouse anti-A2 (1.33 μg/mL) and polyclonal goat anti-vimentin ([protein]=0.195 mg/mL). To control for staining specificity, isotype controls were incubated with a non-immune antibody solution containing mIgG2a (1.33 μg/mL) and goat serum ([protein]=0.71 mg/mL). After 3 PBS washes, the primary antibodies were detected with Cy^3-conjugated donkey anti-mouse IgG (0.125 μg/mL) and FITC-conjugated rabbit anti-goat IgG (1.66 μg/mL). The nuclei were then stained with

25 ng/mL DAPI (for thrombin and TRAP treated cells), and the cells were mounted and visualized as described in 2.1.2.

2.4 PLASMINOGEN BINDING AND ACTIVATION

2.4.1 Examination of S741C-Fluorescein Plasminogen Binding by Fluorescence Microscopy.

Thrombin and TRAP treated HUVEC were washed with HBS/BSA, and incubated with 150 nM S741C-Fluorescein plasminogen (F-Plg) for 30 minutes at 37°C in the dark. After 3 HBS/BSA washes, the cells were fixed with 4% paraformaldehyde and 0.25% gluteraldehyde in HBS. The nuclear DNA was the stained with DAPI (25 ng/mL), and the cells were mounted and visualized as described in section 2.1.2.

In the case of antibody inhibition experiments both the recovery media and the F-Plg solutions contained either polyclonal rabbit anti-p11 antibody or non-immune rabbit IgG, at a concentration of 100 nM.

2.4.2 Western Blot Analysis of S741C-Biotin Plasminogen Binding.

After washing once with HBS/BSA, S741C-Biotin plasminogen binding to the surface of thrombin or TRAP treated cells was evaluated by incubating the cells with 150 nM S741C-Biotin plasminogen in HBS/BSA for 30 minutes at 37°C. After 3 HBS/BSA washes, the cells were lysed by the addition of sample buffer with DTT (12.5 mg/mL), followed by boiling at 95°C for 2 minutes. The proteins were separated by SDS-PAGE on 10% polyacrylamide gels, and transferred to

PVDF membranes. Biotinylated proteins were observed by probing the membrane with HRP-avidin followed by detection with chemilumminescence. To ascertain that equivalent amounts of cells were loaded in each lane, an actin blot was performed on the membranes, as described previously.

In the case of the unlabeled Glu-plasminogen and ε-ACA inhibition experiments the S741C-Biotin plasminogen solution contained either 1.5 μM Glu-plasminogen or 3mM ε-ACA.

2.4.3 Observation of Plasminogen Activation by Chromogenic Assay.

HUVEC grown to confluence in 48 well culture plates were treated with 8nM thrombin and 10 μM TRAP as described previously, and were allowed to recover in IMDM* for 30 minutes at 37°C. After the recovery period, the cells were incubated with 5 nM recombinant tPA in HBS/BSA for 20 minutes at 37°C with occasional shaking. 150 μM Glu- or Lys-plasminogen was then added to the reaction mixture, and 15 μL aliquots were removed at various time points, added to 80 μL of S2251 chromogenic substrate (500 μM), and the amount of plasmin generated was measured by reading the absorbance at 405 nM. To control for cellular tPA production or the presence of plasminogen in the culture media, the experiment was repeated omitting the tPA, the plasminogen, or both. To ensure that the activity observed was plasmin dependent, the experiment was also performed with aprotinin (100 Kiu) present in the tPA solution.

A plasmin standard curve was completed by incubating 15 μL of Lys-plasmin, at concentrations from 10 nM to 300 nM, with 80 μL S2251 (500 μM) and reading the absorbance at 405 nM.

3. RESULTS

3.1 IDENTIFICATION OF ISOLATED CELLS AS HUMAN UMBILICAL VEIN ENDOTHELIAL CELLS.

3.1.1 von Willebrand Factor Staining of Isolated Cells.

von Willebrand Factor (vWF) is a 260 kDa protein produced specifically in endothelial cells and megakaryocytes (226). Once vWF has been synthesized, it is either secreted directly into plasma and the subendothelium or stored in in specialized endothelial cell compartments called Weibel-Palade bodies (226). Thus, the vWF-staining pattern of endothelial cells should appear punctate in nature. Because vWF is expressed in endothelial cells, but is absent from contaminating cells obtained during the HUVEC isolation procedure, such as smooth muscle cells or fibroblasts (225-227), immunofluorescence microscopy staining for vWF was undertaken to demonstrate that the cells isolated from the human umbilical veins were of endothelial origin (Figure 9, Panel A). To ensure that the vWF staining we observed was specific for the anti-vWF antibody, we repeated the experiment omitting the primary antibody (Panel A: frame b). This specificity control was void of staining, thereby indicating that the vWF staining observed was specific, and not due to interactions between the secondary antibodies and the cells. Panel A, frame a, shows the vWF factor distribution in the isolated cells. The punctate staining pattern observed is characteristic of vWF staining of endothelial cells, indicating that our cells are positive for vWF. Staining the nuclei with DAPI (Panel A: frames a',b') was used to determine the proportion of cells in Panel A were positive for vWF. As observed in Panel A, a

Figure 9: Identification of Endothelial Cells by Immunofluorescence Microscopy and Morphological Observation. Isolated cells grown to confluence on gelatin coated coverslips were simultaneously fixed and permeabilized with 4% paraformaldehyde, 0.25% gluteraldehyde, and 0.2% TritionX-100. Cells were subsequently incubated with rabbit anti-von Willebrand Factor antibody in PBS (Panel A: frame a), or as a negative control PBS alone (Panel A: frame b), for 1 hour at RT. After 3 PBS washes, the primary antibody was detected by treating the cells with FITC-conjugated goat anti-rabbit IgG at RT for 1 hour. The nuclear DNA was then stained with DAPI (Panel A: frame a',b'), the washing steps were repeated, and the cells were mounted and visualized using a Zeiss Axioplan2 epifluorescent microscope. Exposure times were controlled using Northern Eclispe software (Empix). Panel B shows a typical phase-contrast micrographs of the isolated cells at low (frame a) and high (frame a') magnification.

A

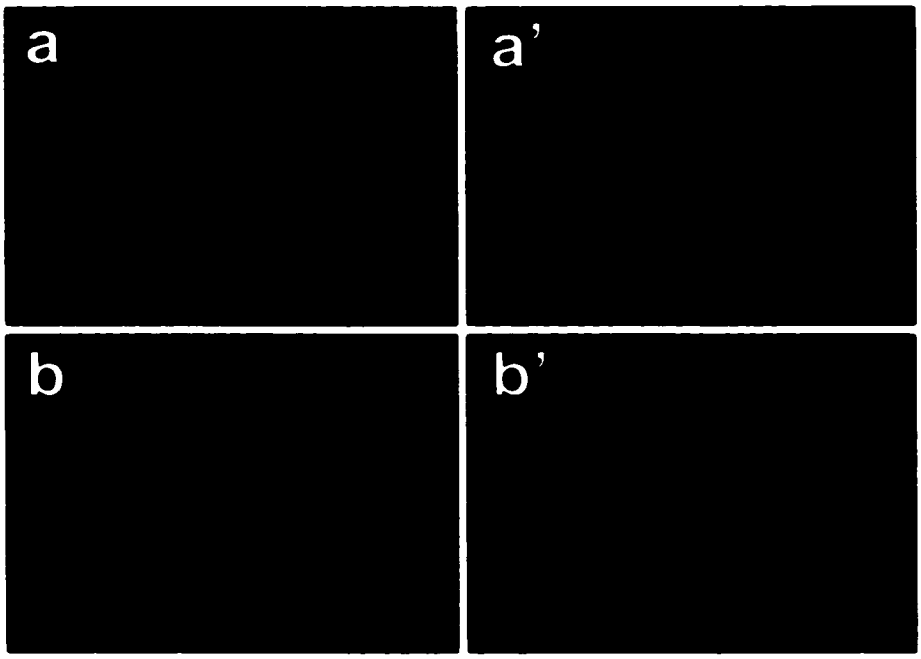

B

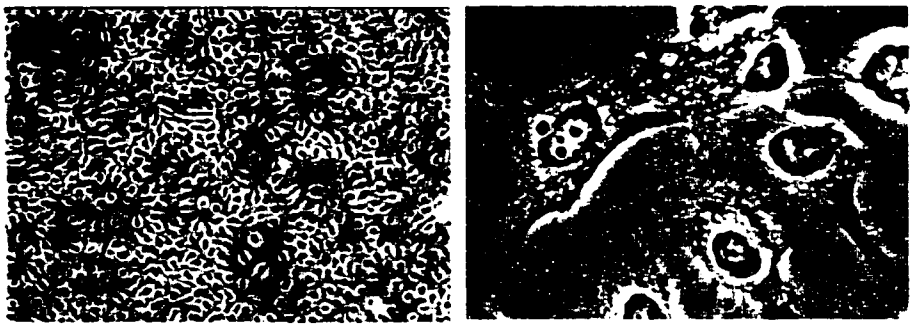

comparison of the DAPI and vWF staining patterns demonstrated that all cells stained positively for vWF.

3.1.2 Phase-contrast Observation of Isolated Cells.

Morphological analysis of the isolated cells by phase-contrast microscopy was used to corroborate the immunofluorescence data (Figure 9, Panel B). Endothelial cells derived from umbilical veins can be easily distinguished from contaminant smooth muscle cells and fibroblasts cells based upon morphological criteria. Examination of cultured HUVEC revealed that they form confluent monolayers void of whorling patterns, while inspection of the cellular morphology demonstrated that the cells were polygonal in shape with indistinct borders and a centrally located nucleus with prominent nucleoli (225;227). The morphology of possible contaminants, fibroblasts and smooth muscle cells, was also studied. Analysis of cultured fibroblasts demonstrated that they form confluent monolayers with overlapping layers and visible whorling patterns (225). Observation of individual fibroblasts revealed that they were long and slender. Smooth muscle cells had a similar phenotype to fibroblasts, but did not demonstrate whorling.

Knowing the morphology of candidate contaminating cells in HUVEC cultures, we used phase contrast analysis of monolayers at low and high magnification, to determine if the isolated cells were endothelial in nature. In Panel B typical phase-contrast micrographs of the isolated cells are shown. Observation of the cellular morphology demonstrated that the isolated cells were

polygonal with a centrally located nucleus containing prominent nucleoli, which are physical characteristics consistent with those observed for endothelial cells (Panel B: frame a'). Additionally, examination of our cells at low magnification determined that they formed confluent monolayers without overlapping layers or whorling (Panel B: frame a), a phenotype typical of endothelial cells.

Therefore, when combined with the immunofluorescence microscopy, these data allow us to conclude that the cells isolated from the human umbilical veins were of endothelial origin.

3.2 EFFECT OF THROMBIN OR TRAP ON SURFACE ANNEXIN II AND P11.

3.2.1 Surface Annexin II and p11 Levels are Up-regulated by Thrombin or TRAP Stimulation of Human Umbilical Vein Endothelial Cells.

3.2.1.1 Surveillance of Cell Surface Annexin II by Immunofluorescence.

The effect of thrombin and TRAP on the cellular distribution of A2 and p11 was studied in endothelial cells, specifically endothelial cells derived from umbilical veins (HUVEC). Endothelial cells were chosen because they line the bloodstream, and are therefore exposed to thrombin when tissue injury and blood clot formation occur. In addition, the ability of endothelial cells to participate in various hemostatic functions increases their relevance in the study of the effect of thrombin on A2 function in fibrinolysis. Thus, HUVEC cells were chosen as our first cell model.

Figure 10: Isotype Controls for Surface A2 and Vimentin Staining in HUVEC and HFF. HUVEC (Panel A) and HFF (Panel B) were treated with 8 nM thrombin, 10 μM TRAP or mock treated. The cells were the incubated with a non-immune primary antibody solution containing mouse IgG2a and goat serum, washed 3 times with media, and placed in a secondary antibody solution containing Cy^3-conjugated donkey anti-mouse IgG and FITC-conjugated rabbit anti-goat IgG antibodies. The cells were then fixed with 4% paraformaldehyde, and the nuclei were stained with DAPI. The washing steps were repeated, and the cells were mounted and visualized as described in Figure 9. The goat serum and DAPI staining patterns are presented in an overlayed image.

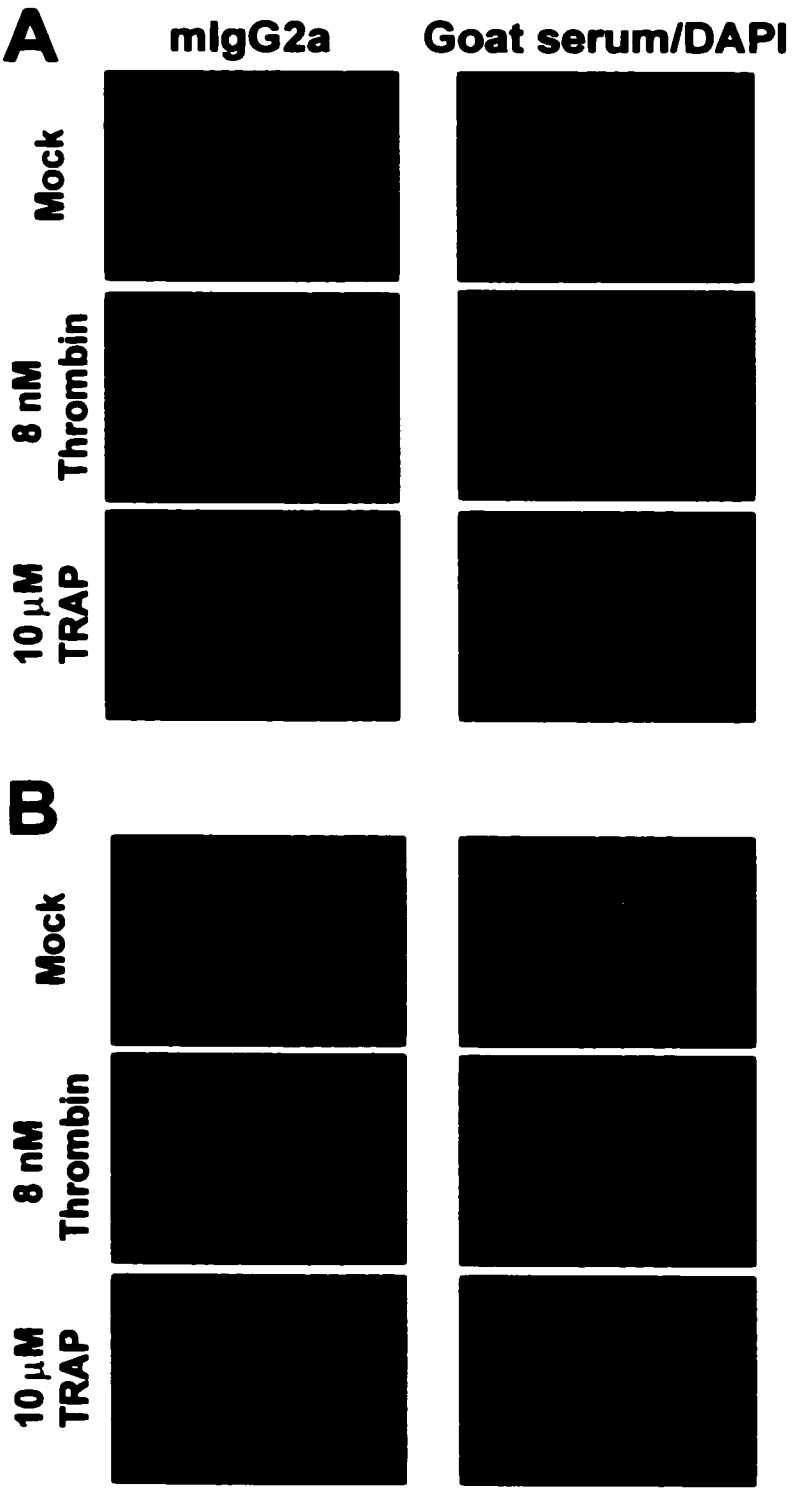
A
mIgG2a
Goat serum/DAPI
Mock
8 nM Thrombin
10 μM TRAP
B
Mock
8 nM Thrombin
10 μM TRAP

To determine if thrombin- or TRAP-mediated stimulation of cells could induce the expression of surface A2, the effect of thrombin or TRAP on surface A2 was evaluated by two-color immunofluorescence microscopy staining of A2 and vimentin in live, unfixed HUVEC, followed by staining of the genetic material in the nuclei with DAPI.

To ensure that our experimental system was appropriate, we performed isotype controls substituting our primary antibodies for non-immune mouse IgG2a and goat serum (Figure 10: Panel A for HUVEC, Panel B for HFF). These isotype controls allowed us to test for staining specificity and ensured that our antibodies were not interacting with the cell surface independently of the antigen-binding region. These isotype controls were negative, thus confirming that all the A2, p11 and vimentin staining observed was specifically antibody-antigen mediated. In addition, the isotype controls also demonstrated that thrombin and TRAP treatment of cells did not affect the non-specific interactions between the cell surface and the primary or secondary antibodies.

To ensure that inadvertent permeabilization did not occur during the staining procedure, the cells were double stained for vimentin, an intermediate filament of the cytoskeleton (Figure 11, for thrombin treatment; Figure 12 for TRAP treatment). The vimentin staining patterns were void of the characteristic spindles seen in permeabilized cells (see Figure 23), demonstrating that the cells being studied were not permeabilized. By this criterion, any A2 staining observed was due solely to the accessible surface pool. Staining of the genetic material in the nuclei with DAPI was also undertaken to determine the number of

Figure 11: Immunofluorescence Microscopy analysis of Surface A2 in Thrombin Treated HUVEC. HUVEC treated with 0.8 to 8 nM thrombin or mock treated were stained for surface A2 and vimentin (Vim) by incubation with monoclonal anti-A2 and polyclonal goat anti-vimentin antibodies, followed by washes with media. The cells were subsequently placed in a secondary antibody solution containing Cy^3-conjugated donkey anti-mouse IgG and FITC-conjugated rabbit anti-goat IgG. After a second round of washing, the cells were fixed with 4% paraformaldehyde and 0.25% gluteraldehyde, the nuclear DNA was stained with DAPI, and the cells were visualized as described in Figure 9. Overlay images of the vimentin and DAPI are shown.

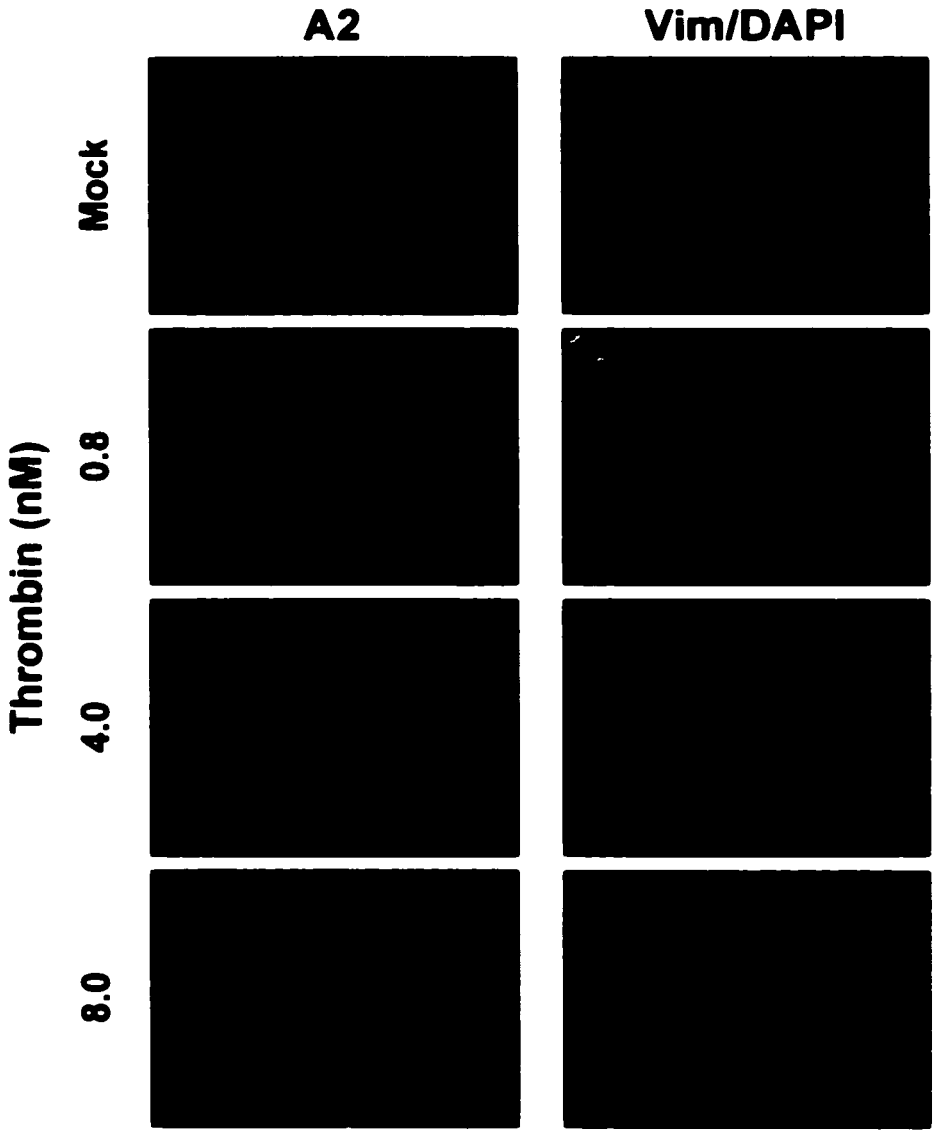
A2
Vim/DAPI
Thrombin (nM)
Mock
0.8
4.0
8.0

Figure 12: Analysis of Surface A2 in TRAP Treated HUVEC by Immunofluorescence Microscopy. HUVEC treated with 0.1 to 1 μM TRAP or mock treated were stained for surface A2, surface vimentin (Vim) and DAPI as described in Figure 11. The DAPI and vimentin staining patters are shown as an overlay image.

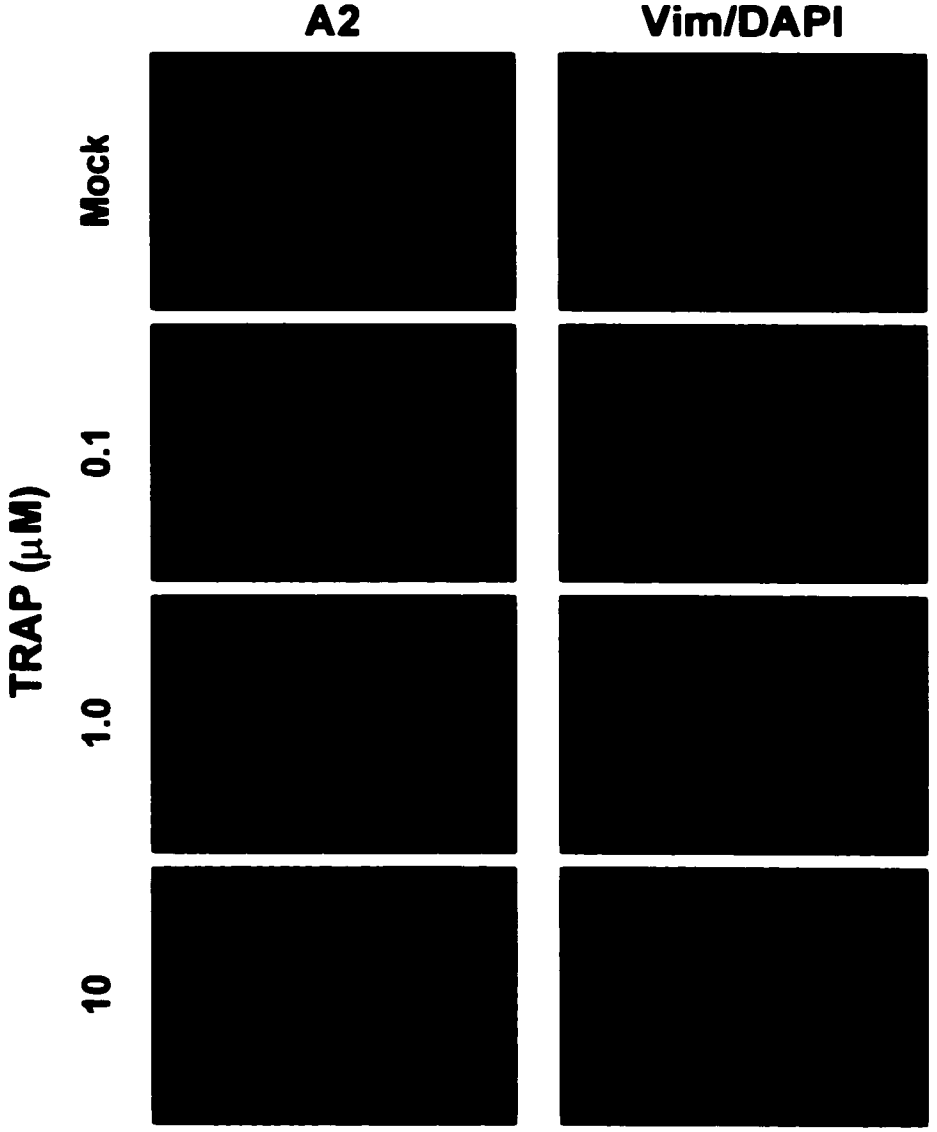
A2
Vim/DAPI
TRAP (μM)
Mock
0.1
1.0
10

cells in each field (Figure 11, for thrombin treatment; Figure 12 for TRAP treatment). This allowed us to easily ascertain that equivalent numbers of cells were being in each field.

The immunofluorescence microscopy experiments revealed that A2 staining levels were elevated in cells treated with 0.8 to 8 nM thrombin (Figure 11) or 1 to 10 μM TRAP (Figure 12) compared to those observed for mock treated cells (Figures 11 for thrombin treatment; Figure 12 for TRAP treatment). These increases in the exposure of the A2 epitope on the cell surface appeared to be dose dependent with increasing thrombin or TRAP concentrations.

3.2.1.2 Analysis of Extracellular Annexin II and p11 by Chemical Modification of the Cell Surface.

Initially, we attempted to visualize surface proteins by staining the surface of cells after fixation in the absence of detergent. However, when cells were fixed prior to staining, a small amount of vimentin and actin staining (data not shown) was observed. Thus, to ensure the exclusive detection of cell surface antigens, the antibody incubations were performed on live unfixed cells. Unfortunately, all available anti-p11 antibodies were unable to detect p11 unless prior fixation was performed (data not shown). Therefore, surface p11 was detected by chemically modifying the surface of live cells, with a hydrophilic biotin derivative, which is incapable of crossing the plasma membrane.

The effect of thrombin or TRAP on surface A2 was further as evaluated by biotinylation of the cell surface, followed by affinity-depletion of biotinylated

Figure 13: Effect of Thrombin or TRAP on Surface A2 and p11 in HUVEC as Observed by Cell Surface Labeling with Biotin. In Panel A, the surface proteins of HUVEC treated with 8 nM thrombin, 10 μM TRAP or mock treated were labeled with biotin. The surface A2 was then affinity-depleted with avidin-Sepharose beads, separated on a 15% polyacrylamide gel by SDS-PAGE, transferred to PVDF, and probed with a monoclonal anti-A2 antibody. The surface p11 was immuno-depleted by treating the sample with monoclonal anti-p11 antibody, followed by incubation with protein A/G-Sepharose beads. The biotinylated surface p11 was separated by SDS-PAGE on 15% polyacrylamide gels, transferred to PVDF, and the membranes were probed with HRP-avidin. Lane 1 in Panel A represents a purified protein control visualized by western blotting for A2 or p11. In Panel B, quantification of film exposures of the western blots using Northern Eclipse software (Empix) is shown (black bar: A2, gray bar: p11; n=3, treated cells are significantly different from non-treated cells at $*p<0.01$ or $\blacklozenge p<0.05$).

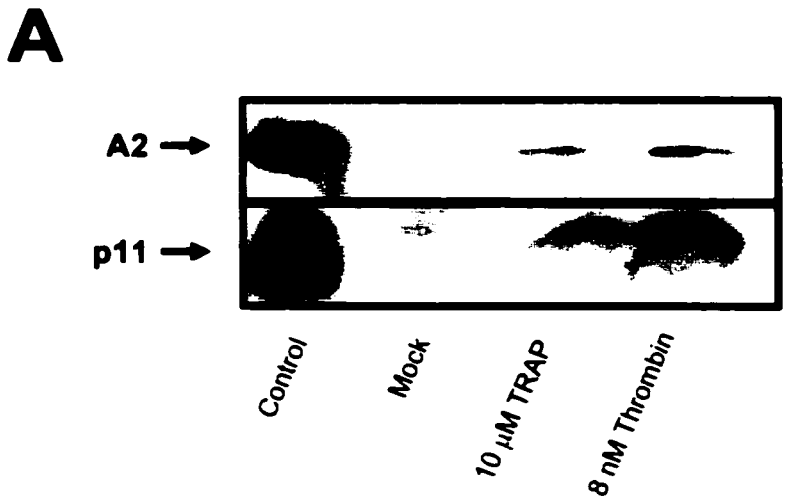
A
A2
p11
Control
Mock
10 μM TRAP
8 nM Thrombin

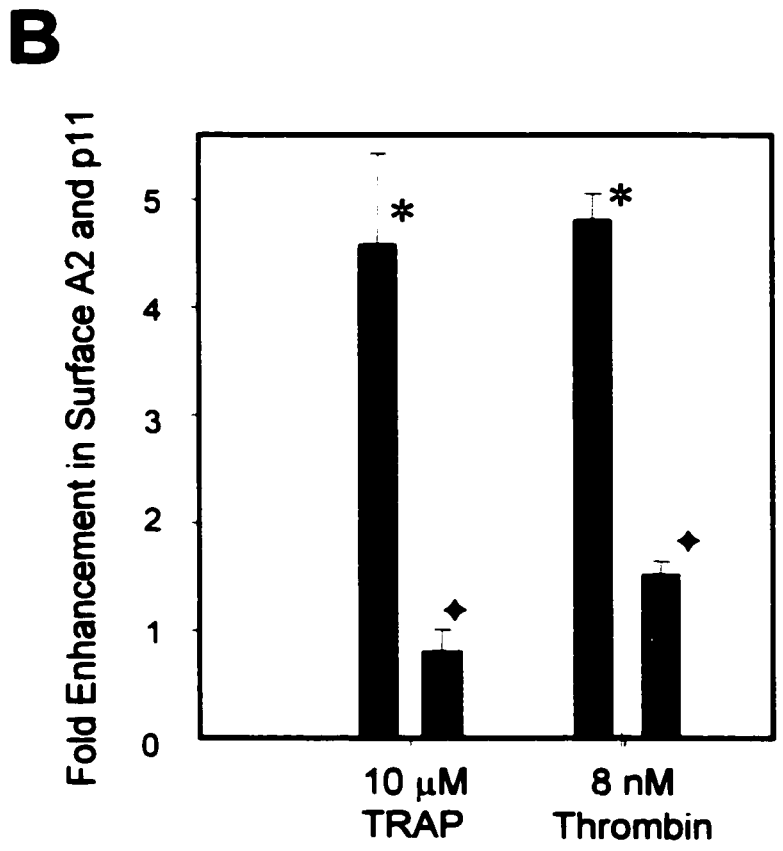
B
Fold Enhancement in Surface A2 and p11
0
1
2
3
4
5
*
*
10 μM TRAP
8 nM Thrombin

surface proteins with avidin-coated Sepharose beads, and visualization by western blot analysis with a monoclonal anti-A2 antibody is shown in Figure 13 (Panel A). Observation of the western blots revealed that HUVEC treated with 8 nM thrombin or 10 μM TRAP had enhanced amounts of surface A2 when compared to mock treated cells. Identification of the bands was performed by comparing the antigenisity and mobility observed to those of a purified A2 positive control .

Western blot analysis for p11 preformed on the surface proteins isolated by affinity-depletion with avidin-Sepharose did not detect any surface p11 (data not shown). Thus, the effect of thrombin and TRAP on surface p11 was evaluated by cell surface biotinylation followed by direct immuno-depletion. Total (surface and intracellular) p11 was isolated from thrombin and TRAP treated HUVEC with anti-p11 IgG, followed by incubation with protein A/G coated-sepharose beads, and was visualized by western blotting with HRP-avidin (Figure 13, Panel A). Western blot analysis demonstrated that 8 nM thrombin and 10 μM TRAP increased surface p11 levels with respect to mock treated cells. To confirm the identity of the observed p11 bands, the membranes were re-probed with an anti-p11 antibody (purified p11 positive control shown in Panel A lane 1). As a control for specificity the immuno-depletion was conducted in the presence of non-immune mouse IgG1 antibody (data not shown). These isotype controls were void of observable p11 staining by western blotting with an anti-p11 antibody or HRP-avidin.

Quantification of the surface A2 levels obtained by western blotting, revealed that both thrombin and TRAP increased the amount of surface A2 observed 5-fold compared to mock treated cells (Figure 13, Panel B; $p<0.01$). Surface p11 levels were approximately doubled by TRAP, and increased 1.5-fold by thrombin (Figure 13, Panel B; $p<0.05$). However, the heterogeneous glycosylation of p11 makes the p11 bands observed on western blots quite diffuse. This characteristic makes these bands difficult to quantify with our current software; therefore the quantification of p11 western blots must be considered only an estimate of relative amounts.

3.2.1.3 Examination Ca^{2+}-dependent Surface Annexin II.

To investigate whether Ca^{2+} was required to maintain the interaction between newly exposed A2 and the HUVEC surface, we observed the effect of thrombin or TRAP on the Ca^{2+}-dependent surface A2. Proteins associated with the surface of thrombin or TRAP treated cells Ca^{2+}-dependently were dissociated by chelation of Ca^{2+} with 20 mM EGTA, and were separated by SDS-PAGE, and were subsequently subjected to western blot analysis for A2 (Figure 14, Panel A). We observed that cells treated with 8 nM thrombin or 10 μM had higher levels of eluted A2 than mock treated cells. To exclude the possibility that this observation was simply due to cells becoming more fragile as a consequence of thrombin treatment, cell eluates contained no detectable A2 when washing was conducted in the presence of 3 mM Ca^{2+}. The bands were identified by the

Figure 14: Effect of Thrombin or TRAP on Ca^{2+}-Dependent Surface A2. The Ca^{2+}-dependent surface proteins of HUVEC treated with 8 nM thrombin, 10 μM TRAP or mock treated were eluted with 20 mM EGTA or 3mM Ca^{2+}. Eluted proteins were separated on 15% polyacrylamide gels by SDS-PAGE, transferred to PVDF, and probed with a monoclonal anti-A2 antibody, as observed in Panel A (a). Lane 5 represents a HUVEC lysate used as an A2 positive control. The PVDF membranes were subsequently stained for total protein with Coomassie blue (Panel A, b). Panel B shows the results obtained from quantification of the western blots with Northern Eclipse software (n=3, treated cells are significantly different from non-treated cells at $*p<0.01$).

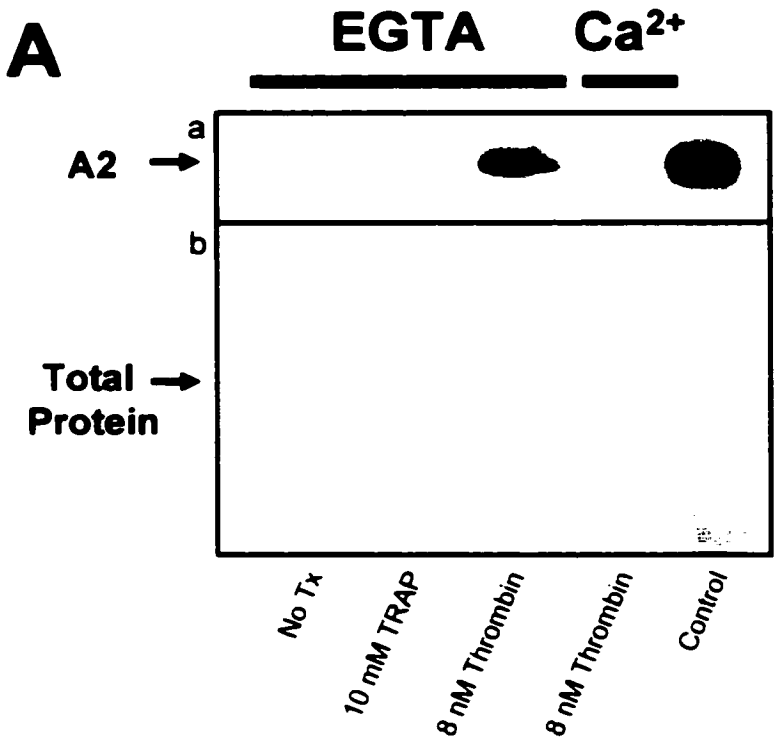
A
EGTA
Ca2+
a
A2
b
Total Protein
No Tx
10 mM TRAP
8 nM Thrombin
8 nM Thrombin
Control

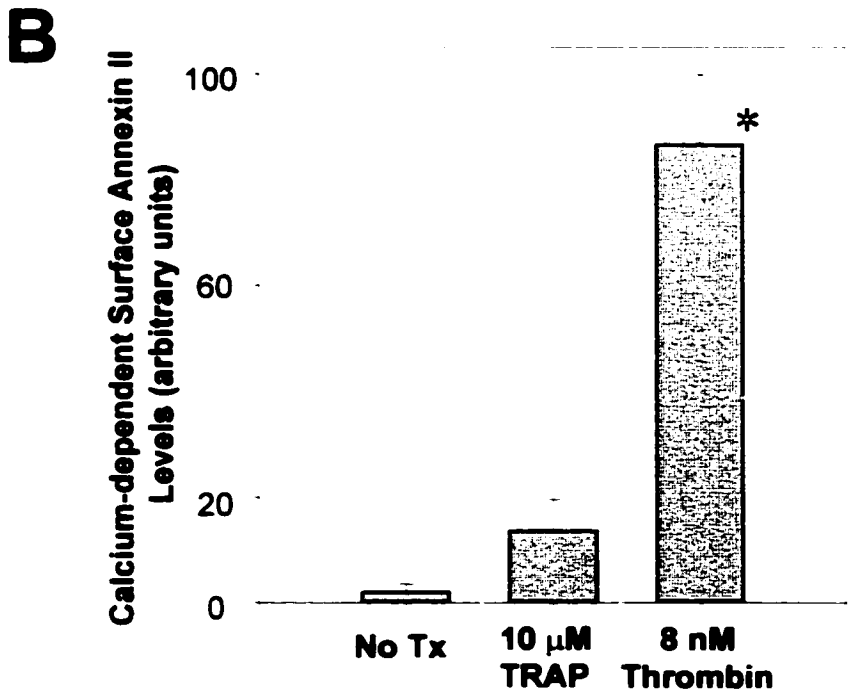
B
Calcium-dependent Surface Annexin II Levels (arbitrary units)
100
60
20
0
*
No Tx
10 μM TRAP
8 nM Thrombin

inclusion of a HUVEC lysate positive control that is known to contain A2 (Panel A, lane 5).

The PVDF membranes were subsequently stained for total protein using Coomassie Blue to control for cell lysis (Figure 14, Panel A). Coomassie Blue staining revealed no detectable bands in the EGTA or Ca^{2+} elution lanes when compared to the cell lysate positive control (Panel A, lane 5), indicating that inadvertent permeabilization did not occur.

In Panel B, quantification and statistical analyses of the western blots are shown. Thrombin treatment lead to an 80-fold enhancement in calcium-dependent A2, while TRAP treatment caused a 4-fold enhancement, both of which were significantly different from mock treated cells at $p<0.01$.

3.2.2 Thrombin or TRAP Treatment of Human Foreskin Fibroblast Cells Induces Cell Surface Annexin II and p11 Exposure.

3.2.2.1 Immunocytological Observation of Surface Annexin II.

HFF cells were chosen as a second cell line to substantiate the results that were obtained for HUVEC. HFF cells are commonly used in laboratory studies of CMV infectivity, and will therefore provide a suitable cell model to study the effect of thrombin on A2 function in CMV infection. Thus, the effect of thrombin or TRAP on the cell surface A2 distribution was evaluated by three-color immunofluorescence microscopy as described in Section 3.2.1.1 for HUVEC.

Figure 15: Immunofluorescence Microscopy Analysis of Surface A2 in Thrombin or TRAP Treated HFF. Confluent HFF monolayers were treated with 8 nM thrombin, 10 μM TRAP or mock treated. After treatment the surface A2 and vimentin (Vim), and the nuclear DNA were visualized by three-color immunofluorescence microscopy as described in Figure 11. The vimentin and DAPI staining patterns are displayed as a merged image.

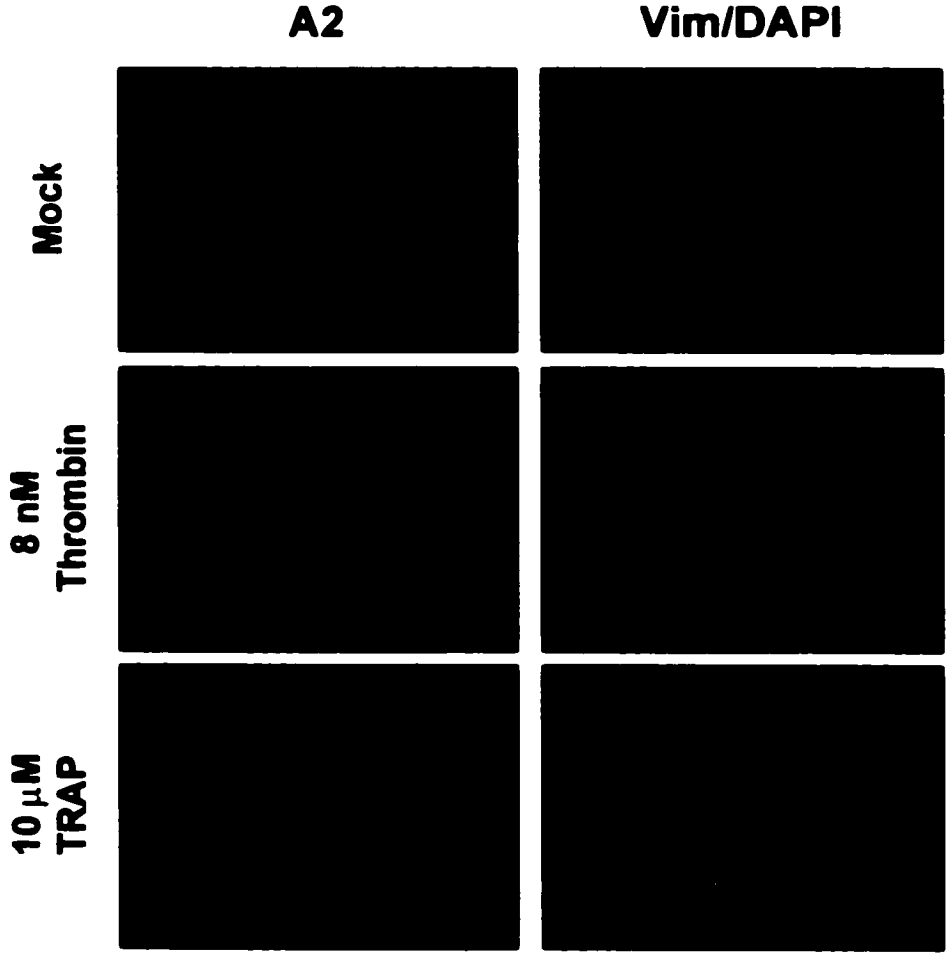
A2
Vim/DAPI
Mock
8 nM Thrombin
10 μM TRAP

As described in Section 3.2.1.1, isotype controls were performed to develop a baseline level for non-specific staining. As observed previously for HUVEC, the isotype controls were negative (Figure 10, Panel B), allowing us to conclude that all staining observed was due to antibody-antigen interactions. Additionally, thrombin and TRAP treatment showed no observable increases in the amount of non-specific staining, demonstrating that thrombin and TRAP did not affect interaction of the primary or secondary antibodies with the cell surface. Similarly, staining for vimentin and nuclear genetic material were performed to control for permeabilization and cell number, as described in Section 3.2.1.1. The vimentin staining patterns, seen in Figure 15, are void of the characteristic spindles representative of permeabilized cells, thereby indicating that the cells observed are not permeabilized, and that the A2 staining observed corresponds to surface A2. In addition, staining of the nuclei with DAPI was performed that similar numbers of cells were being compared in each field.

In Figure 15, surface A2 levels were followed after treatment of HFF cells with thrombin or TRAP. We observed that treatment with 8 nM thrombin or 10 μM TRAP increased the A2 staining intensity with respect to mock treated cells, indicating that thrombin and TRAP treatment of HFF enhanced surface A2 epitope expression levels.

3.2.2.2 Examination of Surface Annexin II and p11 by Cell Surface Biotinylation.

As for HUVEC, staining of live HFF cells prior to fixation with all available anti-p11 antibodies revealed no demonstrable detection of surface p11. Thus,

Figure 16: Effect of Thrombin or TRAP on Surface A2 and p11 in HFF as Determined by Cell Surface Biotinylation. In Panel A, the surface proteins of HFF treated with 8 nM thrombin, 10 μM TRAP or mock treated were biotinylated, and the surface A2 and p11 were visualized as described in Figure 13. Lane 1 in Panel A represents a purified A2 or p11 positive control. Film exposures of the western blots were quantified with Northern Eclipse software (Empix) as shown in Panel B (black bar: A2, gray bar: p11; n=3, treated cells are significantly different from non-treated cells at $*p<0.01$).

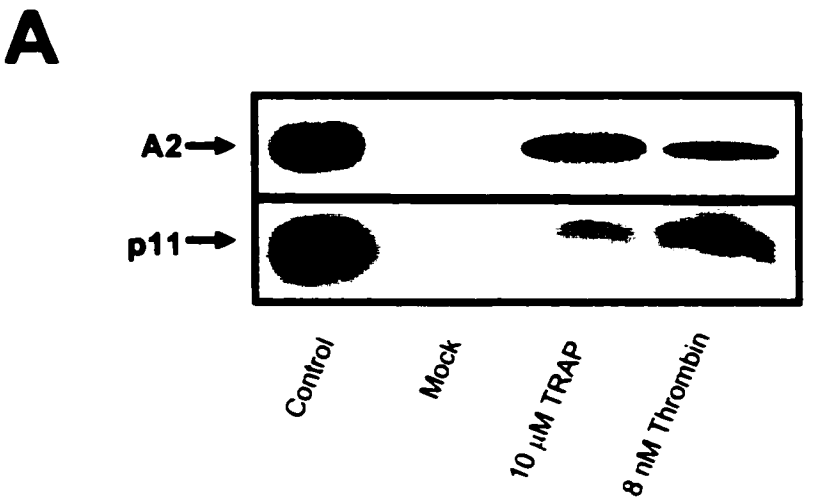
A
A2
p11
Control
Mock
10 μM TRAP
8 nM Thrombin

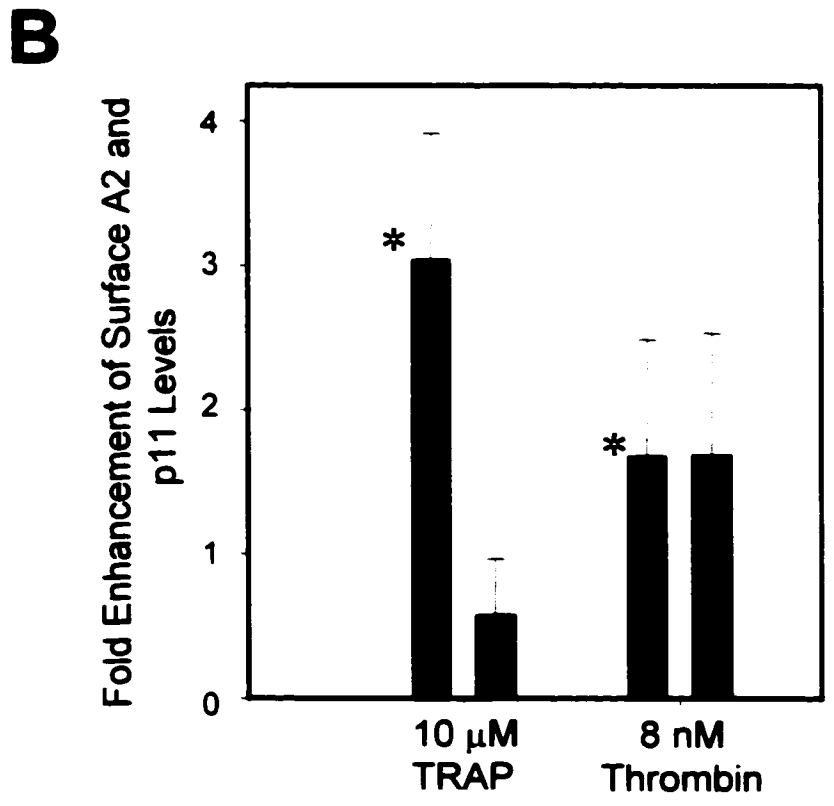
B
Fold Enhancement of Surface A2 and p11 Levels
0
1
2
3
4
*
*
10 μM TRAP
8 nM Thrombin

surface p11 was followed by chemically modifying the cell surface as described for HUVEC. As observed in Figure 16 (Panel A), surface proteins of thrombin- or TRAP-treated HFF were labeled by biotinylation, followed by affinity-depletion of surface A2 with avidin coated Sepharose beads, or immuno-depletion of total p11 with anti-p11 and protein A/G coated Sepharose beads, followed by visualization by western blotting. We observed that compared to mock treated cells , cells treated with 8 nM thrombin, or 10 μM TRAP had enhanced levels of surface A2. Analysis of surface p11 as described in Figure 13, demonstrated that surface p11 was also increased in HFF after thrombin or TRAP treatment with respect to mock treated cells. Re-probing the membrane with anti-p11 IgG (Panel A, lane 1 is a purified p11 positive control) allowed us to confirm that the band visualized in the surface p11 lanes was specific to p11. Immunoprecipitations conducted with mouse IgG1 were void of p11 staining by western blotting (data not shown).

Quantification of the western blots (Figure 16, Panel B) established that thrombin treatment enhanced surface p11 and A2 approximately 1.75-fold. Similarly, quantification of TRAP treated cells confirmed that A2 was increased 3-fold, while p11 levels were enhanced approximately 1-fold ($p<0.01$).

3.2.2.3 Ca^{2+}-Dependent Surface Annexin II.

In Figure 17, the Ca^{2+}-dependence of the interaction of A2 with the HFF surface after treatment with thrombin or TRAP cells was followed by elution of Ca^{2+}-dependent surface proteins with EGTA, as described for HUVEC in Figure

Figure 17: Effect of Thrombin or TRAP on Ca^{2+}-dependent Surface A2 in HFF. In Panel A, A2 associated Ca^{2+}-dependently with the surface of HFF cells treated with 8 nM thrombin, 10 μM TRAP or mock treated was eluted with 20 mM EGTA or 3mM Ca^{2+}, and visualized by SDS-PAGE and western blotting as described in Figure 14 (a: anti-A2 western blot, b: Coomassie blue protein stain). Lane 5 in Panel A represents a HUVEC lysate used as an A2 positive control. Quantification of the western blots using Northern Eclipse software (Empix) is shown in Panel B (n=3, treated cells are significantly different from non-treated cells at ♦ $p<0.01$).

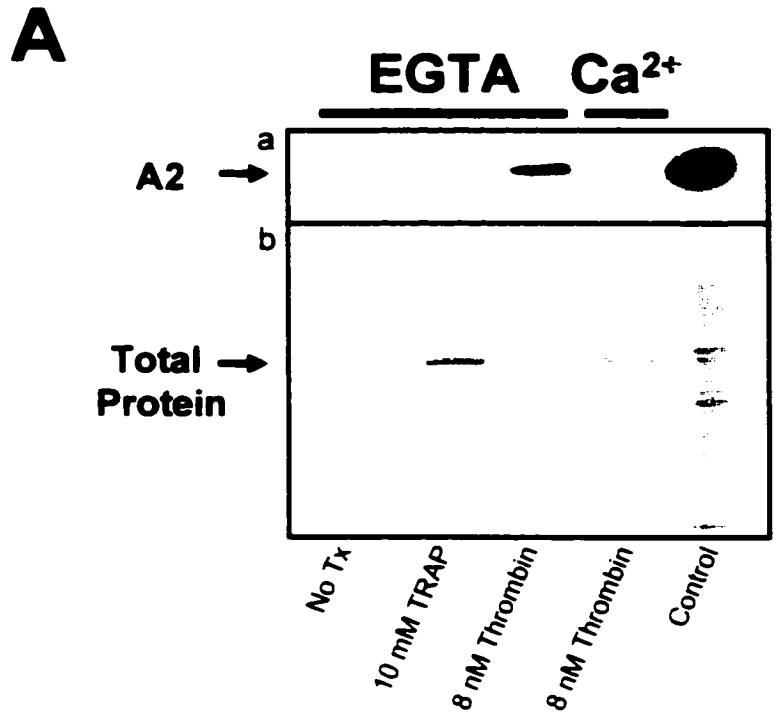
A
EGTA
Ca2+
a
A2
b
Total Protein
No Tx
10 mM TRAP
8 nM Thrombin
8 nM Thrombin
Control

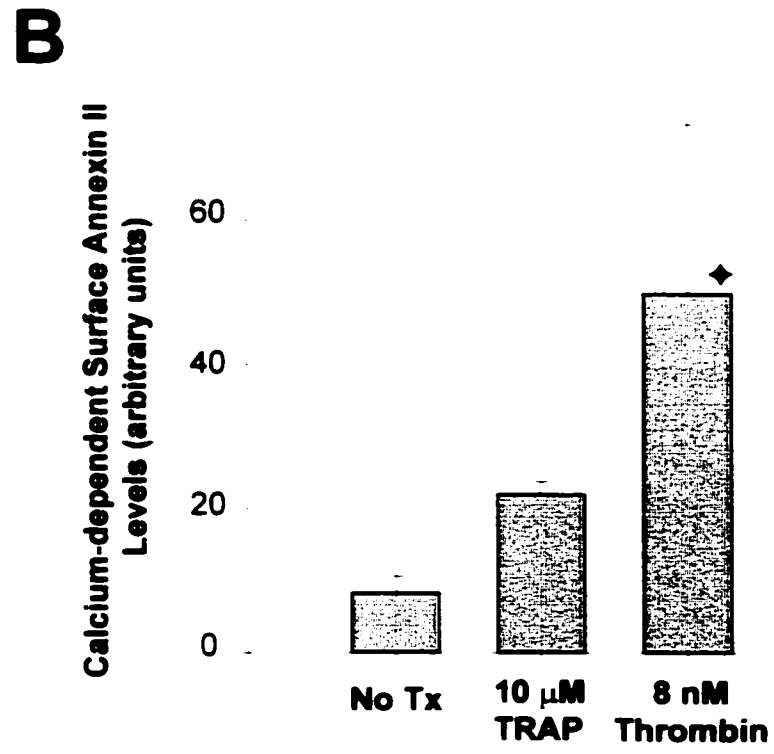
B
Calcium-dependent Surface Annexin II Levels (arbitrary units)
60
40
20
0
No Tx
10 μM TRAP
8 nM Thrombin

14. Western blot analysis of the eluates revealed that HFF treated with 8 nM thrombin or 10 μM TRAP had higher levels of eluted A2 than mock-treated cells. The bands were identified by the inclusion of a HUVEC cell lysate positive control, which is known to contain A2. The absence of A2 in cells eluted with 3 mM Ca^{2+} excluded the possibility that A2 eluted after EGTA treatment was simply due to increased fragility after thrombin or TRAP stimulation. Staining the PVDF membranes with Coomassie Blue was undertaken to visualize the total protein levels in the eluates. The Coomassie blue staining was void of large amounts of protein that would be released by permeabilization of the cells, as was seen in the cell lysate positive control (Panel A, lane 5). This demonstrated that the EGTA step was not causing inadvertent cell rupture to occur.

Quantification of the western blots (Figure 17, Panel B) revealed that calcium dependent surface A2 was enhanced 5.5-fold by thrombin, and 2.5-fold by TRAP. These values were shown to be significantly different from the mock treated cells with $p<0.01$.

3.3 EFFECT OF THROMBIN OR TRAP ON INTRACELLULAR A2 AND p11.

3.3.1 Thrombin- or TRAP-mediated Enhancement of p11 Levels in Human Umbilical Vein Endothelial Cells.

3.3.1.1 Analysis of Intracellular Annexin II and p11 by Immunofluorescence.

To determine if the thrombin- or TRAP-mediated increases in surface A2 and p11 were due to a concomitant rise in intracellular A2 and p11

Figure 18: Isotype Controls for Intracellular p11, A2, and Vimentin Staining of HUVEC and HFF. HUVEC (Panel A) and HFF (Panel B) cells treated with 8 nM thrombin, 10 μM TRAP or mock treated were fixed and permeabilized as described in Figure 9. After fixation the cells were incubated with mouse IgG1 for 1 hour at RT, followed by 3 PBS washes. The non-specific antibody-cell interactions were then detected by the addition of Cy^3-conjugated donkey anti-mouse IgG for 1 hour at RT. The nuclear DNA was then stained with DAPI, followed by 3 PBS washes, and the cells were visualized as described in Figure 9. The photomicrographs show the superimposition of the mIgG1 and DAPI staining patterns.

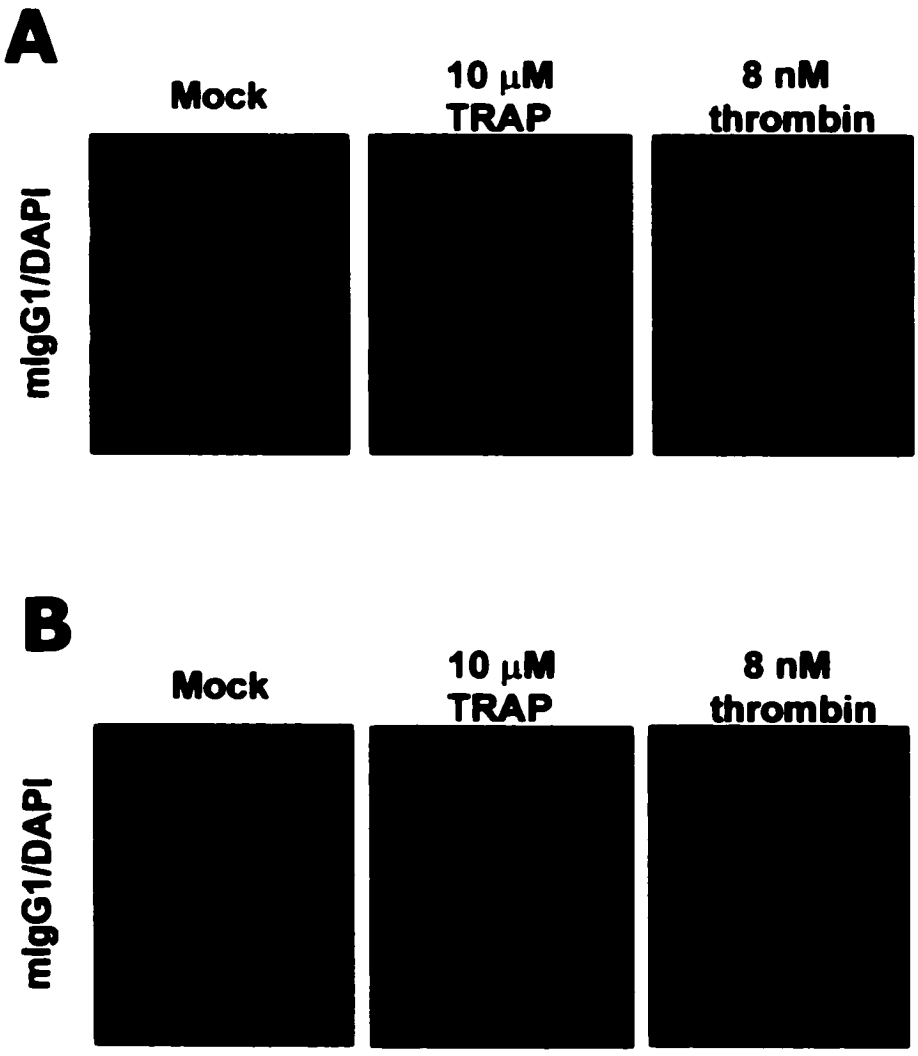
A
Mock
10 μM TRAP
8 nM thrombin
mIgG1/DAPI
B
Mock
10 μM TRAP
8 nM thrombin
mIgG1/DAPI

concentrations, intracellular A2 and p11 were evaluated after thrombin or TRAP treatment.

In order to ascertain that the intracellular A2, p11 and vimentin staining observed was due to antibody-antigen recognition, and not non-specific interactions between the antibodies and the cells, we performed isotype controls by substituting the primary antibodies for non-immune mouse IgG1 (Figure 18, Panel A for HUVEC, Panel B for HFF). These isotype controls were void of staining, thereby demonstrating that all staining observed was specific for A2, p11 and vimentin. Furthermore, it was observed that thrombin or TRAP did not affect non-specific interactions between antibodies and the cells (Figure 18, Panel A for HUVEC, Panel B for HFF).

Identically treated cells were stained for the intermediate filament vimentin, for use as a permeabilization marker (Figure 19). Vimentin staining was undertaken to ensure all cells were equally permeabilized, and that thrombin or TRAP did not affect the level of permeabilization. The vimentin staining patterns observed were equal in intensity and distribution, demonstrating that all cells underwent equivalent levels of permeabilization, and that thrombin or TRAP had no effect of permeabilization. Staining the nuclei with DAPI was used to calculate the number of cells per field for use in quantification (Figure 19).

As shown in Figure 19, the potential effects of 8 nM thrombin (Panel A) or 10 μM TRAP (Panel B) on intracellular A2 and p11 levels were observed by two-color immunofluorescence microscopy. When HUVEC were treated with thrombin or TRAP, the amount of p11 staining was enhanced compared to mock

Figure 19: Effect of Thrombin or TRAP on Intracellular A2 and p11 in HUVEC. HUVEC treated with 8nM thrombin (Panel A), 10 μM TRAP (Panel B) or mock treated (Panel A and Panel B) were fixed and permeabilized as described in Figure 9. Fixation was followed by staining for A2, p11, or vimentin (Vim) by incubating the cells with the corresponding monoclonal antibodies for 1 hour at RT. The cells were subsequently washed 3 times with PBS, and the primary antibodies were detected by treating the cells with Cy^3-conjugated donkey anti-mouse antibody at RT for 1 hour. The nuclear DNA was then stained with DAPI, and the cells were mounted and visualized (as described in Figure 9). The photomicrographs were obtained by superimposing the DAPI images obtained with their corresponding antibody staining patterns.

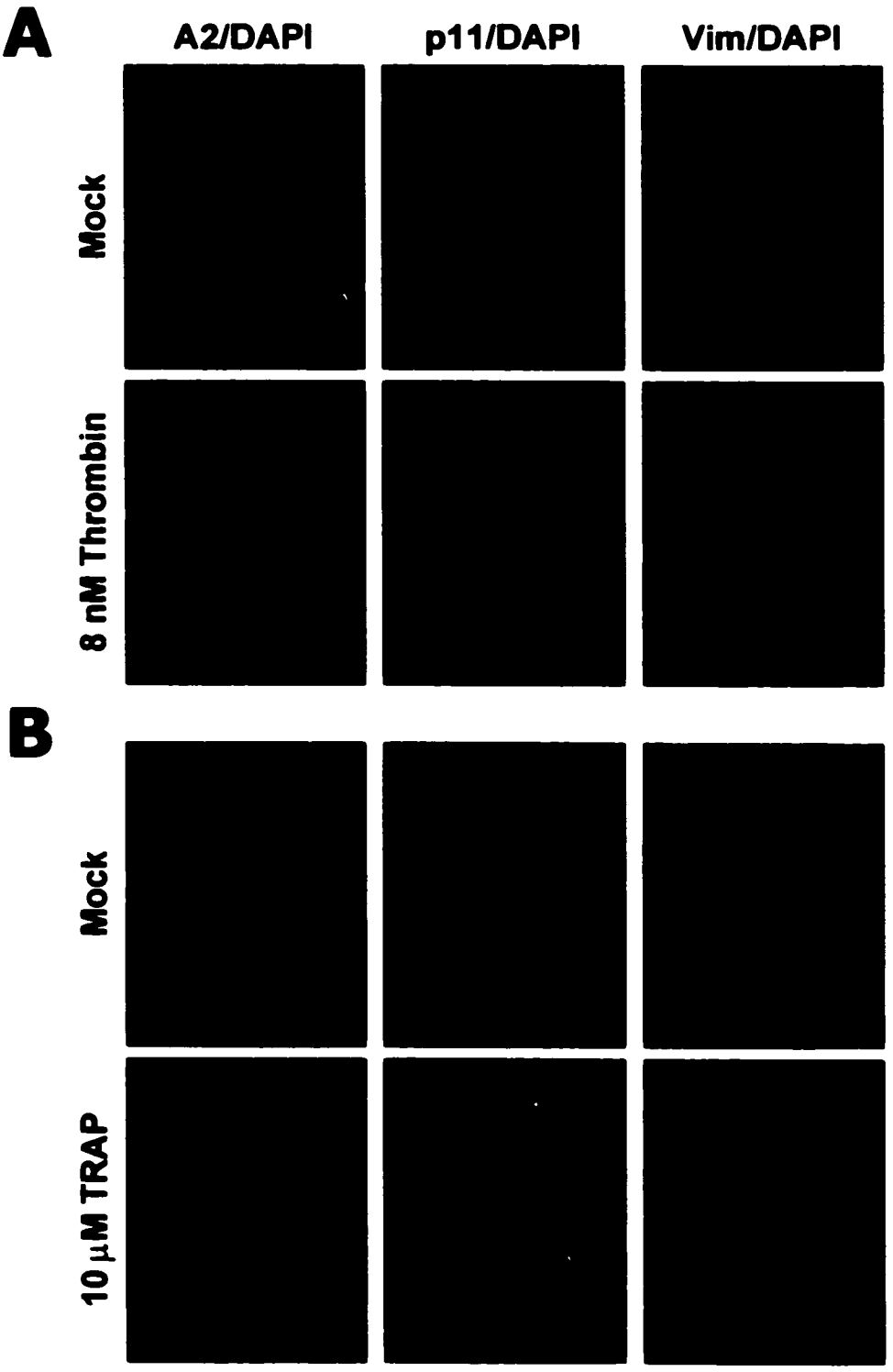
A
A2/DAPI
p11/DAPI
Vim/DAPI
Mock
8 nM Thrombin
B
Mock
10 μM TRAP

Figure 20: Results of Quantification of Immunofluorescence Microscopy of HUVEC. The fluorescence microscopy data was quantified using Northern Eclipse software (Empix). Briefly, the total A2 and p11 fluorescence intensity for each field was calculated (minimum 5 fields per experiment), and the fluorescence intensity/cell was obtained by dividing the total fluorescence intensity by the number of nuclei present in the field (as determined by staining with DAPI). The fluorescence intensity/cell for cells treated with thrombin (Panel A) or TRAP (Panel B) were compared to the levels obtained for the non-treated cells to obtain the fold enhancement/cell of intracellular A2 (∇) and p11 ($\bullet$) levels (n=3, $*$ statistically different from mock treated cells at $p<0.01$).

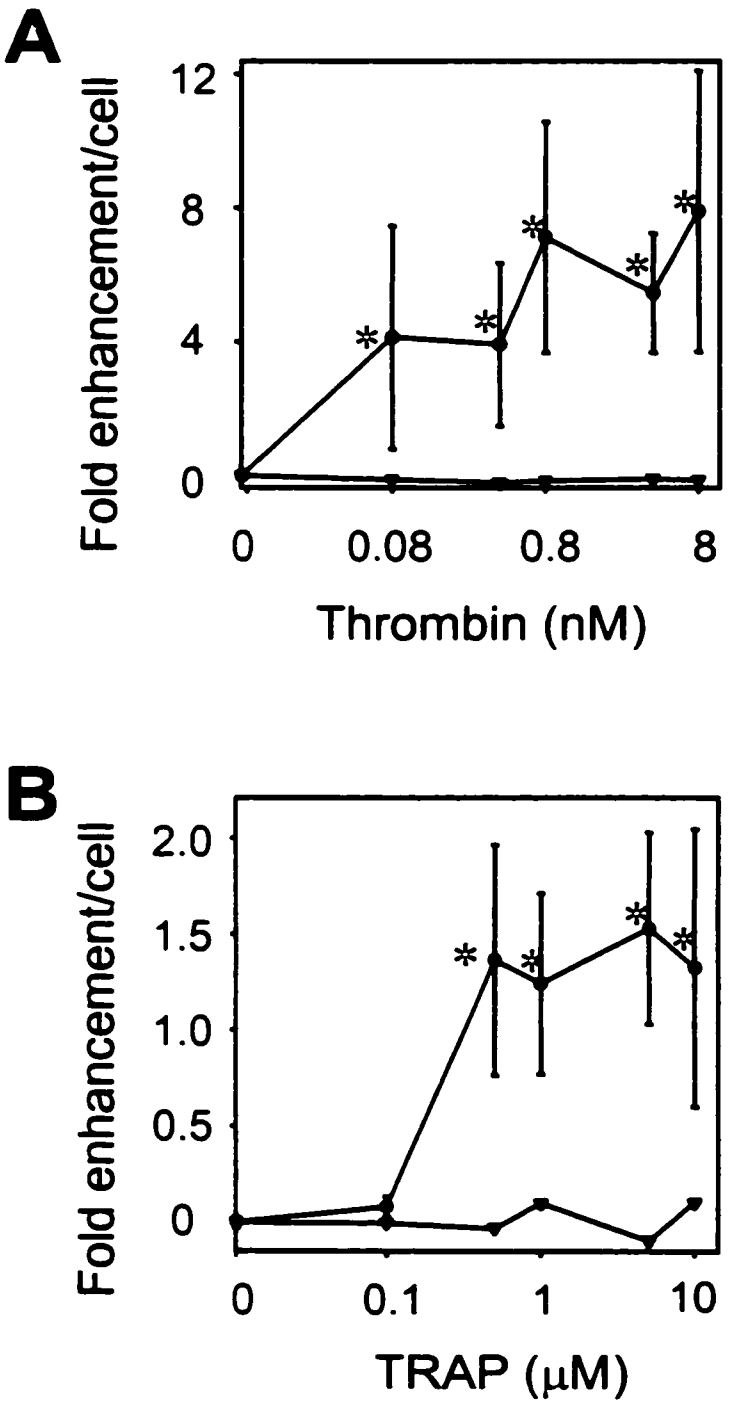
A
Fold enhancement/cell
12
8
4
0
0
0.08
0.8
8
Thrombin (nM)
B
Fold enhancement/cell
2.0
1.5
1.0
0.5
0
0
0.1
1
10
TRAP (μM)

treated cells, while A2 staining levels appeared unchanged. Quantification of fluorescence intensity revealed that over a titration range of 0.8 to 8nM thrombin (Figure 20, Panel A) intracellular p11 levels were enhanced to a maximum of 8-fold/cell, while the 0.1 to 10 μM TRAP titration range (Figure 20, Panel B) led to an approximate 1.5-fold enhancement/cell. In contrast, A2 levels remained constant throughout the thrombin and TRAP titration ranges. Statistical analysis revealed that the p11 levels in thrombin and TRAP treated cells were significantly different from the mock treated cells ($p<0.01$).

3.3.1.2 Antigenic Analysis of Cellular Lysates.

To substantiate the effect of thrombin or TRAP on intracellular A2 or p11 observed by immunofluorescence microscopy, quantitative western blot analysis of A2 and p11 levels in HUVEC treated with 0.8 to 8 nM thrombin (Figure 21, Panel A) or 0.1 to 10 μM TRAP (Figure 21, Panel B) were undertaken. The western blots showed that p11 levels were enhanced with increasing concentrations of thrombin or TRAP, while A2 levels remained unchanged. Identification of the bands was performed by the inclusion of purified protein positive controls (Panels A and B, lane 1). The PVDF membranes were subsequently re-probed for the cytoskeletal protein β-actin. β-actin staining was employed as a loading control, to ensure identical numbers of cells were being loaded in each lane. This loading control allowed us to accurately quantify the levels of A2 and p11 after thrombin or TRAP treatment.

Figure 21: Effect of Thrombin or TRAP on Total A2 or p11 in HUVEC. Confluent HUVEC monolayers were treated with thrombin (Panel A) or TRAP (Panel B). After recovery the cells were lysed with sample buffer containing dithiothreitol (DTT), separated on 15% polyacrylamide gels by SDS-PAGE, transferred to PVDF, and probed with monoclonal anti-A2 or anti-p11 antibodies, followed by HRP-conjugated goat anti-mouse IgG. To ensure equal amounts of sample were loaded in each lane, the membranes were subsequently reprobed with a monoclonal anti-β-actin antibody.

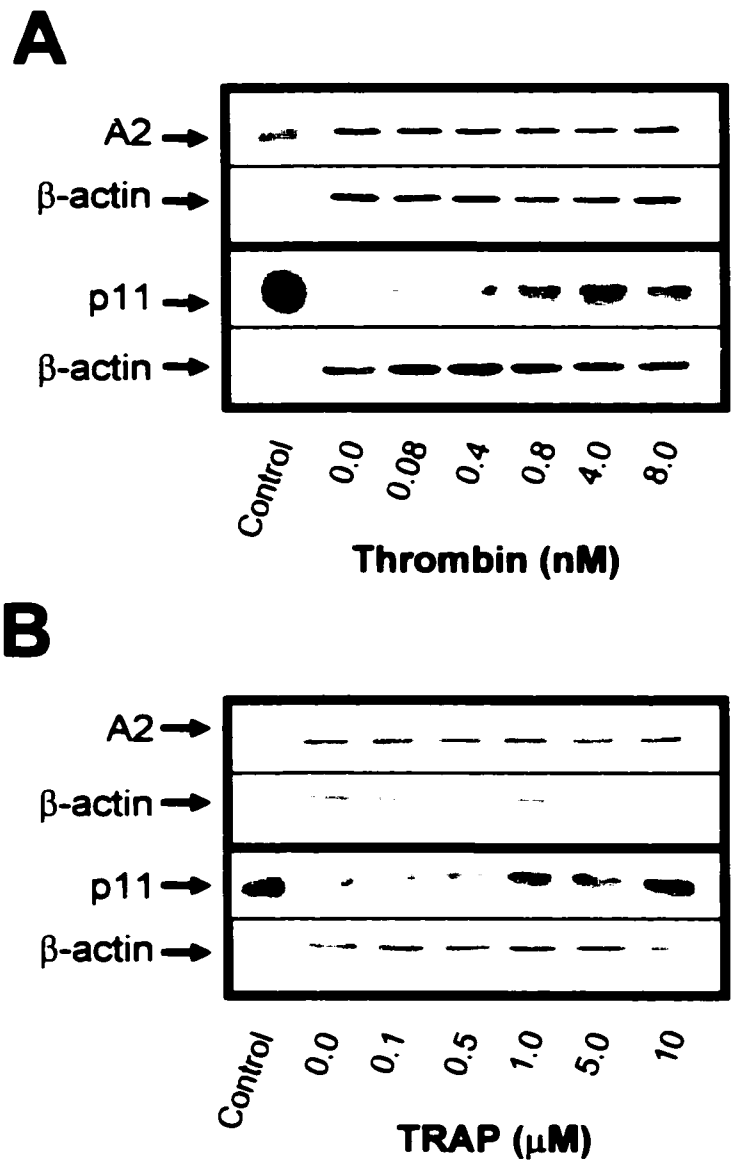
A
A2
β-actin
p11
β-actin
Control
0.0
0.08
0.4
0.8
4.0
8.0
Thrombin (nM)
B
A2
β-actin
p11
β-actin
Control
0.0
0.1
0.5
1.0
5.0
10
TRAP (μM)

Figure 22: Quantification of Western Blot Analysis of HUVEC. The A2 and p11 blots were quantified using Northern Eclipse software (Empix). The A2/actin, and the p11/actin ratios of thrombin (Panel A) and TRAP (Panel B) treated cells were compared to the ratios observed for non-treated cells, to obtain the fold enhancement of A2 (▽) and p11 (•) (n=3, treated cells are significantly different from non-treated cells at ✱$p<0.01$ or ✦$p<0.05$).

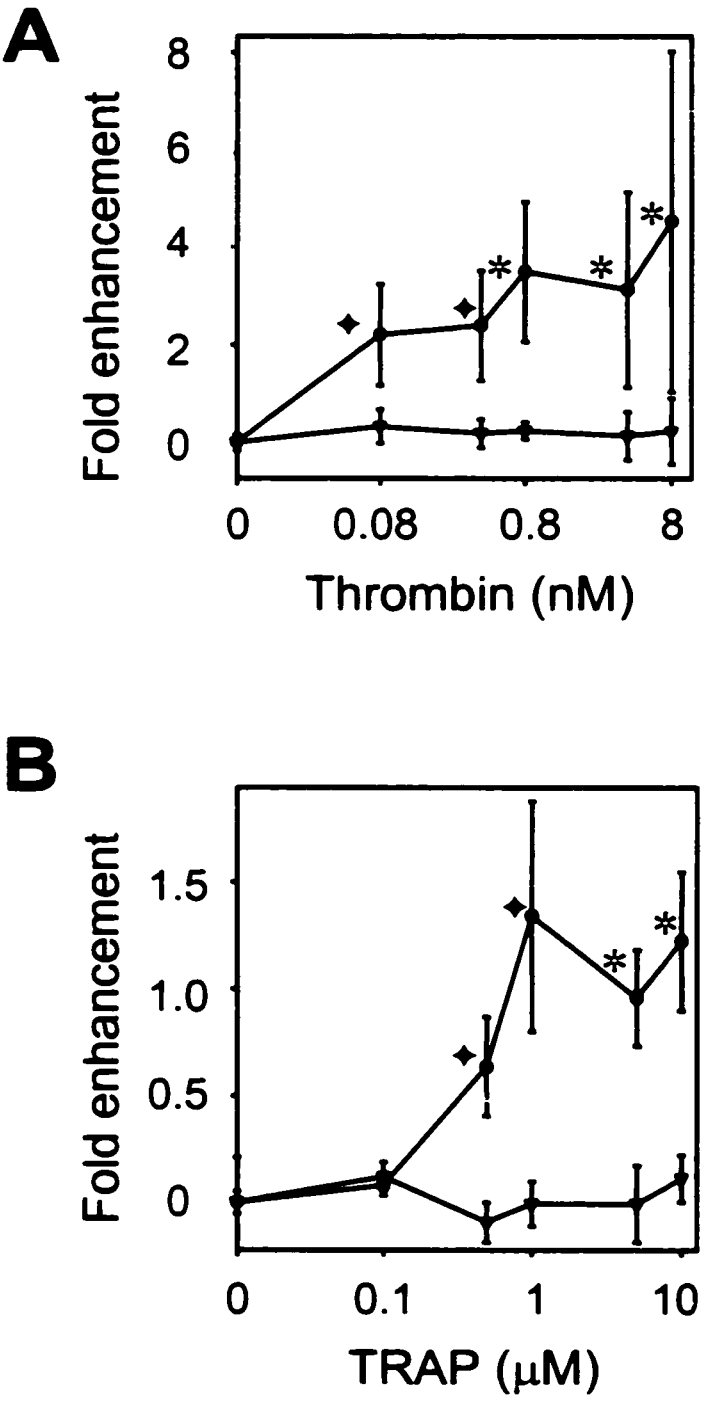
A
Fold enhancement
8
6
4
2
0
0
0.08
0.8
8
Thrombin (nM)
B
Fold enhancement
1.5
1.0
0.5
0
0
0.1
1
10
TRAP (μM)

Quantification of the p11 blots revealed a maximal 4-fold augmentation in the amount of intracellular p11 in thrombin treated cells (Figure 22, Panel A), while TRAP treatment caused an approximate 1.25-fold enhancement (Figure 22, Panel B). Quantification of the A2 blots demonstrated that thrombin and TRAP had no effect on intracellular A2. Subsequent statistical analysis demonstrated that the data obtained was statistically significant (*<0.01 or ♦$p<0.05$).

3.3.2 Up-regulation of Intracellular Annexin II and p11 in Human Foreskin Fibroblasts by Thrombin or TRAP.

3.3.2.1 Observation of Intracellular Annexin II and p11 by Immunocytology.

In order to ascertain the origin of the newly expressed surface A2 and p11, analysis of intracellular A2 and p11 in HFF cells after thrombin or TRAP treatment was undertaken. As described in Section 3.3.1.1 isotype (Figure 18, Panel B) and permeabilization controls (Figure 23, Panels A and B: images) were first performed to ensure that our experimental system was appropriate. The isotype controls were negative, indicating that the A2, p11 and vimentin staining observed was specific. As for HUVEC, we observed that thrombin or TRAP had no effect on non-specific interactions between antibodies and the cells. In addition, vimentin staining was performed to ascertain that all cells received identical levels of permeabilization (Figure 23). The vimentin staining patterns were similar in intensity, signifying that equivalent permeabilization was achieved.

Figure 23: Effect of Thrombin or TRAP on Intracellular A2 and p11 in HFF. HFF grown to 80% confluence on glass coverslips were treated with 8 nM thrombin (Panel A), 10 μM TRAP (Panel B) or mock treated (Panels A and B), and stained for A2, p11, or vimentin (Vim) and DAPI as described in Figure 19. All images are displayed as overlays between the antigenic and the DAPI staining patterns.

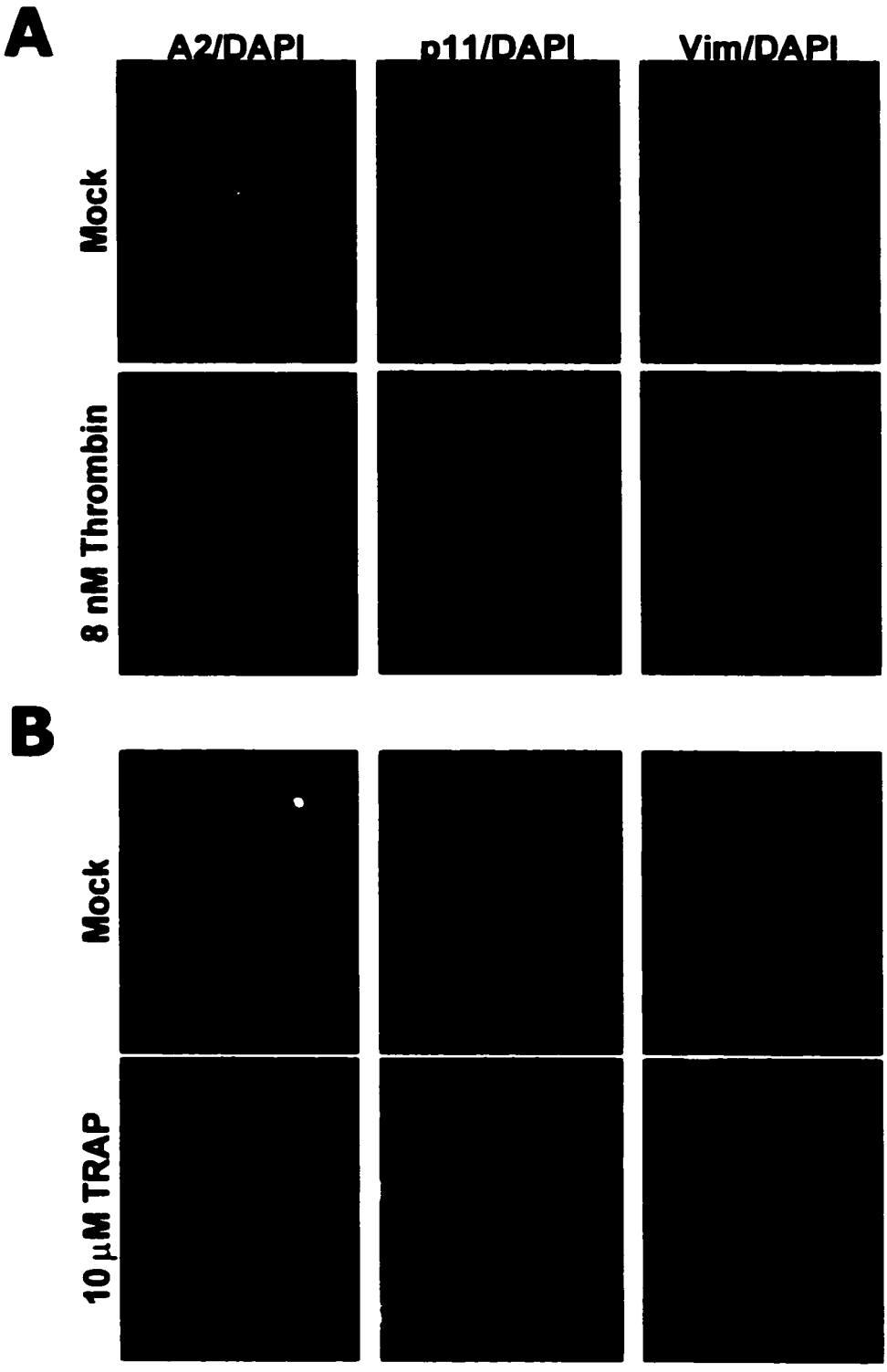
A
A2/DAPI
p11/DAPI
Vim/DAPI
Mock
8 nM Thrombin
B
Mock
10 μM TRAP

Figure 24: Quantification of the Immunofluorescence Analysis of HFF. The fold enhancement/cell of A2 (∇) and p11 ($\bullet$) levels in thrombin (Panel A) and TRAP (Panel B) treated cells were obtained as described in Figure 20 (n=3, treated cells are significantly different from non-treated cells at $*p<0.01$).

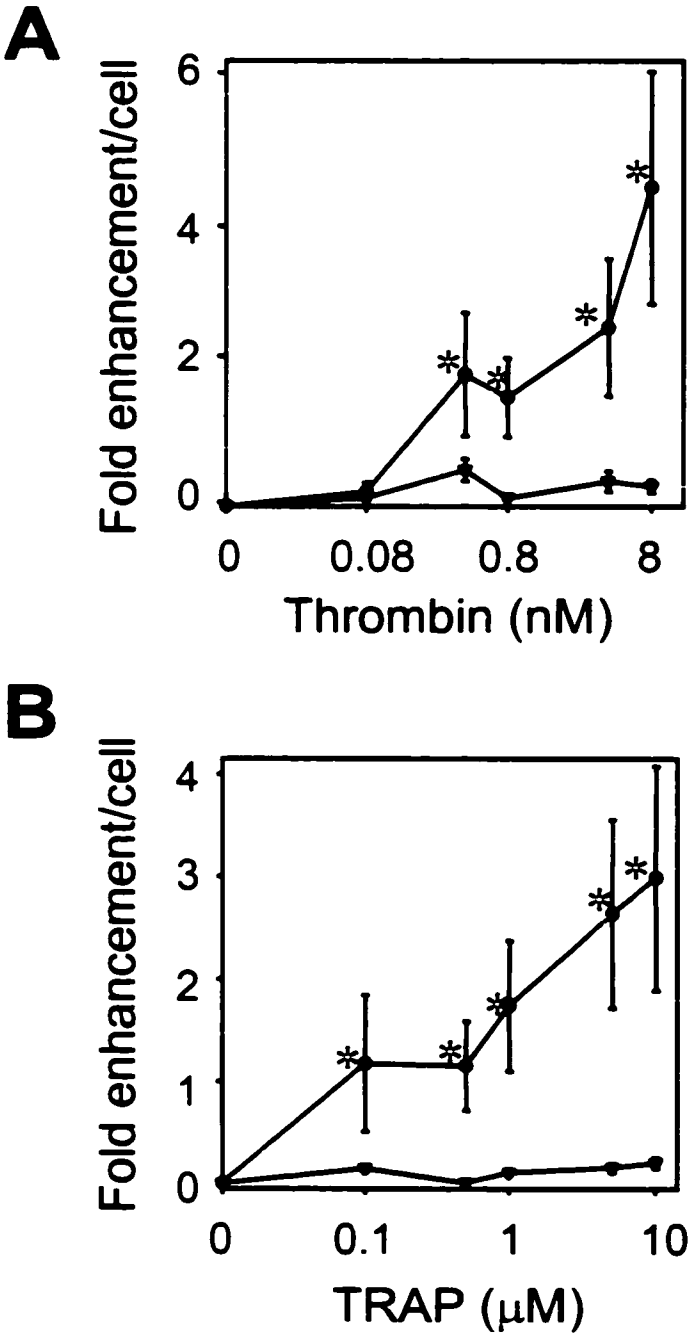
A
Fold enhancement/cell
6
4
2
0
0
0.08
0.8
8
Thrombin (nM)
B
Fold enhancement/cell
4
3
2
1
0
0
0.1
1
10
TRAP (μM)

In Figure 23 the effect of thrombin (Panel A) or TRAP (Panel B) on intracellular A2 and p11 was followed by immunofluorescence microscopy as described previously. Stimulation of HFF with 8 nM thrombin or 10 μM TRAP resulted in an increase the amount of p11 staining intensity, when compared to the levels observed in mock treated cells. In contrast, the A2 staining intensity remained constant regardless of treatment, indicating that A2 levels were unaffected by thrombin or TRAP. Staining the nuclei with DAPI allowed us to calculate the number of cells, which was later used as a denominator for quantification.

The results of the quantification of the immunofluorescence microscopy experiments performed for HFF cells are shown in Figure 24. 0.8 to 8 nM thrombin (Panel A) was observed to enhance intracellular p11 levels a maximum of 4.5-fold, while 0.1 to 10 μM TRAP lead to a maximal 3-fold enhancement. In both cases A2 levels appeared to remain constant throughout the titration ranges (Figure 24, Panel B). Statistical analysis of the results revealed that the values obtained for the treated cells were statistically significant ($p<0.01$).

3.3.2.2 Western Blot Analysis of Cellular Lysates.

As previously described for HUVEC, western blot analysis of A2 and p11 levels in thrombin or TRAP treated HFF cell lysates was undertaken as a second method to confirm our immunofluorescence microscopy results (Figure 25). In Panel A, we observe that treating HFF cells with increasing thrombin concentrations (from 0.8 to 8 nM) results in a dose dependent increase of total

Figure 25: Effect of Thrombin and TRAP on Total A2 and p11 in HFF. The effect of thrombin (Panel A) or TRAP (Panel B) on total A2 and p11 in HFF was followed by quantitative western blotting as described in Figure 21.

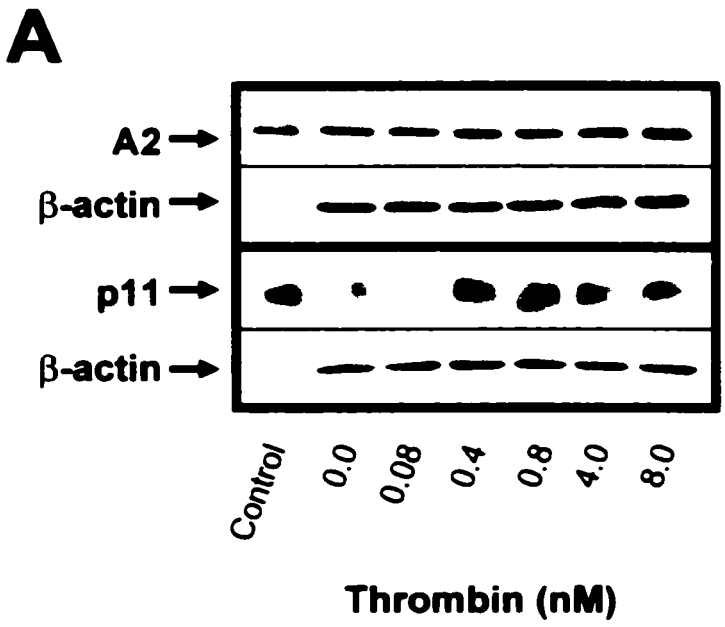
A
A2
β-actin
p11
β-actin
Control
0.0
0.08
0.4
0.8
4.0
8.0
Thrombin (nM)

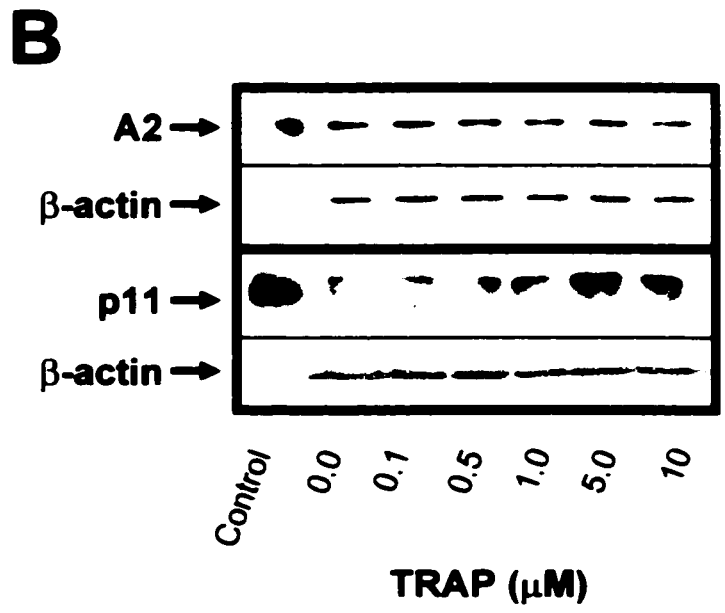
B
A2
β-actin
p11
β-actin
Control
0.0
0.1
0.5
1.0
5.0
10
TRAP (μM)

Figure 26: Quantification of Total A2 and p11 Levels Obtained by Western Blot Analysis HFF. The fold enhancement in total A2 (∇) and p11 (•) levels in thrombin (Panel A) and TRAP (Panel B) treated cells were quantified as described in Figure 22 (n=3, treated cells are significantly different from non-treated cells at *$p<0.01$ or ✦$p<0.05$).

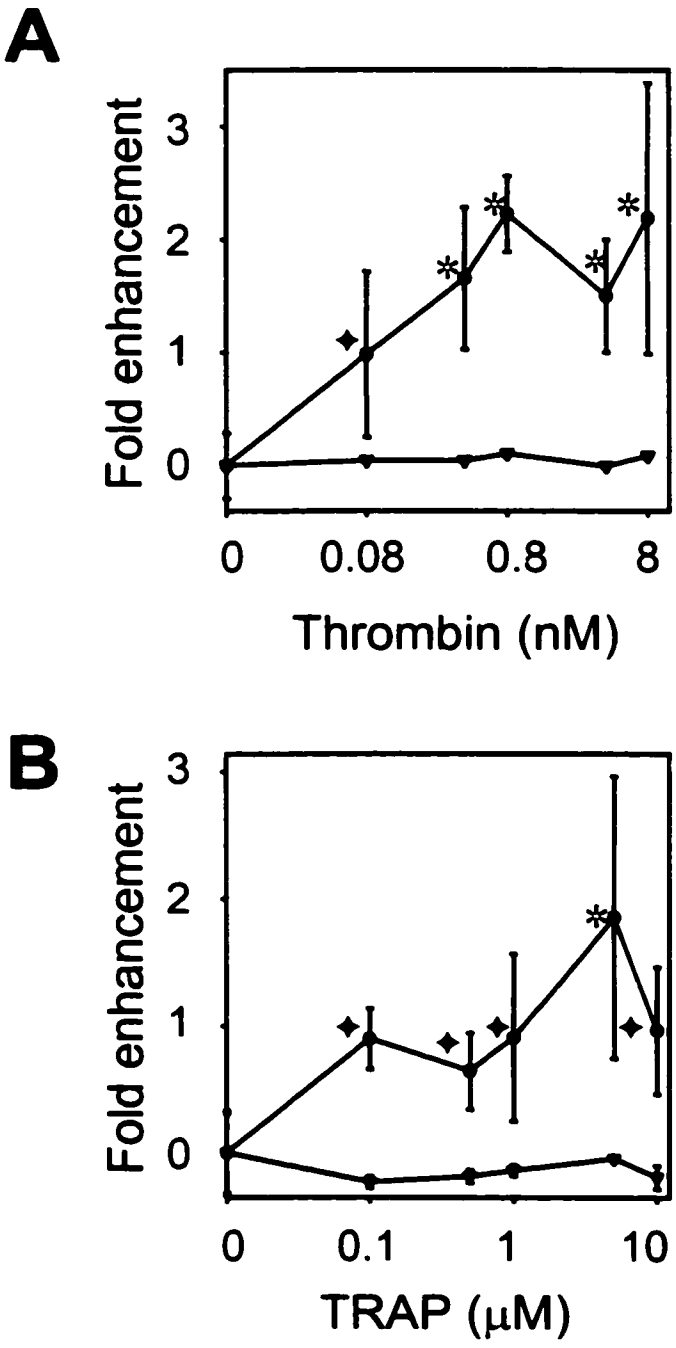
A
Fold enhancement
3
2
1
0
0
0.08
0.8
8
Thrombin (nM)
B
Fold enhancement
3
2
1
0
0
0.1
1
10
TRAP (μM)

p11 levels, while having no effect on total A2. Similar results were observed after treatment with 0.1 to 10 μM TRAP (Panel B). Re-probing the membranes with anti-β-actin served as a loading control and as a baseline for quantification.

Quantification of the western blots (Figure 26) established that both thrombin (Panel A) and TRAP (Panel B) enhanced intracellular p11 levels approximately 2-fold, while quantification of the A2 blots confirmed that A2 levels were unaffected by thrombin or TRAP treatment. The data obtained for treated cells was shown to be significantly different from the mock-treated cells at $p<0.05$ or $p<0.01$.

3.4 EFFECT OF THROMBIN OR TRAP ON SUB-MEMBRANOUS ANNEXIN II

3.4.1 Sub-membranous Pools of Annexin II in Human Umbilical Vein Endothelial Cell are Enhanced by Thrombin or TRAP Stimulation.

The inability of thrombin or TRAP to enhance intracellular A2 levels in HUVEC indicated that the thrombin- or TRAP-mediated increase in surface A2 might be due to a redistribution of intracellular A2 pools and not new protein synthesis.

Immunofluorescence microscopy observation of annexin I in cells extracted using different concentrations of fixative and detergent proposed the existence of sub-membranous annexin I pools that colocalized with cytoskeletal elements (228). Subsequent observation of similarly treated cells by electron microscopy revealed that the annexin I pools were in fact located just beneath the plasma membrane. The existence of sub-membranous A2 pools, which could

Figure 27: Isotype Controls for Membrane-bound A2 and Vimentin Staining in HUVEC and HFF. HUVEC (Panel A) and HFF (Panel B) treated with 8nM thrombin, 10 μM TRAP or mock treated were fixed with 4% paraformaldehyde and 0.25% gluteraldehyde. The cells were then incubated with a primary antibody solution containing mouse IgG2a and goat serum. After 3 PBS washes, the primary antibodies were detected by treating the cells with a secondary antibody solution containing Cy^3-conjugated donkey anti-mouse IgG and FITC conjugated rabbit anti-goat IgG. The nuclei were then stained with DAPI (shown merged with the vimentin staining), and the cells were visualized as in Figure 9.

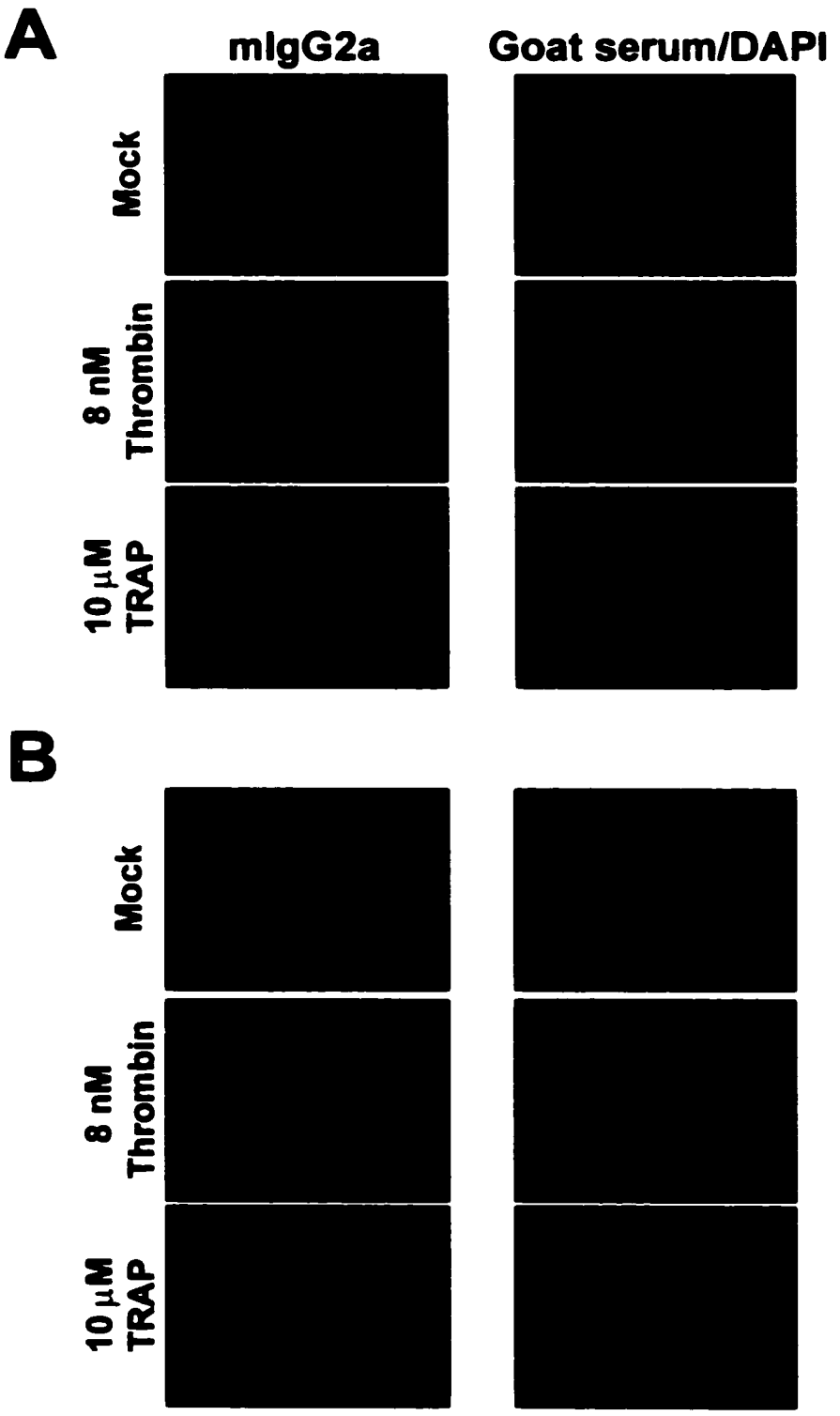
A
mIgG2a
Goat serum/DAPI
Mock
8 nM Thrombin
10 μM TRAP
B
Mock
8 nM Thrombin
10 μM TRAP

be shuttled to the surface after thrombin or TRAP stimulation may in part explain the observed increases in surface A2. Therefore, to determine if these pools exist for A2, and if they may be enhanced by thrombin or TRAP we performed immunofluorescence microscopy by triple staining paraformaldehyde and gluteraldehyde fixed HUVEC for A2, vimentin and DAPI following treatment by thrombin or TRAP.

A baseline for non-specific staining was established by performing isotype controls, where non-immune mouse IgG2a and goat serum were substituted for the primary antibodies (Figure 27, Panel A). These controls were negative demonstrating that all staining observed was due to specific interactions between the primary antibodies and the cellular A2 or vimentin. Furthermore, we observed that thrombin and TRAP

had no effect on non-specific interactions between the primary and secondary antibodies and the cells.

Observation of A2 staining demonstrated that compared to mock treated cells, cells treated with 8 nM thrombin or 1 μM TRAP had increased A2 fluorescence levels (Figure 28). The A2 staining was localized in specific areas throughout the cells. Observation of the vimentin staining patterns showed a similar localization of staining. The absence of the typical vimentin spindles normally seen in permeabilized cells indicated that complete permeabilization did not occur. Merged images of the A2 and vimentin staining patterns demonstrated that there was colocolization between certain A2 and vimentin pools. Staining the nuclei with DAPI was performed to control for cell number.

Figure 28: Effect of Thrombin and TRAP on Membrane-bound A2 in HUVEC. HUVEC treated with 8 nM thrombin, 10 μM TRAP or mock treated were fixed with 4% paraformaldehyde and 0.25% gluteraldehyde. After fixation the cells were simultaneously stained for A2 and vimentin (Vim) by the addition of a primary antibody solution containing monoclonal anti-A2 and polyclonal goat anti-vimentin antibodies. After 3 PBS washes, the primary antibodies were detected by incubation with Cy^3-conjugated donkey anti-mouse IgG and FITC conjugated rabbit anti-goat IgG. The nuclei were stained with DAPI, the washing steps were repeated, and the cells were visualized as described in Figure 9. Overlays of the vimentin and DAPI, as well as the A2 and DAPI staining patterns are shown.

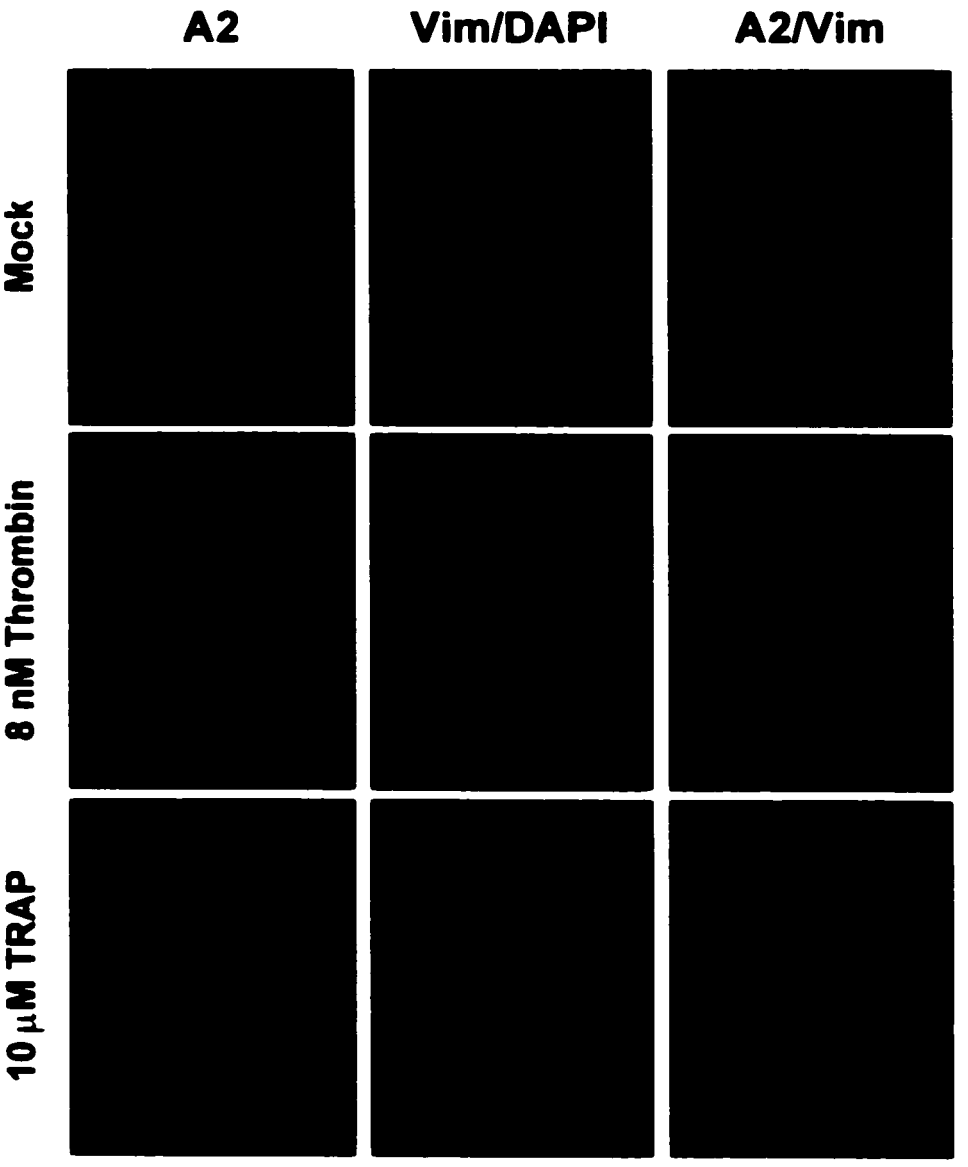
A2
Vim/DAPI
A2/Vim
Mock
8 nM Thrombin
10 μM TRAP

Thus, the sub-membranous A2 pools colocalized with cytoskeletal elements, demonstrating that these A2 pools occur at junctions between the plasma membrane and cytoskeleton.

3.4.2 Thrombin- or TRAP-Mediated Augmentation of Sub-membranous Annexin II Pools in Human Foreskin Fibroblasts.

To determine if HFF contained the sub-membranous A2 pools observed in HUVEC, and if these pools could be increased by thrombin- or TRAP-mediated stimulation, the effect of thrombin or TRAP on membrane associated A2 pools in HFF was followed by three-color immunofluorescence microscopy as described in Section 3.4.1.

As for HUVEC, isotype controls were undertaken to determine the baseline of our system (Figure 27, Panel B). The primary antibodies were substituted with non-immune mIgG2a and goat serum to determine whether non-specific antibody-antigen interactions were contributing to the observed staining. The isotype controls were negative, demonstrating that the A2 and vimentin staining was specific, and that non-specific antibody-cell interactions were unaffected by thrombin or TRAP.

In Figure 29, the sub-membranous A2 staining pattern in HFF cells is shown. We observed that A2 staining was elevated after treatment with 8 nM thrombin or 1 μM TRAP, compared to mock treated cells. The sub-membranous A2 distribution appeared more diffuse than in HUVEC, however certain areas did appear to have a more intense point-like staining. The vimentin-staining pattern

Figure 29: Effect of Thrombin and TRAP on Sub-membranous A2 in HFF. HFF cells treated with 8 nM thrombin, 10 μM TRAP or mock treated were simultaneously stained for A2, vimentin (Vim) and DAPI by three-color immunofluorescence microscopy as described in Figure 28. Merged images of the A2/vimentin, and the vimentin/DAPI staining patterns have been provided.

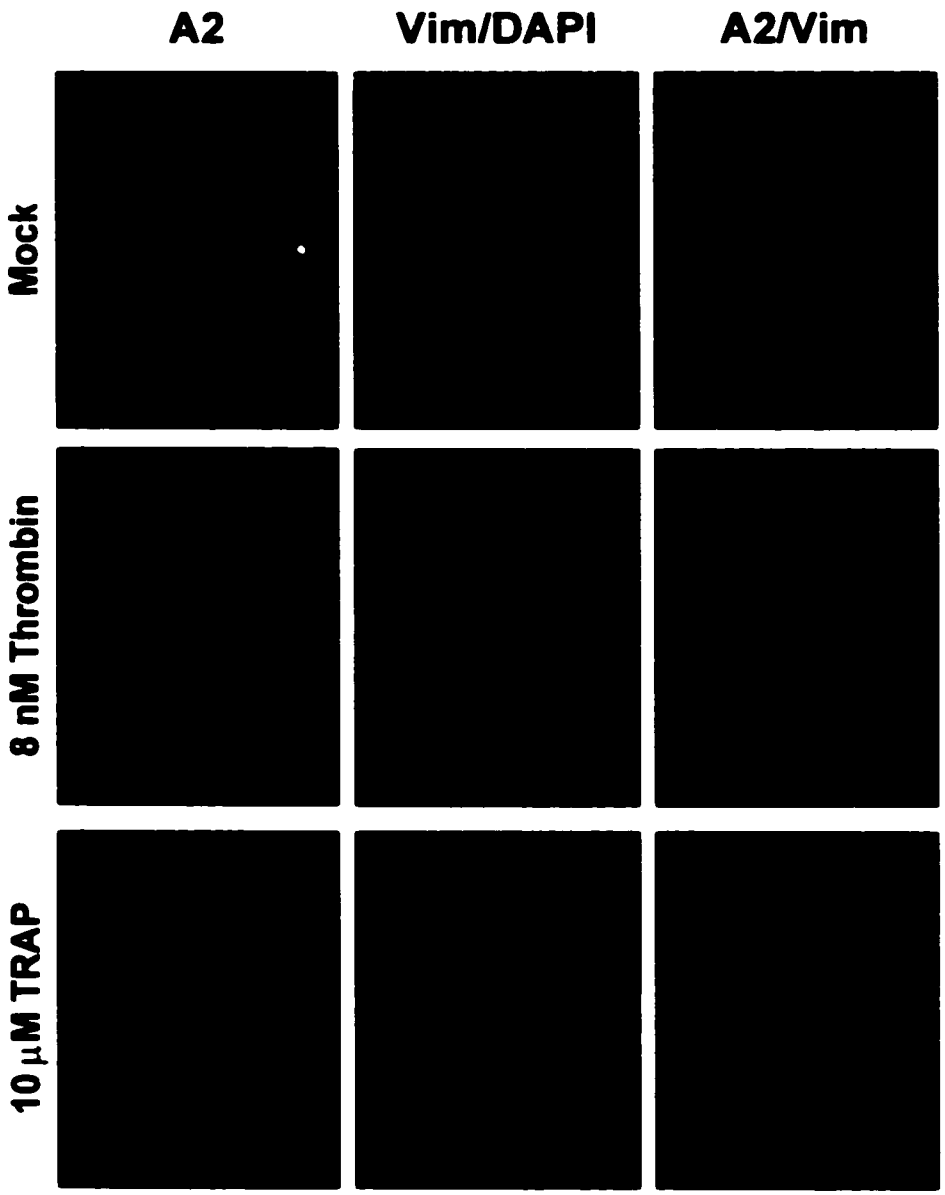
A2
Vim/DAPI
A2/Vim
Mock
8 nM Thrombin
10 μM TRAP

was highly punctate in nature. The absence of visible spindles in the vimentin staining patterns indicated that complete permeabilization did not occur. Nuclear staining with DAPI was used to ascertain equal numbers of cell were being compared in each field. Examination of overlays of the A2 and vimentin distributions revealed that a proportion of the A2 pools appear to colocolize with vimentin. Therefore, certain sub-membranous pools of A2 occur in regions of the plasma membrane interacting with cytoskeletal elements.

3.5 EFFECT CMV ON INTRACELLULAR AND SUB-MEMBRANOUS A2.

3.5.1 CMV-mediated Up-regulation of Sub-membranous Annexin II in Human Umbilical Vein Endothelial Cells.

A2 has been proposed to be a cell surface receptor for CMV (125;147). Therefore, the ability of CMV to produce thrombin on its surface (174), and the capability of the virus to stimulate cells through direct virus-cell contact (229), were studied as triggers for the redistribution of cellular A2 pools. Preliminary immunofluorescence microscopy experiments were conducted to follow intracellular and sub-membranous A2 pools in HUVEC after CMV treatment (as described in Sections 3.3.1 and 3.4.1).

The isotype controls for intracellular and sub-membranous A2 are shown in Figure 30. These controls, completed by incubating identically treated cells with non-immune mIgG2a and goat serum in place of the primary antibodies, were performed to determine the baseline level of staining in our experiments. As observed in Figure 30, the controls were void of staining, confirming that all

Figure 30: Isotype Controls for Intracellular and Sub-membranous A2 Staining in CMV Treated Cells. HUVEC grown to confluence were treated with 7.14 x 10^4 CMV particles/mL. The cells were subsequently fixed with 4 % paraformaldehyde and 0.25 % gluteraldehyde (sub-membranous staining), or fixed and permeabilized with 4 % paraformaldehyde, 0.25 % gluteraldehyde and 0.2 % Triton X-100 (intracellular staining). Non-specific interactions between the antibodies and the cells were detected by incubation with mouse IgG2a and goat serum. The cells were washed 3 times with PBS, followed by treatment with a secondary antibody solution containing FITC-conjugated rabbit anti-goat IgG and Cy^3-conjugated donkey anti-mouse IgG. The washing steps were repeated, and the cells were visualized with a Zeiss epifluorescent microscope at a magnification of 1260 (exposure times: 30 seconds for mIgG2a, 60 seconds for goat serum).

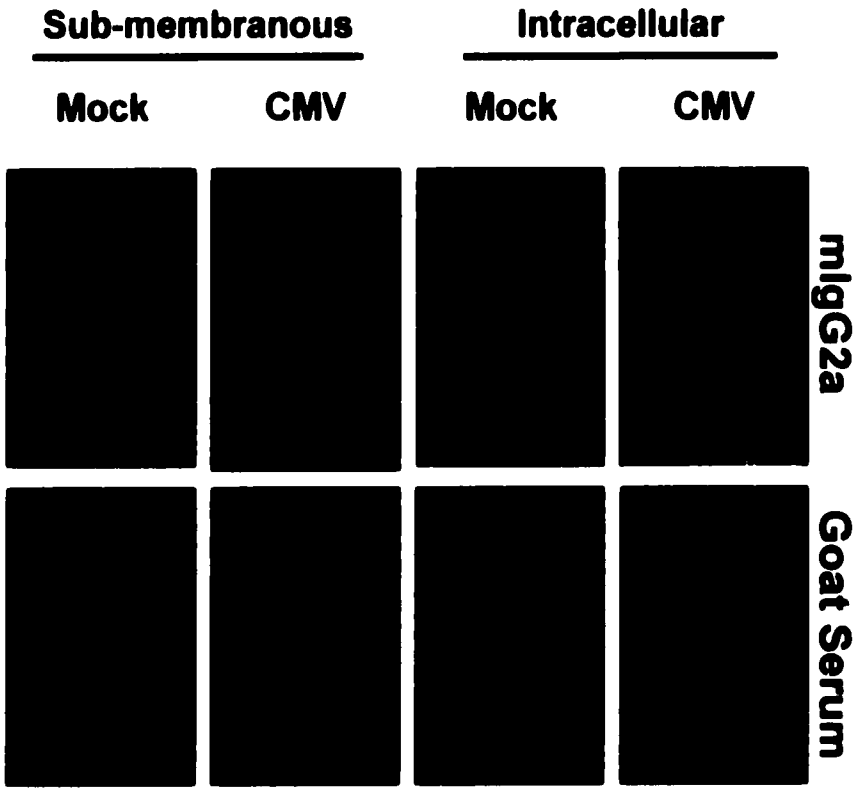
Sub-membranous
Intracellular
Mock
CMV
Mock
CMV
mIgG2a
Goat Serum

A2 and vimentin staining observed was specific and that CMV treatment did not affect the levels of non-specific antibody-cell interactions. In addition vimentin staining was undertaken to control for the levels of permeabilization caused by the various fixation procedures (Figure 31).

In Figure 31, the effect of CMV on intracellular A2 is shown. Intracellular A2 levels remained constant regardless of treatment, demonstrating that CMV had no effect on the amount intracellular A2. Staining for vimentin was performed to ensure all cells received identical levels of permeabilization. The vimentin staining patterns of CMV and mock treated cells were identical, ensuring that equivalent permeabilization occurred, and that permeabilization was unaffected by CMV treatment.

The effect of CMV on sub-membranous A2 pools is also shown in Figure 31. The sub-membranous A2 was dramatically enhanced in CMV treated cells when compared to mock treatment. Observation of the A2 distribution demonstrated that it was restricted to specific areas within the cells. The vimentin staining patterns are void of the spindles characteristic of a permeabilized vimentin stain, and was also localized to distinct areas inside the cells. Due to the high degree of similarity between the A2 and vimentin staining patterns we can conclude that there is colocolization of of certain sub-membranous A2 and vimentin pools. Hence, the membrane associated A2 pools were observed in distinct areas throughout the cell, which correspond to linkages between the plasma membrane and cytoskeleton.

Figure 31: Effect of CMV on the Distribution of Intracellular and Sub-membranous A2 in HUVEC. HUVEC grown to confluence were treated with 7.14 x 10^4 CMV particles/mL. The cell were subsequently fixed (sub-membranous staining), or fixed and permeabilized (intracellular staining) as described in Figure 30. A2 and vimentin were detected by incubation with monoclonal mouse anti-A2 and polyclonal goat anti-vimentin antibodies, followed by washing with PBS. The cells were then treated with a secondary antibody solution containing FITC-conjugated rabbit anti-goat IgG and Cy^3-conjugated donkey anti-mouse IgG. After antibody incubations the cells were mounted and visualized as described in Figure 30 (exposure times: 30 seconds for A2, 60 seconds for vimentin).

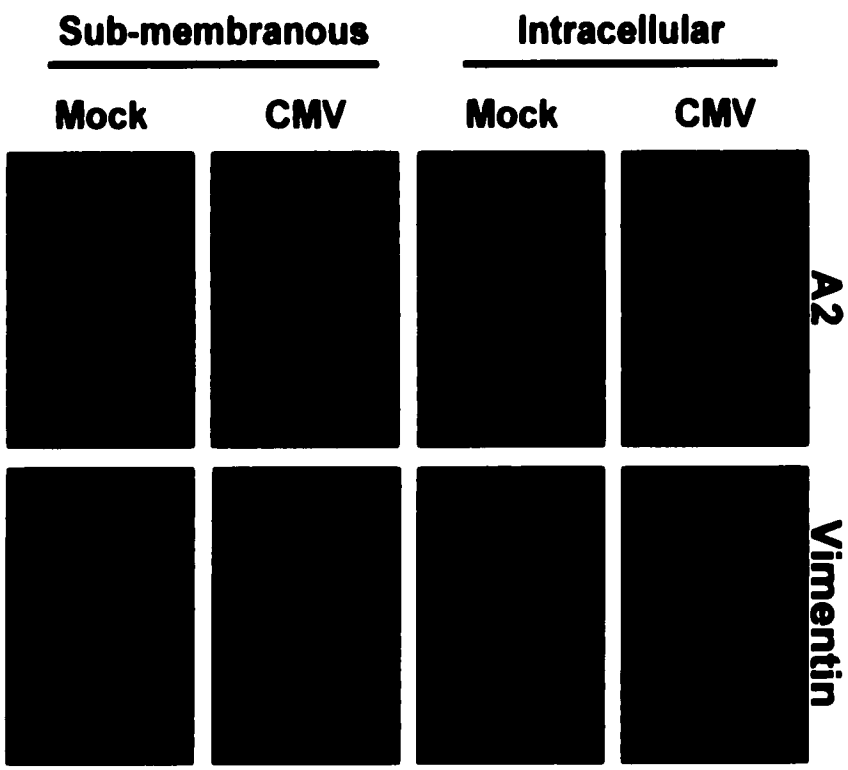
Sub-membranous
Intracellular
Mock
CMV
Mock
CMV
A2
Vimentin

3.5.2 Total Annexin II Levels are Unaffected by CMV Treatment.

To substantiate the immunofluorescence microscopy results, total A2 levels were observed after CMV treatment of HUVEC and HFF by western blot analysis of cellular lysates. Figure 32 shows the results of a time course of CMV treatment followed by a 1 hour recovery period (Panel A), and a 5 minute CMV treatment followed by a time course recovery period (Panel B) in HUVEC (Panels A and B: a) and HFF cells (Panels A and B: b). We observed that neither a time course CMV treatment, nor a time course recovery period had any effect on total A2 levels. The identity of the A2 bands was confirmed by including a purified A2 positive control (Panels A and B: lane 7). The PVDF membranes were stained for total protein with Coomassie Blue to ensure that identical numbers of cells were being loaded in each SDS-PAGE lane.

It has been well documented that CMV envelope contains annexin II (144). To ascertain that the A2 contributed by the added CMV was not significant, controls containing the amount of purified CMV used in each experiment, were performed (Panel B: lane 6). These controls detected little or no measurable A2, demonstrating that CMV was not contributing significant amounts of the protein.

Figure 32: Effect of CMV on Total A2 in HUVEC and HFF. HUVEC (Panels A and B: a) and HFF (Panels A and B: b) grown to confluence were treated with 19.4 x 10^4 CMV particles/cell for 5 to 30 minutes, washed with HBS, and allowed to recover for 1 hour at 37°C (Panel A), or treated with 19.4 x 10^4 CMV particles/cell for 5 minutes, washed with HBS, and allowed to recover for 0 to 60 minutes in fresh media at 37°C (Panel B). After treatment the cells were lysed and placed in sample buffer containing 2% β-mercaptotethanol. 2 μg of each sample (determined by colorimetric assay) were separated on 12% polyacrylamide gels by SDS-PAGE. Western blot analysis was performed using a monoclonal anti-A2 antibody. Total protein was visualized by staining with Coomassie blue.

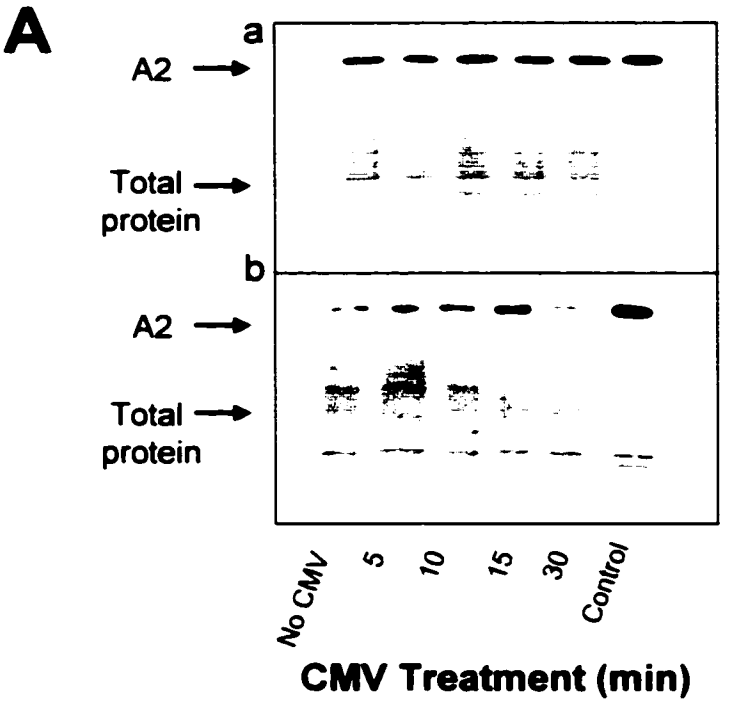
A
a
A2
Total protein
b
A2
Total protein
No CMV
5
10
15
30
Control
CMV Treatment (min)

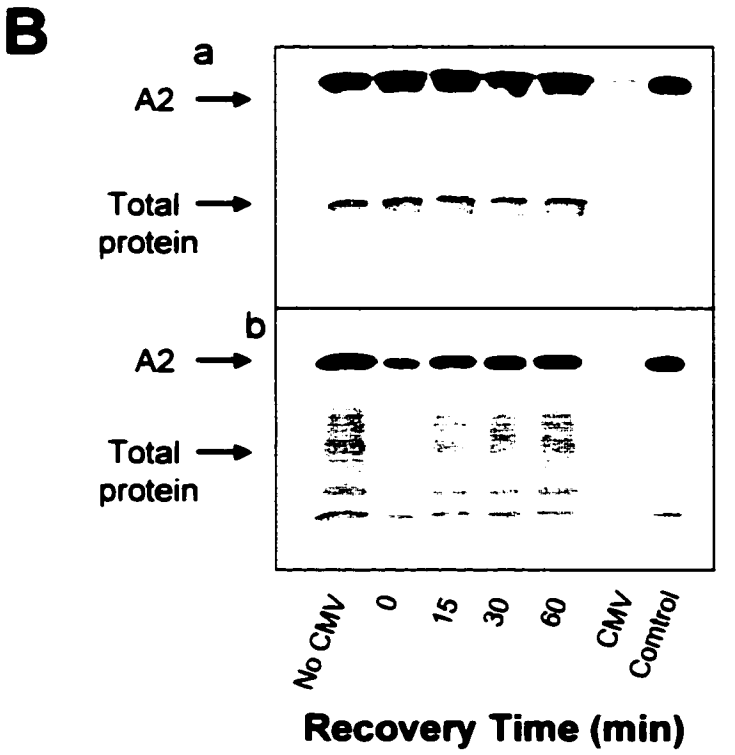
B
a
A2
Total protein
b
A2
Total protein
No CMV
0
15
30
60
CMV
Control
Recovery Time (min)

3.6 FUNCTIONAL EXPERIMENTS

3.6.1 Enhancement of Plasminogen Binding in Thrombin or TRAP Stimulated Human Umbilical Vein Endothelial Cells.

A2 has been identified as an endothelial cell surface co-receptor for plasminogen and tissue plasminogen activator (tPA) (119), and as a cofactor in the tPA-mediated conversion of plasminogen to plasmin (129). To determine whether thrombin- or TRAP-induced enhancement of surface A2 or p11 could play a functional role in fibrinolysis, we studied their effects on the binding of biotinylated (B-Plg)- or fluorescein (F-Plg)-labeled recombinant plasminogen to the HUVEC surface.

3.6.1.1 B-Plg Binding

Binding of B-Plg (Figure 33, Panel A) to cells treated with 8 nM thrombin, 10 μM TRAP or mock treated HUVEC was evaluated by western blot analysis of cell lysates with HRP-avidin, after incubation with B-Plg. We observed that treating HUVEC with either thrombin or TRAP enhanced B-Plg binding when compared to mock treated cells.

The addition of 3 mM ε-ACA, which inhibits the interaction of plasminogen with essential C-terminal lysine residues on known receptors, inhibited B-Plg binding (Panel A). Similarly, the addition of a 10-fold excess of unlabeled purified Glu-plasminogen completely repressed the ability of B-Plg to bind to the HUVEC surface (data not shown). The ability of excess unlabeled Glu-plasminogen to prevent B-Plg binding demonstrated that biotinylation did not affect the specificity

Figure 33: Thrombin or TRAP Treatment of HUVEC Enhances Plasminogen Binding. In Panel A, biotin-plasminogen (B-Plg) binding to the surface of thrombin and TRAP treated HUVEC was evaluated by incubating treated cells with 150 nM B-Plg for 30 minutes at 37°C, lysing the cells, separating the proteins by SDS-PAGE, transferring to PVDF and probing the membranes with HRP-avidin. To ensure similar numbers of cells were loaded in each lane, the blots were reprobed with an anti-β-actin antibody. Quantification of B-Plg binding to the cell surface is shown in Panel B (n=3, treated cells are significantly different from non-treated cells at * $p<0.01$). Fluorescein-plasminogen (F-Plg) binding to HUVEC was evaluated in Panel C, by incubating cells treated with 8 nM thrombin, 10 μM TRAP or mock treated with 150 nM F-Plg for 30 min at 37°C. The cells were subsequently fixed, the nuclear DNA was stained with DAPI, and the cells were mounted and visualized as described in Figure 9.

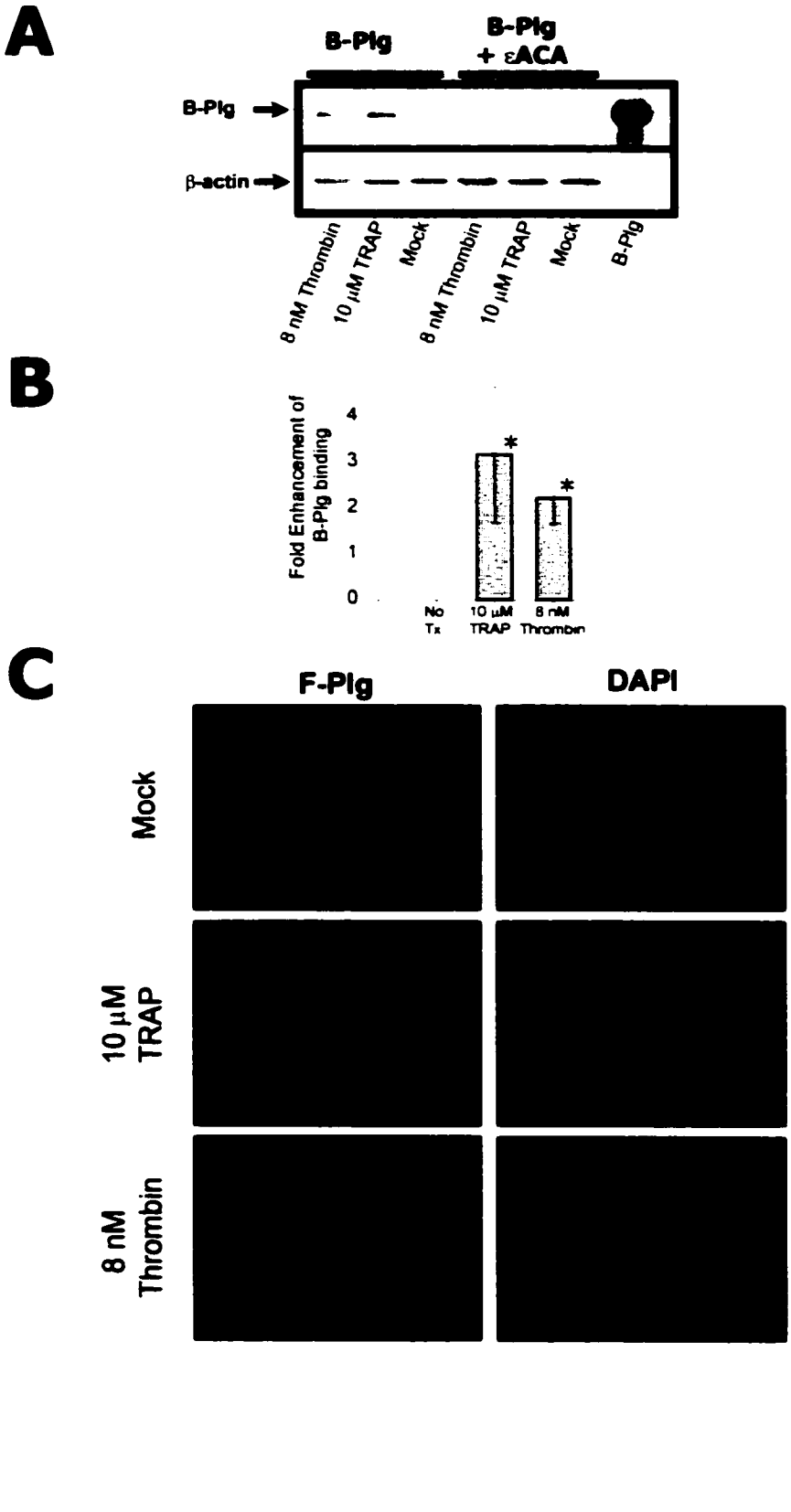
A
B-Plg
B-Plg
+ εACA
B-Plg
β-actin
8 nM Thrombin
10 μM TRAP
Mock
8 nM Thrombin
10 μM TRAP
Mock
B-Plg
B
Fold Enhancement of B-Plg binding
4
3
2
1
0
*
*
No Tx
10 μM TRAP
8 nM Thrombin
C
F-Plg
DAPI
Mock
10 μM TRAP
8 nM Thrombin

of B-Plg binding to the HUVEC surface. Re-probing the PVDF membrane for β-actin served as a loading control, to verify that comparable amounts of each sample were subjected to electrophoresis, and as a baseline for quantification. An SDS-PAGE lane containing B-Plg alone (Panel A, lane 4) was included to identify which bands in the HUVEC lysate corresponded to B-Plg.

The results of quantification and statistical analysis are shown in Panel B. Thrombin treatment enhanced B-Plg binding 2-fold, while TRAP caused a 3-fold increase compared to mock treated HUVEC ($p<0.01$, $n=3$).

3.6.1.2 F-Plg Binding

In Figure 33 Panel C, fluorescence microscopy was used to follow the binding of F-Plg to the surface of live HUVEC treated with 8 nM thrombin, 10 μM or mock treated. We observed an increase in fluorescence in cells treated with thrombin or TRAP, indicating that F-Plg binding to the HUVEC surface was increased. Staining of the nuclear DNA with DAPI was performed to ensure that comparable numbers of cells were being evaluated in each field.

3.6.2 Anti-p11 Inhibition of Thrombin- or TRAP-mediated Increase in F-Plg Binding to Human Umbilical Vein Endothelial Cells.

To determine whether the enhancement of plasminogen binding could be directly attributed to increases in surface A2 and p11, the F-Plg binding experiment described in Figure 33 was repeated including rabbit anti-p11 IgG or control non-immune rabbit IgG (Figure 34). In the absence of antibody we

Figure 34: Inhibition of F-Plg Binding by Interference with p11. F-Plg binding to thrombin, TRAP or mock treated cells was evaluated as in Figure 33. However, both the recovery media, and the F-Plg solution for certain cells contained 100 nM polyclonal rabbit anti-p11. As controls for specificity the experiment was repeated with F-Plg alone and in the presence of 100 nM non-immune rabbit IgG.

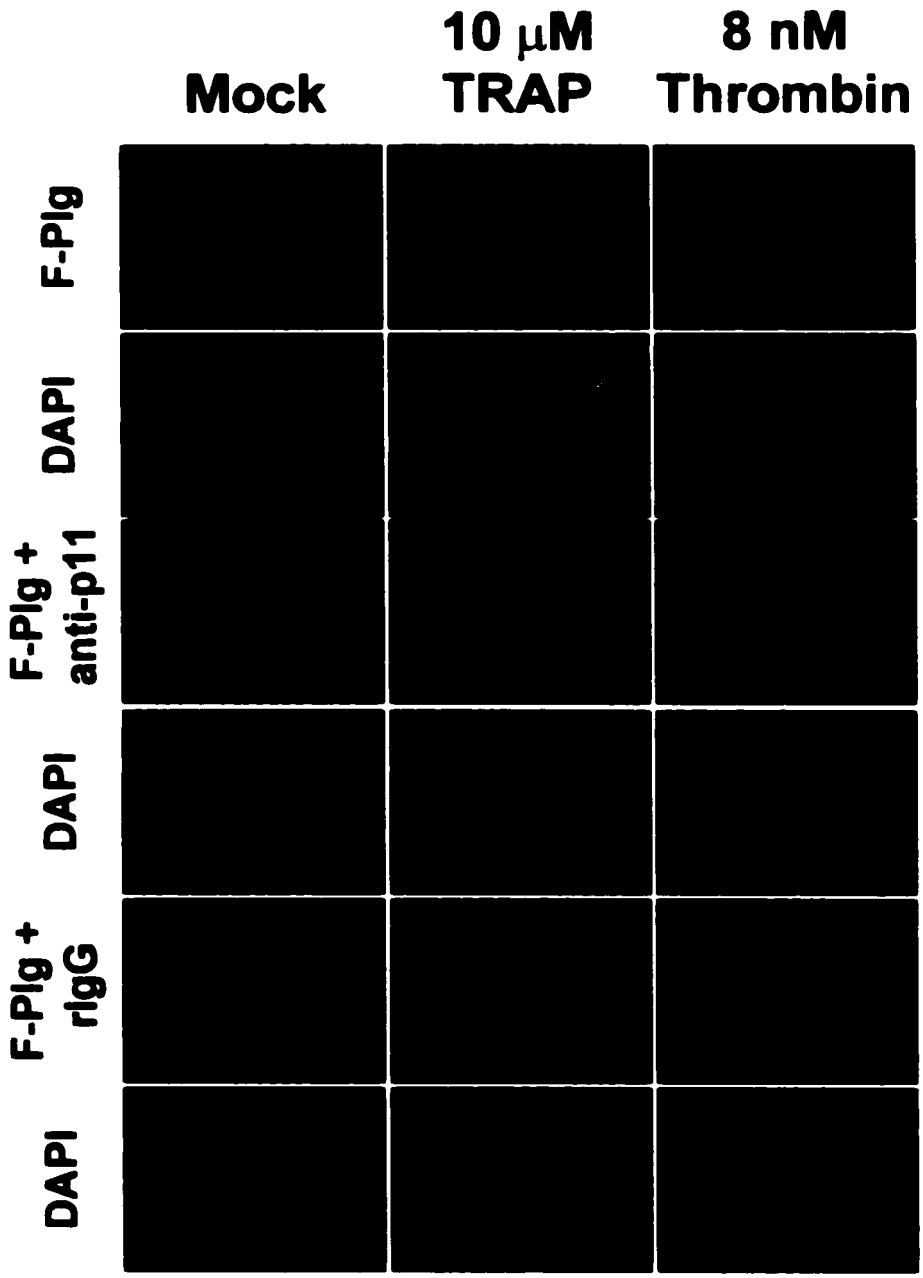
Mock
10 μM TRAP
8 nM Thrombin
F-Plg
DAPI
F-Plg + anti-p11
DAPI
F-Plg + rIgG
DAPI

observed that both 8 nM thrombin and 10 μM TRAP enhanced the level of binding of F-Plg to the HUVEC surface compared to the mock treated cells as seen in Figure 33. However, this increase in F-Plg binding was inhibited by the addition of an anti-p11 antibody but was unaffected by a non-immune rabbit IgG. Thus, interference with p11 inhibits the binding of F-Plg to the HUVEC surface.

3.6.3 Plasmin Generation on the Human Umbilical Vein Endothelial Cell Surface is Enhanced by Thrombin or TRAP Stimulation.

Having established that thrombin- and TRAP-mediated stimulation of HUVEC can enhance plasminogen binding, we then investigated whether this effect translated to increased tPA-mediated plasmin generation on the HUVEC surface (Figure 35). Plasmin produced from Lys- (Panel A) or Glu-plasminogen (Panel B) by recombinant tPA was measured by chromogenic assay. The mOD (mili optical density)/min units obtained from the chromogenic assays were translated into μM plasmin or nM plasmin generated/min with the use of a plasmin standard curve (data not shown).

These experiments demonstrated that both thrombin and TRAP in the case of Lys-Plasminogen, and thrombin alone in the case of Glu-Plasminogen was able to significantly enhance plasmin generation on the HUVEC surface. A maximal 7-fold enhancement was observed in plasmin generation from Lys-plasminogen, while plasmin generation from Glu-plasminogen was enhanced to a maximum of 3-fold. Interestingly unlike Lys-plasminogen, conversion of Glu-

Figure 35: Enhancement of Plasmin Generation on the HUVEC Surface by Thrombin or TRAP. HUVEC treated with 8 nM thrombin (•), 10 μM TRAP (▼), or mock treated (o) were pre-incubated with 5 nM recombinant tissue plasminogen activator (rtPA) at 37°C. After 20 minutes, 150 nM of Lys-plasminogen (Panel A) or Glu-plasminogen (Panel B) was added. Aliquots were then removed at various time points and assayed for plasmin activity by chromogenic assay (n=3). The insets represent specificity controls for cells treated with 8 nM thrombin at the 30 minute time point for Lys-plaminogen and at the 60 minute time point for Glu-plasminogen (Panel A, A: rtPA + plasminogen, B: rtPA omitted, C: plasminogen omitted, D: rtPA + plasminogen + aprotinin; Panel B, A: rtPA + plasminogen, B: rtPA omitted, C: plasminogen omitted).

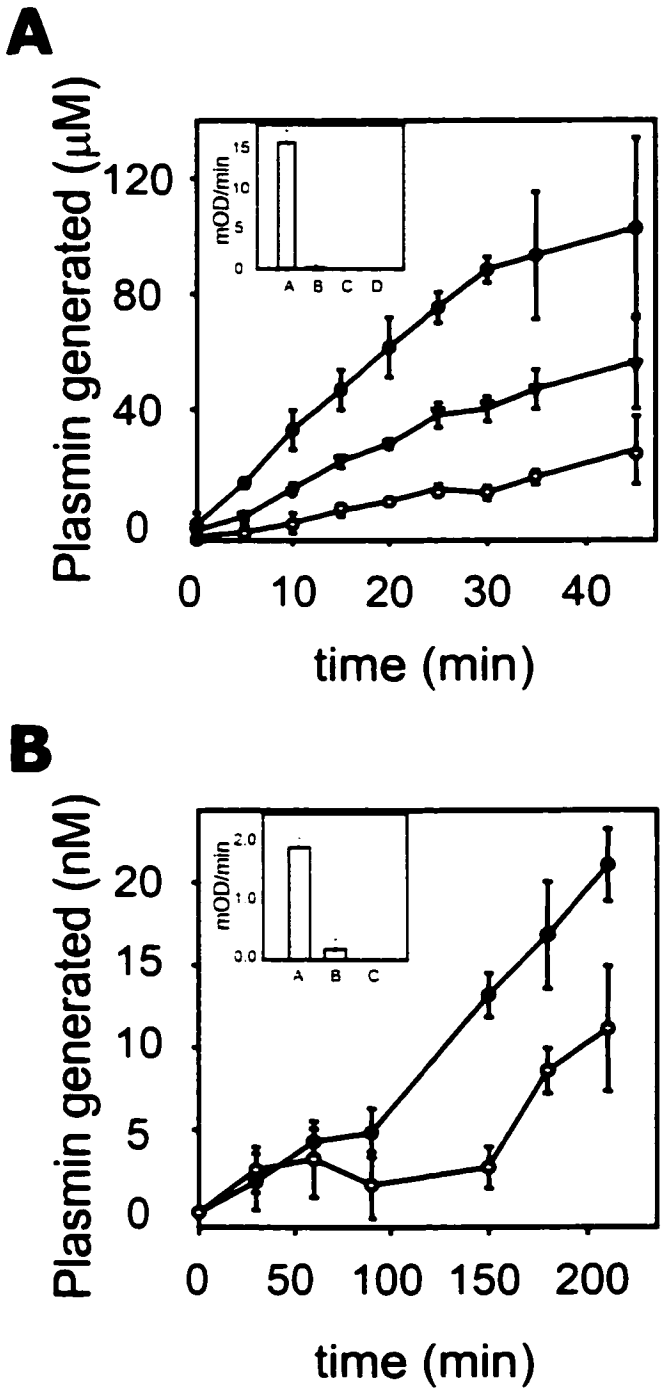
A
Plasmin generated (μM)
120
80
40
0
0
10
20
30
40
time (min)
mOD/min
15
10
5
0
A B C D
B
Plasmin generated (nM)
20
15
10
5
0
0
50
100
150
200
time (min)
mOD/min
2.0
1.0
0.0
A B C

plasminogen to plasmin had a lag phase, which lasted approximately 90 to 105 minutes.

The addition of aprotinin, a relatively specific plasmin inhibitor (230), blocked all chromogenic activity observed, which strongly supported the idea that plasmin and not another enzyme was responsible for the activity observed (Panel A: inset). The aprotinin data for cells treated with 8 nM thrombin shown in Panel A (inset), was characteristic of the data obtained for TRAP and mock treated cells (data not shown). The omission of tPA or plasminogen also resulted in loss of all chromogenic activity, indicating that the cells were not secreting detectable amounts of tPA, and that plasmin generation was dependent solely on exogenous tPA and plasminogen (Panels A and B: insets). The tPA and plasminogen omission controls shown for thrombin (Panels A and B: inset) treated cells were typical of the controls obtained for TRAP and mock treated cells (data not shown). All thrombin controls were taken at the 30 minute time point for Lys-Plg and the 60 minute time point for Glu-Plg.

4. DISCUSSION

4.1 THROMBIN OR TRAP STIMULATION ENHANCES SURFACE ANNEXIN II AND p11 EXPRESSION.

Thrombin has well documented cell-modulating capabilities, which function to regulate hemostasis. The goal of this thesis was to study the effect of thrombin on the cellular distribution of A2, and to determine the role of thrombin on the function of A2 in fibrinolysis. The hypothesis addressed was that thrombin-mediated signaling increases cellular participation in plasmin generation and CMV infection, by enhancing the presentation of A2 on the cell surface. Indeed, antigenic analysis of surface A2 and p11 levels demonstrated that a 5 minute treatment with thrombin or TRAP caused a rapid increase of surface A2 and p11 in HUVEC and HFF cells.

A2 and p11 do not contain secretory signals; thus they cannot exit the cell via the typical endoplasmic reticulum-dependent pathway (121). Although, the mechanism by which A2 and p11 are secreted is undetermined and does not involve typical pathways, both proteins have been identified on the surface of numerous cell types, including keratinocytes (231), endothelial (45;119;142), glioma (45), and large-cell lymphoma cells (117). Our discovery that thrombin can mediate surface A2 and p11 expression represents the first known stimulus capable of inducing their cell surface expression. In addition, we observed that stimulation with TRAP, a PAR-1 activating peptide, triggered the redistribution of A2 and p11 to the exterior of the cell. The ability of PAR-1 activation to induce cell surface A2 and p11 expression provides insight into the mechanism involved,

implicating G protein activation. A more detailed and specific mechanism may be inferred by studying the effects of other cell modulators that have been shown to activate G proteins, on the cellular distribution of A2. Like thrombin, nicotine stimulation of certain cells has been shown to involve G protein activation (232). Analysis of the effects of nicotine treatment on A2 distribution in chromaffin cells demonstrated that cellular stimulation by nicotine caused a translocation of A2m and A2t from the cytosol to caveolar domains (233), plasma membrane invaginations that function in transmembrane trafficking and intracellular signaling (234;235). Additional evidence exists for the presence of A2 in caveolae. It has been observed that A2 is a component of caveolae in various cell types (236), including endothelial cells (237), and cell surface A2 appears to colocalize with caveolae (238). Furthermore, A2 has been implicated in granule-granule and granule-plasma membrane fusion (239), as well as exocytosis (48), two functions that are proposed to involve caveolae. When combined together, these observations may provide a potential explanation into the mechanism by which A2 and p11 are translocated to the cell surface, which we speculate, may involve caveolae.

While our data indicates that surface A2 and p11 are enhanced by thrombin or TRAP, it does not give us any specifications as to whether the A2 and p11 are present as A2t. Studies involving which forms of A2 exist on the cell surface have been reported. It has been demonstrated that 90 to 95 % of endothelial and epithelial A2 exists as A2t (40;240). From analysis of surface A2 and p11 levels, these authors concluded that they are present in equal

concentrations, suggesting that A2t is the dominant form of A2 on the cell surface. Furthermore, cell surface immunofluorescence microscopy verified that staining for A2 colocalized with all observed p11 staining (120). These observations allow us to hypothesize that all p11 present on the cell surface is complexed to A2. Double staining of surface A2 and p11 by immunofluorescence microcopy could test this hypothesis. However, to perform these experiments an anti-p11 antibody that recognizes unfixed p11 would have to be produced.

To ascertain what type of interaction occurs between A2 and the cell surface we attempted to remove surface A2 with EGTA. As a Ca^{2+} chelator, EGTA would induce the dissociation of any A2 associated with the cell surface in a Ca^{2+}-dependent manner. In fact, we observed that EGTA did strip A2 from the cell surface, and that the amount of Ca^{2+}-dependent A2 bound was increased after treatment with thrombin or TRAP. The observed Ca^{2+}-dependence of the interaction of A2 with the cell surface suggests that the newly expressed surface A2 is interacting with the cell surface via anPL. This observation provides further evidence implicating plasma membrane structures in the translocation of A2 from the interior of the cell to the cell surface. However, A2 has also been shown to interact with certain proteins, such as annexins I (241) and V (242), in a Ca^{2+}-dependent manner, and therefore an A2-protein interaction cannot be ruled out. To determine if another protein is involved, chemical crosslinking prior to EGTA elution could be undertaken.

4.2 THROMBIN- OR TRAP-MEDIATED AUGMENTATION OF TOTAL p11.

In order to determine if the thrombin or TRAP-mediated increases in surface A2 and p11 are correlated-to protein synthesis, we analyzed total A2 and p11 levels by antigenic analysis. We observed that while A2 was unaffected by thrombin or TRAP, the amount of intracellular or total p11 increased significantly. It has been demonstrated that surface A2 comprises approximately 4 % of the total cellular pool in endothelial cells (116). Thus, due to the small proportion of surface A2, intracellular A2 can be considered an approximate representation of the total cellular pool of the protein.

The ability of thrombin to modulate cells via the induction of intracellular signaling through cell surface receptors PAR-1, PAR-3 and PAR-4, has been well documented in the literature (166). Along with stimulation of intracellular signaling and second messenger generation, thrombin has been shown to cause the expression of various gene products such as platelet derived growth factor B chain (243), plasminogen activator inhibitor-1 (244), endothelin 1 (178), and gelatinase B (244) to name a few. This enhancement is believed to result from the activation of thrombin inducible transcription factors, including activator protein 1 (AP-1) (244;245), NF-κB (246;247), and DNA binding protein B (248). The ability of thrombin to induce gene expression through the activation of thrombin-sensitive transcription factors, and the existence of thrombin inducible transcription factor binding sites in the p11 gene sequence may explain the increases in total p11 levels. To determine whether the p11 gene contains any of these DNA motifs, we analyzed the promoter region (10 Kbp upstream from the

transcription start site) for transcription factor binding sites with the MatInspector V2.2 program (249). We discovered that the p11 gene contains putative recognition elements for NF-κB. Thus, we propose that the thrombin-induced enhancement of p11 levels we observed may be due to the thrombin-mediated activation of the NF-κB pathways. In contrast, analysis of the promoter region of the A2 gene with the MatInspector V2.2 program revealed that the A2 gene sequence was void of the putative NF-κB transcription factor recognition elements found in the p11 gene (249). Based on this preliminary analysis we propose that total A2 levels are unaffected by treatment with thrombin or TRAP because the gene contains no binding sites for the known thrombin-activated transcription factor NF-κB.

Although protein synthesis may be responsible for the increase in total p11 observed after thrombin or TRAP stimulation, another possible explanation would be decreased degradation or increased half-life. Northern blot analysis of the p11 mRNA, quantitative RT-PCR, or pulse-chase experiments may provide further insight into which mechanism is involved.

Interestingly, we observed that thrombin treatment was able to increase intracellular p11 up to a maximum of 8-fold in HUVEC, while TRAP caused an approximate 1.5-fold increase. Our observation that TRAP, a thrombin signaling peptide specific for PAR-1, enhanced surface A2 and p11 levels indicates at least this member of the PAR family is involved. The discrepancy observed between thrombin and TRAP may be due to the fact that thrombin has numerous receptors on the cell surface, and may activate receptors other than PAR-1.

Other members of the PAR family, including PAR-3, exist on the HUVEC surface, which can be activated by thrombin (216). In addition, thrombin has also been shown to activate cells in a non-proteolytic manner (250). A thrombin peptide, whose sequence is identical to the region of thrombin responsible for high affinity binding to fibroblasts, has been shown to stimulate cells without proteolysis (250). This peptide, but not PAR-1, was able to induce annexin V expression in human fibroblasts (250). Thus, the thrombin mediated increases in intracellular p11, and surface A2 and p11, may be due in part through signaling by a distinct non-PAR receptor.

The ability of coagulation proteases Xa and VIIa to activate PAR-1 and PAR-2 (220-223), suggests that their formation and subsequent receptor activation may elicited the same biochemical responses as thrombin. Thus, Xa or VIIa treatment of our cells may induce the expression of surface A2 and p11, as well as increase the amount of intracellular p11. This effect may or may not be physiologically significant in comparison to thrombin PAR-1 and PAR-3 activation. Analysis of the effects of Xa and VIIa on the cellular distribution of A2 and p11 may elucidate whether thrombin, or other coagulation proteases, are the physiological triggers of protease receptor activation- mediated redistribution of cellular A2 and p11.

The purity of the thrombin utilized in the current experiments, was tested by the supplier with SDS-PAGE analysis, and was subsequently confirmed by SDS-PAGE in our Laboratory. Furthermore, the thrombin must be diluted 10 000 fold to achieve concentrations in the nM range. Any impurities present would

certainly be too diluted to have any substantial effects. In addition, the observation that PAR-1 stimulation by TRAP elicits the same observed effects as thrombin suggests that thrombin, and not an impurity, is causing cell activation. However, the possibility exists that a trace component present in the thrombin, although unlikely, could be participating. To confirm the specificity of the effect on thrombin, experiments could be repeated in the presence of hirudin, a highly specific thrombin inhibitor. If the inclusion of hirudin eradicates all thrombin-associated activity then we could confirm that all observed cellular changes are specific to thrombin

4.3 UP-REGULATION OF MEMBRANE ASSOCIATED ANNEXIN II BY THROMBIN OR TRAP.

Previous studies in A549 cells have shown that fixation of cells with paraformaldehyde and gluteraldehyde causes the plasma membrane to undergo a mild permeabilization (228). This allows distinct areas of the cytoplasm, proposed to occur at junctions between the cytoskeleton and the plasma membrane, to be visualized by immunofluorescence microscopy. Studies using this method revealed that annexin I existed in sub-membranous patches whose staining colocalized with staining for cytoskeletal elements including tubulin and cytokeratin 8 (228). Further characterization with immunogold electron microscopy showed that annexin I was accumulated in electron dense areas just underneath the plasma membrane, indicating that the immunofluorescence staining observed was due to sub-membranous annexin I pools (228). To add

credence to the hypothesis that sub-membranous structures, such as caveolae, are involved in the transmembrane trafficking of A2, we utilized this method of fixation to observe sub-membranous A2 pools, and to determine if they are affected by thrombin or TRAP stimulation. This technique demonstrated that both thrombin and TRAP stimulation dramatically enhance these sub-membranous pools in HUVEC and HFF, which colocalized with the intermediate cytoskeletal component vimentin.

We propose that two interrelated mechanisms may contribute to the augmentation of membrane associated A2. The first mechanism involves the well-documented transient increase in intracellular calcium levels after thrombin stimulation of cells. The intracellular Ca^{2+} concentrations of resting cells (0.01 to 0.1 μM) are raised significantly to 1 to 10 μM (112;251). The Kd (Ca^{2+}) required for A2m binding to PS has been reported to be 2 μM (96). In the Ca^{2+} concentration range displayed in activated cells, A2m present in the cytosol will be able to bind the anPL present on the inner leaflet of the plasma membrane (33;87;96). Thus thrombin-mediated rises in intracellular Ca^{2+} can cause the translocation of A2m from the cytosol to the plasma membrane. The translocation of annexins to membranes after increases in intracellular Ca^{2+} have been well documented in the literature. Annexins II, IV, V, and VI have been shown to translocate to the inner plasma membranes of HFF (252) and neuroblastoma SH-SY5Y cells (253) after treatment with calcium ionophores. In addition, thrombin stimulation of platelets resulted in the relocation of annexin V

to membrane structures (254). Thus the translocation of A2m to the plasma membrane may play a role in the enhancement of sub-membranous A2 pools.

The second part of the mechanism involves the ability of thrombin or TRAP to increase intracellular p11 levels. It is proposed that the additional p11 produced is available to associate with A2m present in the cytosol to form A2t. Because only the tetrameric form of the protein can bind anPL at low μM calcium concentrations, this newly formed A2t will translocate from the cytosol to the inner leaflet of the plasma membrane, thus enhancing the membrane-associated pools of A2. If the total p11 levels were raised sufficiently the amount of A2m translocated to the plasma membrane would be negligible in comparison to the levels of A2t. Thus, this model suggests that A2t would preferentially be translocated to the cell surface, corroborating data demonstrating that A2t is the dominant form of A2 on the cell surface. The translocation of A2m and A2t to the plasma membrane upon thrombin- or TRAP-mediated PAR-1 stimulation suggests that plasma membrane domains, such as caveolae, may play a role in the thrombin induced expression of surface A2t.

A hypothetical model summarizing the effect of thrombin- or TRAP mediated PAR-1 stimulation is presented in Figure 36. Activation of cell surface receptor by thrombin results in G protein linked intracellular signaling. The products of this signaling cascade are a transient elevation in cytosolic calcium concentrations, and an enhancement of intracellular p11 levels. These increases in intracellular calcium and p11 levels will cause a translocation of A2m

Figure 36: Working Model of Thrombin or TRAP Induced Redistribution of Cellular A2 and p11. The increase in intracellular Ca^{2+} concentrations, combined with the enhancement of intracellular p11 levels which occur upon thrombin or TRAP mediated PAR-1 activation result in an enhancement of membrane associated A2m and A2t. These membrane associated pools of A2m and A2t are then shuttled to the cell surface by an as of yet unknown mechanism possibly involving caveolae.

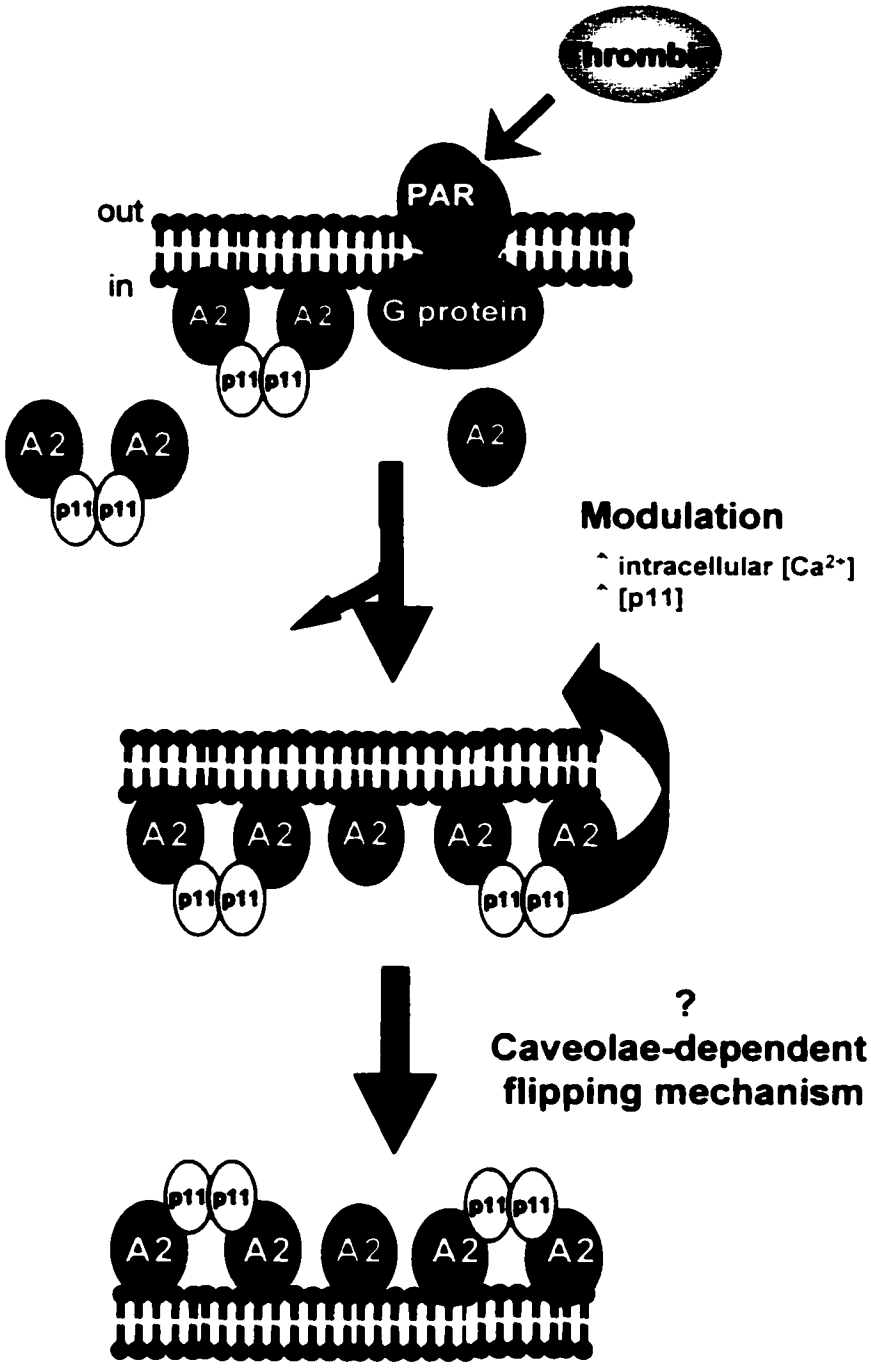
thrombin
PAR
out
in
A2
A2
G protein
p11
p11
A2
A2
p11
p11
A2
Modulation
^ intracellular [Ca2+]
^ [p11]
A2
A2
A2
A2
A2
p11
p11
p11
p11
?
Caveolae-dependent
flipping mechanism
p11
p11
p11
p11
A2
A2
A2
A2
A2

and newly formed A2t to the inner leaflet of the plasma membrane, resulting in an up-regulation of sub-membranous A2 pools. A2t and A2m are subsequently shuttled to the cell surface from the sub-membranous pools, possibly in a caveolae dependent mechanism.

4.4 CMV-MEDIATED ENHANCEMENT OF SUB-MEMBRANOUS ANNEXIN II.

CMV has been shown to interact with the cell surface in a two step mechanism. The first step is a low affinity, heparin inhibitable interaction between glycoprotein CII or B on the virus surface, and cell surface heparan sulfate proteoglycans (HSP) (255;256). This is followed by a second higher affinity interaction between the virus surface and the putative second receptor A2, and fusion of the viral envelope with the cell membrane (125;147). An additional consequence of CMV infection is cellular activation (for review see (229;257)). The ability of CMV to stimulate cell through direct CMV-cell contact has been demonstrated in the literature (258), however, the discovery that CMV can produce thrombin on its surface (174) suggests that CMV may potentially stimulate cells indirectly through thrombin production and cell surface thrombin receptor activation.

In the present study, we addressed the hypothesis that CMV treatment of cells can induce the expression of cell surface A2 for use as a viral receptor. We propose that treatment with CMV could prime cells for further infectibility by causing intracellular events capable of inducing the expression of its own high affinity second receptor, A2. Thus, the long-term goals of this portion of the

project are to determine whether the CMV-cell interaction, or the production of thrombin on the CMV surface, can induce the expression of cell surface A2. As an initial investigation, we evaluated the effect of CMV on intracellular and membrane-associated A2. Antigenic analysis of total, and sub-membranous A2 pools revealed that CMV treatment considerably enhanced the amount of sub-membranous A2, while total and intracellular A2 levels were unaffected. In our experiments the CMV stimulation took place in media containing fetal calf serum. Fetal calf serum contains clotting factors that could interact with tissue factor and anPL present on the CMV surface to generate thrombin. Therefore, our results cannot distinguish between the CMV-cell interaction, or the production of thrombin on the virus surface, as cell stimulatory triggers. In order to determine which pathway is responsible, experiments isolating one or the other must be undertaken. To isolate the CMV-HSP interaction, the CMV stimulation must be performed in the absence of serum, thereby preventing the generation of thrombin and other activated clotting factors. Enzymatic removal of cell surface heparan sulfate proteoglycans with heparinase or heparitinase prior to CMV stimulation in the presence of serum would allow the effect of thrombin produced on the virus surface to be evaluated.

If the CMV-mediated enhancement of sub-membranous A2 pools occurs through thrombin generation by CMV, and the subsequent binding of thrombin to its cell surface receptors, we propose that the mechanism by which CMV increases membrane associated A2 pools is identical to the one described previously for thrombin stimulation. However, if the enhancement of sub-

membranous A2 pools is due to the direct interaction between CMV and the cell surface that the mechanism involved may be related to the mechanism by which CMV has been shown to activate cells. It has been observed that the interaction of CMV with the cell surface can cause potent intracellular changes, including hydrolysis of membrane phospholipids and the production of the second messengers inositol 1,4,5-triphosphate and 1,2-diacylglycerol (259), an increase in the cytosolic Ca^{2+} concentration (260), a sodium influx (261), an enhancement in cyclic AMP and GMP levels (257). CMV exerts these intracellular changes through the activation of cell surface kinases such as phospholipase A2 (262), protein kinase C and A (262;263), and pertussis toxin sensitive G proteins (264;265). Stimulation of these cell membrane proteins also results in an increase in AP-1, NF-κB, and CREB transcription factors, thereby stimulating cellular and viral DNA synthesis (263;265). Although the intracellular changes described above could be due to thrombin production on the virus surface, there is some evidence of the ability of CMV to directly activate cells. CMV glycoprotein B has been shown tc initiate intracellular signaling (258), and modulate cellular transcription of CMV infected cells (266).

Thus, the ability of CMV to elevate NF-κB could possibly result in an up-regulation in total p11 levels, by the mechanism proposed previously for thrombin. Therefore, we suggest that the mechanism by which direct CMV-cell contact causes the enhancement of membrane bound A2 involves two separate but related phenomena, increases in cytosolic Ca^{2+} concentrations and elevation of total p11 levels. The ability of CMV to activate transcription factors such as

NF-κB may lead to increased p11 protein levels, due to the existence of putative NF-κB binding sites in the promoter region of the p11 gene. This enhancement of intracellular p11 levels would result in the formation of additional A2t, which would translocate to the plasma membrane, resulting in enhanced membrane associated A2t pools. The documented rise in intracellular Ca^{2+} concentrations that occurs upon interaction of CMV with the cell surface might allow A2m to bind to the inner leaflet of the plasma membrane. Thus the calcium spike observed after CMV-cell interactions could lead to the enhancement of sub-membranous pools of A2m. The sub-membranous A2 may then be shuttled to the surface by a caveolae-dependent mechanism resulting in greater exposure of A2 on the cell surface, as described for thrombin stimulation. It should be noted that these are only speculations, as direct experiments have not been conducted at this time. However, immunofluorescence microscopy analysis of intracellular p11 and cell surface A2, combined with an analysis of surface p11 by chemical modification of surface proteins after CMV treatment may provide insight as to whether the mechanism of CMV-mediated enhancement of membrane associated A2 mirrors that of thrombin.

4.5 ANNEXIN II-MEDIATED STIMULATION OF FIBRINOLYSIS.

4.5.2 Thrombin or TRAP enhanced Plasminogen Binding by Human Umbilical Vein Endothelial Cells.

A2 has been identified as an endothelial cell surface co-receptor for tPA and plasminogen (119), and a cofactor in the tPA dependent conversion of

plasminogen to plasmin (129). Our observation that both surface A2 and p11 were increased after thrombin treatment of HUVEC led us to test whether this correlated to enhanced fibrinolytic cell surface activity. Indeed, as predicted, enhanced binding of biotinylated and fluorescein labeled plasminogen to the HUVEC surface was observed after thrombin or TRAP-mediated HUVEC stimulation (Figure 24). The plasminogen concentrations used in our experiments (150 nM) were well below the plasma concentration of plasminogen (2.4 μM) (267). Therefore, the thrombin or TRAP mediated enhancement of plasminogen binding could occur at physiological plasminogen concentrations.

Although the ability of A2 to bind plasminogen is well documented, there is some controversy in the literature over which form of A2, A2m or A2t, is the functional one. Early binding experiments demonstrated that A2 bound plasminogen, and that this binding was inhibited by carboxypeptidase B treatment of A2 (119). Mutation of Lys residues 307 and 328 present in the C-terminus portion of the protein revealed, that residue Lys^{307} was necessary for plasminogen binding (119) (see Figure 36). Therefore, the authors concluded that the plasminogen binding site on A2 is the Lys^{307} residue, which is exposed upon cleavage of the Lys^{307}-Arg^{308} peptide bond by an unidentified plasmin-like protease (119) (see Figure 37). More recently, the presence of endogenous C-terminal Lys residues on the p11 subunit of A2t has shifted the focus to the effect of A2t in plasminogen binding and tPA acceleration. A2t was shown to bind plasminogen (120), and to enhance the rate of Glu-plasminogen activation by tPA (120), indicating that the presence of the p11 subunit of A2t may play an

Figure 37: Location of Putative Plasminogen Binding Sites in A2 and p11. The sequences of the C-terminal regions of A2 (Panel A) and p11 (Panel B) are shown. The position of the C-terminal lysine residues of A2 and p11 proposed to interact with plasminogen are highlighted in red. The black arrow indicates the proposed Lys^{307}-Arg^{308} cleavage site in A2 that would expose the putative C-terminal lysine residue upon cleavage by an unidentified plasmin-like protease.

A

300 338

KIRSEFKRKYGKSLYYYIQQ DTKGDYQKAL LYLCGGDD

B

58 96

DLDQCRDGKVGFQSFFSLIAGLTIACNYFVVHMKQKGKK

important role in tPA acceleration by A2. Because p11 contains endogenous C-terminal Lys residues, the plasminogen binding site may be located in the p11 subunit of A2t. Experiments involving recombinant proteins demonstrated that t-PA-dependent Glu-plasminogen activation was stimulated and 46-fold by recombinant p11 (205). Binding of Glu-plasminogen to a p11-affinity column, and competition studies using peptides with sequences identical to the last 12 residues (residues 85-96) of p11 demonstrated p11 could bind plasminogen, and that the plaasminogen binding site was located in the last 12 residues of the protein (205). Mutational analysis of the endogenous C-terminal Lys residues of p11 demonstrated that p11 mutant missing residues Lys^{95} and Lys^{96} from the C-terminus retained only approximately 15% of total activity (205). Thus, the Lys^{95} and Lys^{96} residues of p11 appear to be involved in plasminogen binding by p11 (see Figure 37). In addition, a mutant A2t composed of wild type A2m and the C-terminal Lys p11 deletion mutant lost 88% of its activity (205). These data indicate that the p11 subunit, and in particular residues Lys^{95} and Lys^{96} of p11, may participate in both the plasminogen binding and tPA acceleration functions of A2. The remaining 12% activity of the mutant A2t may be accounted for by the wild type A2m subunits of the protein.

Thus, the p11 subunit of A2t appears to play an important role in the plasminogen binding and tPA acceleration functions of A2. Therefore, the role of p11 in F-Plg binding to thrombin treated HUVEC was evaluated by antibody-mediated interference with p11.

4.5.2 Cellular Evidence for p11-mediated Binding of Plasminogen.

Because thrombin may enhance numerous putative plasminogen receptors on the cell surface, it was necessary to correlate the thrombin- or TRAP-mediated enhancement of surface A2m and A2t with the increased plasminogen binding observed in thrombin or TRAP treated cells. A direct involvement was demonstrated by the observation that anti-p11, and not a control rabbit IgG, was able to inhibit the thrombin or TRAP induced increase in F-Plg binding.

The ability of the anti-p11 antibody to inhibit plasminogen binding confirms the importance of the p11 subunit of A2t. While these data strongly support a role for p11, we cannot exclude the possibility that AII is also involved. Steric hindrance caused by binding of the anti-p11 antibody to A2t may indirectly prevent plasminogen from reaching its binding site on the A2m subunit. In order to rule out this second possibility, the F-Plg binding experiment needs to be repeated with an antibody specific for A2. Because this experiment was not performed, we cannot exclude the possibility of simultaneous involvement of A2 and p11 in plasminogen binding and activation. However, the ability of an anti-p11 antibody to eradicate plasminogen binding is consistent with the role for p11 in plasminogen binding and activation described previously.

4.5.3 Enhancement of Plasmin Generation on the Human Umbilical Vein Endothelial Cell Surface.

Plasmin (83 kDa) is generated from full-length plasminogen (Glu-plasminogen) by hydrolysis of the Arg ^{560}-Val ^{561} peptide bond by plasminogen activators such as tPA (268). Once activated, plasmin can convert Glu-plasminogen (88 kDa) to Lys-plasminogen (83 kDa) by cleavage of the Lys^{76}-Lys^{77} peptide bond, which is subsequently converted to Lys-plasmin (268). It has been demonstrated that Lys-plasminogen has a higher affinity for fibrin (269;270) and is more readily activated by tPA (271) and urokinase plasminogen activator (272) *in vitro* than Glu-plasminogen. Studies of fibrinolysis *in vitro* have revealed that the conversion of Glu- to Lys-plasminogen does occur during fibrinolysis *in vitro* (273), indicating that the conversion step is not an artifact. *In vivo* experiments have demonstrated that the Glu- to Lys- plasminogen conversion dramatically enhanced plasmin generation on the HUVEC surface corroborating the *in vitro* observations (274).

To ascertain whether the thrombin or TRAP-mediated enhancement of plasminogen binding to the cell surface could be translated into increased plasmin generation, we tested the effect of thrombin or TRAP treatment on the tPA dependent conversion of Glu- and Lys-plasminogen to plasmin. Using chromogenic assays, we demonstrated that thrombin or TRAP-mediated PAR-1 stimulation enhanced tPA dependent plasmin generation from Glu- or Lys-plasminogen on the HUVEC surface (Figure 26). Conversion of Lys-plasminogen to plasmin occurred at a constant rate, while a substantial lag

phase was observed for plasmin generation from Glu-plasminogen. This lag phase may be due to the conversion of Glu-plasminogen to Lys-plasminogen prior to plasmin activation.

Thus, we can conclude that the thrombin-mediated increases in surface A2t and A2m results in an enhanced ability to activate plasminogen, through the action of A2 and p11 as accelerators of tPA activity. However, to substantiate the involvement of A2 and p11 in the enhancement of plasmin generation observed after thrombin treatment, the experiments need to be repeated in the presence of antibodies directed against A2 and p11.

5. CONCLUSION

In this work we tested the hypothesis that thrombin could enhance the expression of cell surface A2t. Our results indicate that thrombin-mediated stimulation of its cell surface receptors can cause increases in total p11, combined with a concomitant formation and translocation of A2t to the inner leaflet of the plasma membrane. The end result of these intracellular changes is shuttling of A2t to the cell surface. Furthermore, we observed that the newly exposed surface A2t could play a functional role in fibrinolysis by conferring enhanced plasminogen binding and plasmin generation activity to the surface of HUVEC. Thus, a novel feedback regulatory step in hemostasis is indicated that links thrombin, the biological effector of coagulation, to enhanced cellular production of the fibrinolytic enzyme, plasmin (Figure 38).

Cell surface A2 has been suggested to have importance in a number of processes, such as tenascin C-binding, CMV infection, and tumor invasion and metastasis. Therefore the finding that exposure of cell surface A2 can be stimulus-induced may have implications in areas additional to fibrinolysis. Thus we propose that transbilayer shuttling of A2 to the cell surface may be involved as an important regulatory event in a number of biological processes, including fibrinolysis. Defects in the mechanism of cell surface expression of A2 could be the basis of diseases involving deregulated surface A2 expression such as in promyelocytic leukemia (136). Therefore, a more complete understanding of the mechanisms by which A2 is translocated to the cell surface may lead to new

Figure 38: Thrombin Regulated Activation of Fibrinolysis. Thrombin stimulation of cell surface receptors, including PAR-1, results in a transient rise in intracellular Ca^{2+} concentrations along with an observed increase in the amount of intracellular p11. Combined together, these biochemical phenomena cause the formation of additional A2t, and the translocation of cytosolic A2m and the newly formed A2t to the inner leaflet of the plasma membrane. These sub-membranous pools of A2m and A2t can then be shuttled to the cell surface by an unknown mechanism. This newly expressed surface A2 may then function as a tPA and plasminogen receptor and as an accelerator of tPA activity.

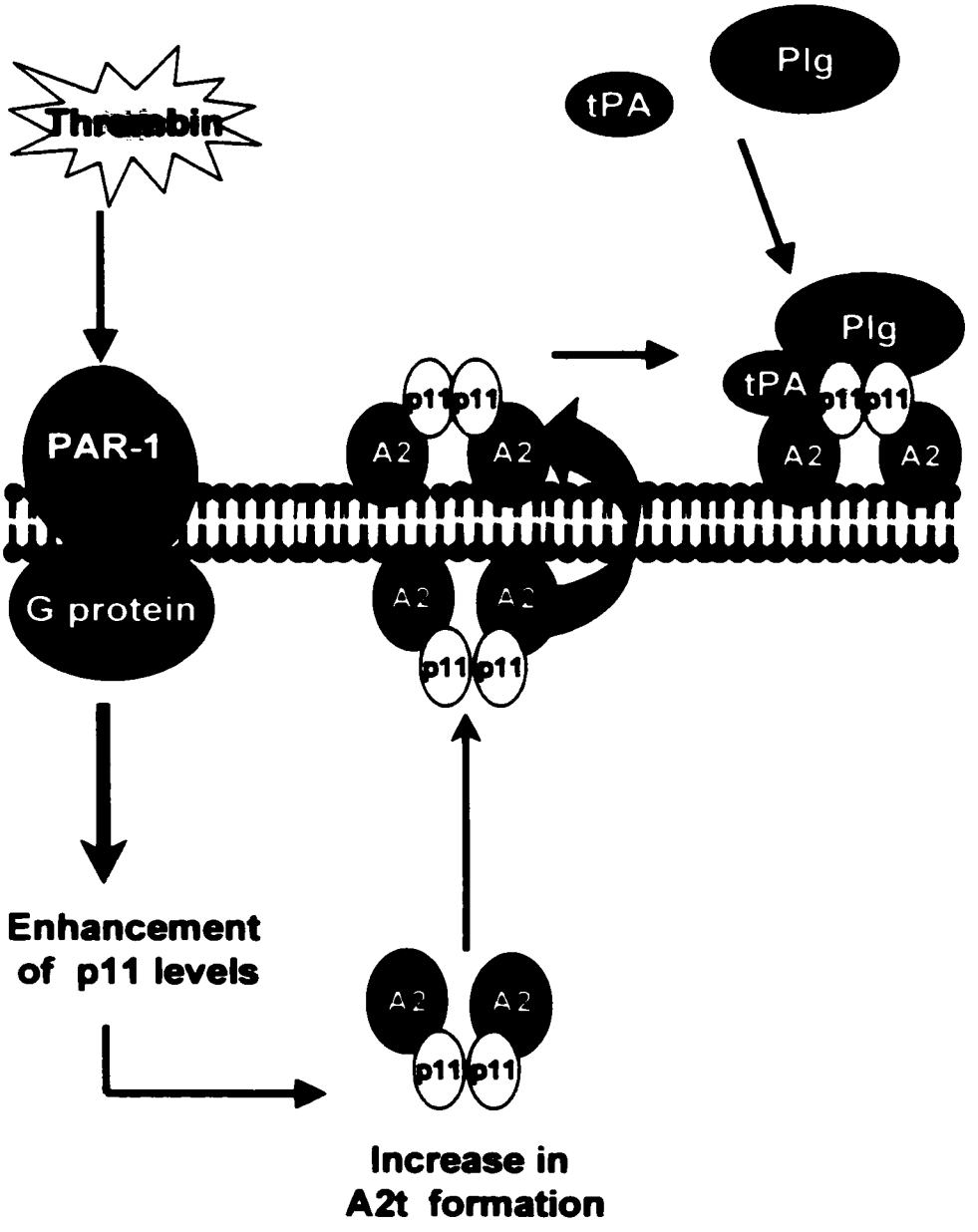
Thrombin
tPA
Plg
Plg
tPA
p11
p11
A2
A2
PAR-1
G protein
Enhancement
of p11 levels
Increase in
A2t formation

therapies for diseases involving the over-expression and the under-expression of surface A2.

6. REFERENCES

1. **Gerke, V. and S.E. Moss**. 1997. Annexins and membrane dynamics. Biochem. Biophys. Acta **1357**:129-154.

2. **Swairjo, M.A. and B.A. Seaton**. 1994. Annexin structure and membrane interactions: A molecular perspective. Annu. Rev. Biophys. Biomol. Struct. **23**:193-213.

3. **Benz, J. and A. Hofmann**. 1997. Annexins: From Structure to Function. Biol. Chem. **378**:177-183.

4. **Geisow, M.J.** 1986. Common domain structure of Ca^{2+} and lipid-binding proteins. FEBS Lett. **203**:99-103.

5. **Geisow, M.J., U. Fritsche, J.M. Hexham, B. Dash, and T. Johnson**. 1986. A consensus amino-acid sequence repeat in Torpedo and mammalian Ca(2+)-dependent membrane-binding proteins. Nature **320**:636-638.

6. **Saris, C.J.M., B.F. Tack, T. kristensen, J.R. Glenney, and T. Hunter**. 19860. The cDNA sequence for the protein tyrosine kinase substrate p36 (calpactin I heavy chain) reveals a multidomain protein with internal repeats. Cell **46**:201-212.

7. **Rodriguez-Garcia, M.I., C.A. Kozak, R.O. Morgan, and M.P. Fernandez**. 19960. Mouse annexin V chromosomal location, cDNA sequence conservation, and molecular evolution. Genomics **31**:151-157.

8. **Weng, X., H. Luecke, I.S. Song, D.S. Kang, S.-H. Kim, and R. Huber**. 1993. Crystal structure of annexin I at 2.5 Å resolution. Prot. Sci. **2**:448-458.

9. **Burger, A., R. Berendes, S. Liemann, J. Benz, A. Hofmann, P. Gottig, R. Huber, V. Gerke, C. Thiel, J. Romisch, and K. Weber**. 1996. The crystal structure and ion channel activity of human annexin II, a peripheral membrane protein. J. Mol. Biol. **257**:839-847.

10. **Favier-Perron, B., A. Lewit-Bentley, and F. Russo-Marie**. 1996. The high-resolution crystal structure of human annexin III shows subtle differences with annexin V. Biochem. **35**:1740-1744.

11. **Huber, R., J. Römisch, and E.P. Paques**. 1990. The crystal and molecular structure of human annexin V, an anticoagulant protein that binds to calcium and membranes. EMBO J **9**:3867-3874.

12. **Benz, J., A. Bergner, A. Hofmann, P. Demange, P. Göttig, S. Liemann, R. Huber, and D. Voges**. 1996. The structure of recombinant human

annexin VI in crystals and membrane-bound. J. Mol. Biol. **260**:638-643.

13. **Huber, R., R. Berendes, A. Burger, M. Schneider, A. Karshikiov, H. Luecke, J. Romisch, and E. Paques**. 1992. Crystal and molecular structure of human annexin V after refinement. J. Mol. Biol. **223**:683-704.

14. **Declerc, J.P., B. Tinant, J. Parello, G. Etienne, and R. Huber**. 1988. Crystal structure determination and refinement of Pike 4.10 parvalbumin (minor component from Esox lucius). J. Mol. Biol. **202**:349-353.

15. **McPhalen, C.A., N.C.J. Strynadka, and M.N.G. James**. 1991. Calcium-binding in proteins: a structural perspective. Adv. Protein Chem. **42**:77-144.

16. **Smith, V.L., M.A. Kaetzel, and J.R. Dedman**. 1990. Stimulus-response coupling: the search for intracellular calcium mediator proteins. Cell Reg. **1**:165

17. **Huber, R., M. Schneider, I. Mayr, J. Romisch, and E. Paques**. 1990. The calcium binding sites in human annexin V by crystal structure analysis at 2.0 A resolution. FEBS Lett. **275**:15-21.

18. **Verheij, H.M., J.J. Volwerk, E.H.J.M. Jansen, W.C. Puyk, B.W. Dijkstra, J. Drenth, and G.H. de Haas**. 1980. Methylation of histidine-48 in pancreatic phopholipase A_2. Role of histidine and calcium ion in the catalytic mechanism. Biochem. **19**:743-750.

19. **Huber, R., R. Berendes, A. Burger, H. Luecke, and A. Karshikov**. 1992. Annexin V: crystal structure and its implications on function., p. 105-124. In S.E. Moss (ed.), The Annexins. Portland Press Ltd, Chapel Hill.

20. **Thiel, C., K. Weber, and V. Gerke** . 1991. Characterization of a Ca(2+)-binding site in human annexin II by site-directed mutagenesis. J. Biol. Chem. **266**:14732-14739.

21. **Jost, M., C. Thiel, K. Weber, and V. Gerke**. 1992. Mapping of three unique Ca(2+)-binding sites in human annexin II. Eur. J. Biochem. **207**:923-930.

22. **Jost, M., K. Weber, and V. Gerke**. 1994. Annexin II contains two types of calcium-binding sites. Biochem. J. **298**:553-559.

23. **Gerke, V. and K. Weber**. 1985. Calcium-dependent conformational changes in the 36-kDa subunit of intestinal protein I related to the

cellular 36 kDa target of Rous sarcoma virus tyrosine kinase. J. Biol. Chem. **260**:1688-1695.

24. **Pigault, C., A. Follenius-Wund, B. Lux, and D. Gerard**. 1990. A fluorescence spectroscopy study of the calpactin I complex and its subunits p11 and p36: calcium-dependent conformation changes. Biochim. Biophys. Acta **1037**:106-114.

25. **Concha, N.O., J.F. Head, M.A. Kaetzel, J.R. Dedman, and B.A. Seaton**. 1993. Rat annexin V crystal structure: Ca^{2+}-induced conformational changes. Science **261**:1321-1324.

26. **Meers, P., D. Daleke, K. Hong, and D. Papahadjopoulos**. 1991. Interactions of annexins with membrane phospholipids. Biochem. **30**:2903-2908.

27. **Meers, P.** 1990. Location of tryptophans in membrane-bound annexins. Biochem. **29**:3325-3330.

28. **Meers, P. and T. Mealy**. 1993. Relationship between annexin V tryptophan exposure, calcium, and phospholipid binding. Biochem. **32**:5411-5418.

29. **Brisson, A., Mosser, G., and Huber, R.** 1991. Structure of soluble and membrane-bound human annexin V. J. Mol. Biol. 220:199-203.

30. **Mosser, G., C. Ravanat, J.-M. Freyssinet, and A. Brisson**. 1991. Sub-domain structure of lipid-bound annexin V resolved by electron image analysis. J. Mol. Biol. **217**:241-245.

31. **Voges, D., R. Berendes, A. Burger, P. Demange, W. Baumeister, and R. Huber**. 1994. Three-dimensional structure of membrane-bound annexin V-A correlative electron microscopy-X-ray crystallography study. J. Mol. Biol. **238**:199-213.

32. **Scott, D.L., S.P. White, Z. Otwinowski, W. Yuan, M.H. Gelb, and P.B. Sigler**. 1990. Interfacial catalysis: the mechanism of phospholipase A_2. Science **250**:1541

33. **Blackwood, R.A. and J.D. Ernst**. 1990. Characterization of Ca(2+)-dependent phospholipid binding, vesicle aggregation and membrane fusion by annexins. Biochem. J. **266**:195-200.

34. **Liu, L., J.Q. Tao, and U.J.P. Zimmerman**. 1997. Annexin II binds to the membrane of A549 cells in a calcium-dependent and calcium-independent manner. Cell Signal. **9**:299-304.

35. **Jost, M., D. Zeuscher, J. Seeman, K. Weber, and V. Gerke**. 1997. Identification and characterization of a novel type of annexin-membrane interaction - Calcium is not required for the association of annexin II with early endosomes. J. Cell Sci. **110**:221-228.

36. **Meers, P., T. Mealy, and N. Pavlotsky**. 1992. Annexin I-mediated vesicular aggregation: Mechanism and role on human neutrophils. Biochem. **31**:6372-6382.

37. **Raynal, P. and H.B. Pollard**. 1994. Annexins: the problem of assessing the biological role for a gene family of multifunctional calcium- and phospholipid-binding proteins. Biochim. Biophys. Acta. **1197**:63-93.

38. **Creutz, C.E.** 1992. The annexins and exocytosis. Science **258**:924-931.

39. **Glenney, Jr.J.R., B. Tack, and M.A. Powell**. 1987. Calpactins: two distinct Ca^{++}-regulated phospholipid- and actin-binding proteins isolated from lung and placenta. J. Cell Biol. **104**:503-511.

40. **Gerke, V. and K. Weber**. 1984. Identity of p36K phosphorylated upon Rous sarcoma virus transformation with a protein purified from brush borders: calcium-dependent binding to non-erythroid spectrin and F-actin. EMBO J. **3**:227-233.

41. **Tanaka, K., T. Tashiro, S. Sekimoto, and Y. Komiya**. 1994. Axonal transport of actin and actin-binding proteins in rat sciatic nerve. Neuroscience Res. **19**:295-302.

42. **Cheney, R.E. and M.B. Willard**. 1989. Characterization of the interaction between calpactin I and fodrin (non-erythroid spectrin). J. Biol. Chem. **264**:18068-18075.

43. **Bianchi, R., M. Garbuglia, M. Verzini, I. Giambanco, and R. Donato**. 1994. Calpactin I binds to the glial fibrillary acidic protein (GFAP) and cosediments with glial filaments in a Ca(2+)-dependent manner: implications for concerted regulatory effects of calpactin I and S100 proteins on glial filaments. Biochim. Biophys. Acta **1223**:361-367.

44. **Pfäffle, M., M. Borchert, R. Deutzmann, K. von der Mark, M.P. Fernandez, O. Selmin, Y. Yamada, G. Martin, F. Ruggiero, and R. Garrone**. 1990. Anchorin CII, a collagen-binding chondrocyte surface protein of the calpactin family. Prog. Clin. Biol. Res. **349**:147-157.

45. **Chung, C.Y. and H.P. Erickson**. 1994. Cell surface annexin II is a high affinity receptor for tenascin-C. J. Cell Biol. **126**:539-548.

46. **Chung, C.Y., J.E. Murphy-Ullrich, and H.P. Erickson**. 1996. Mitogenisis, cell migration, and loss of focal adhesions induced by tenascin-C

interacting with its cell surface receptor, annexin II. Mol. Biol. Cell **7**:883-892.

47. **Emans, N., J.-P. Gorvel, C. Walter, V. Gerke, R. Kellner, and G. Griffiths**. 1993. Annexin II is a major component of fusogenic endosomal vesicles. J. Cell Biol. **120**:1357-1369.

48. **Konig, J., J. Prenen, B. Nilius, and V. Gerke**. 1998. The annexin II-p11 complex is involved in regulated exocytosis in bovine pulmonary artery endothelial cells. J. Biol. Chem. **273**:19679-19684.

49. **Burgoyne, R.D., S.E. Handel, A. Morgan, M.E. Rennison, M.D. Turner, and C.J. Wilde**. 1991. Calcium, the cytoskeleton and calpactin (annexin II) in exocytotic secretion from adrenal chromaffin and mammary epithelial cells. Biochem. Soc. Trans. **19**:1085-1090.

50. **Reutelingsperger, C.P.M., G. Hornstra, and H.C. Hemker**. 1985. Isolation and partial purification of a novel anticoagulant from arteries of human umbilical cord. Eur. J. Biochem. **151**:625-629.

51. **Buhl, W.J.** 1992. Annexins and phospholipase A2 inhibition. Eicosanoids **5**:S26-S28

52. **Tait, J., M. Sakata, B.A. McMullen, C.H. Miao, T. Funakoshi, L.E. Hendrickson, and K. Fujikawa**. 19980. Placental anticoagulant proteins: Isolation and comparative characterization of four members of the lipocortin family. Biochem. **27**:6268-6276.

53. **Funakoshi, T., R.L. Heimark, L.E. Hendrickson, B.A. McMullen, and K. Fujikawa**. 1987. Human placental anticoagulant protein: Isolation and characterization. Biochem. **26**:5572-5578.

54. **Andree, H.A., C.P. Reutelingsperger, R. Hauptmann, H.C. Hemker, W.T. Hermens, and G.M. Willems**. 1990. Binding of vascular anticoagulant alpha (VAC alpha) to planar phospholipid bilayers. J. Biol. Chem. **265**:4923-4928.

55. **Andree, H.A., M.C. Stuart, W.T. Hermens, C.P. Reutelingsperger, H.C. Hemker, P.M. Frederik, and G.M. Willems**. 1992. Clustering of lipid-bound annexin V may explain its anticoagulant effect. J. Biol. Chem. **267**:17907-17912.

56. **Bohn, E., V. Gerke, H. Kresse, B.M. Loffler, and H. Kunze**. 1992. Annexin II inhibits calcium-dependent phospholipase A1 and lysophospholipase but not triacyl glycerol lipase activities of rat liver hepatic lipase. FEBS Lett. **296**:237-240.

57. **Huang, K.S., B.P. Wallner, R.J. Mattaliano, R. Tizard, C. Burne, A. Frey, C. Hession, P. McGray, L.K. Sinclair, E.P. Chow, J.L. Browning, K.L. Ramachandran, J. Tang, J.E. Smart, and R.B. Pepinsky**. 1986. Two human 35 kd inhibitors of phospholipase A2 are related to substrates of pp60v-src and of the epidermal growth factor receptor/kinase. Cell **46**:191-199.

58. **Khanna, N.C., M. Hee-Chong, D.L. Severson, M. Tokuda, S.M. Chong, and D.M. Waisman**. 19860. Inhibition of phospholipase A2 by protein I. Biochem. Biophys. Res. Comm. **139**:455-460.

59. **Bastian, B.C., C. Sellert, A. Seekamp, J. Romisch, E.P. Paques, and E.B. Brocker**. 1993. Inhibition of human skin phospholipase A2 by 'lipocortins' is an indirect effect of substrate/lipocortin interaction. J. Invest. Dermatol. **101**:359-363.

60. **Huang, K.S., P. McGray, R.J. Mattaliano, C. Burne, E.P. Chow, L.K. Sinclair, and R.B. Pepinsky**. 1987. Purification and characterization of proteolytic fragments of lipocortin I that inhibit phospholipase A2. J. Biol. Chem. **262**:7639-7645.

61. **Cirino, G., C. Cicala, L. Sorrentino, G. Ciliberto, G. Arpaia, M. Perretti, and R.J. Flower**. 1993. Anti-inflammatory actions of an N-terminal peptide from lipocortin I. Br. J. Pharmacol. **108**:573-574.

62. **Russo-Marie, F.** 1992. Annexins, phospholipase A_2 and the glucocorticoids., p. 35-46. In S.E. Moss (ed.), The Annexins. Portland Press Research Monography, Chappel Hill.

63. **Russo-Marie, F.** 1992. Annexins, phospholipase A_2 and the glucocorticoids., p. 35-46. In S.E. Moss (ed.), The Annexins. Portland Press Research Monography, Chappel Hill.

64. **Kim, S., J. Ko, J.H. Kim, E.C. Choi, and D.S. Na**. 2001. Differential effects of annexins I, II, III, and V on cytosolic phospholipase A2 activity: specific interaction model. FEBS Lett. **489**:243-248.

65. **Errasfa, M. and F. Russo-Marie**. 1989. A purifed lipocortin shares the anti-inflammatory effect of glucocorticosteroids in vivo in mice. Br. J. Pharmacol. **97**:1051-1058.

66. **Cirino, G., S.H. Peers, R.J. Flower, J.L. Browning, and R.B. Pepinsky**. 1989. Human recombinant lipocortin I has acute local anti-inflammatory properties in the rat paw edema test. Proc.Natl.Acad.Sci U.S.A. **89**:3428-3432.

67. **Rojas, E., N. Arispe, H.T. Haigler, A.L. Burns, and H.B. Pollard**. 1992. Identification of annexins as calcium channels in biological membranes. Bone and Mineral **17**:214-218.

68. **Pollard, H.B., H.R. Guy, N. Arispe, M. de la Fuente, G. Lee, E. Rojas, J.R. Pollard, M. Srivastava, Z.Y. Zhang-Keck, N. Merezhinskaya, and et al**. 1992. Calcium channel and membrane fusion activity of synexin and other members of the annexin gene family. Biophys. J. **62**:15-18.

69. **Rojas, E. and H.B. Pollard**. 1987. Membrane capacity measurements suggest a calcium-dependent insertion of synexin into phosphatidylserine bilayers. FEBS Lett. **217**:25-31.

70. **Pollard, H.B. and E. Rojas**. 1988. Calcium-activated synexin forms highly selective, voltage gated calcium channels in phosphatidylserine bilayer membranes. Proc.Natl.Acad.Sci U.S.A. **85**:2974-2978.

71. **Burns, A.L., K. Magendzo, A. Shirvan, M. Srivastava, E. Rojas, M.R. Alijani, and H.B. Pollard**. 1989. Calcium channel activity of purified human synexin and structure of the human synexin gene. Proc.Natl.Acad.Sci.USA **86**:3798-3802.

72. **Berendes, R., A. Burger, D. Voges, P. Demange, and R. Huber**. 1993. Calcium influx through annexin V ion channels into large unilamellar vesicles measured with fura-2. FEBS Lett. **317**:131-134.

73. **Rojas, E., H.B. Pollard, H.T. Haigler, C. Parra, and A.L. Burns**. 1990. Calcium-activated endonexin II forms calcium channels across acidic phospholipid bilayer membranes. J. Biol. Chem. **265**:21207-21215.

74. **Rojas, E., H.B. Pollard, H.T. Haigler, C. Parra, and A.L. Burns**. 1990. Calcium-activated endonexin II forms calcium channels across acidic phospholipid membranes. J. Biol. Chem. **265**:21207-21215.

75. **Berendes, R., D. Voges, P. Demange, R. Huber, and A. Burger**. 1993. Structure-function analysis of the ion channel selectivity filter in human annexin V. Science **262**:427-430.

76. **Waisman, D.M.** 1995. Annexin II tetramer: structure and function. Mol. Cell. Biochem. **149/150**:301-322.

77. **Glenney, J.R., Jr.** 1985. Phosphorylation of p36 *in vitro* with $pp60^{src}$. Regulation by Ca^{2+} and phospholipid. FEBS Lett. **192**:79-82.

78. **Hagiwara, M., M. Ochiai, K. Owada, T. Tanaka, and H. Hidaka**. 1988. Modulation of tyrosine phosphorylation of p36 and othe substrates by the S-100 protein. J. Biol. Chem. **263**:6348-6441.

79. **Karasik, A., R.B. Pepinsky, S.E. Shoelson, and C.R. Kahn**. 1988. Lipocortins 1 and 2 as substrates for the insulin receptor kinase in rat liver. J. Biol. Chem. **263**:11862-11867.

80. **Isacke, C.M., I.S. Trowbridge, and T. Hunter**. 1986. Modulation of p36 phosphorylation in human cells: studies using anti-p36 monoclonal antibodies. Mol. Cell Biol. **6**:2745-2751.

81. **Weber, K., N. Johnsson, U. Plessmann, P.N. Van, H.D. Soling, C. Ampe, and J. Vandekerckhove**. 1987. The amino acid sequence of protein II and its phosphorylation site for protein kinase C; the domain structure Ca2+-modulated lipid binding proteins. EMBO J **6**:1599-1604.

82. **Gould, K.L., J.R. Woodgett, C.M. Isacke, and T. Hunter**. 1986. The protein-tyrosine kinase substrate p36 is also a substrate for protein kinase C in vitro and in vivo. Molecular & Cellular Biology **6**:2783-2744.

83. **Johnsson, N., P. Nuguyen-Van, H.D. Soling, and K. Weber**. 1986. Functionally distinct serine phosphorylation site of p36, the cellular substrate of retroviral protein kinase; differential inhibition of reassociation with p11. EMBO J. **5**:3455-3460.

84. **Jost, M. and V. Gerke**. 1996. Mapping of a regulatory important site for protein kinase C phosphorylation in the N-terminal domain of annexin II. Biochim. Biophys. Acta **1313**:283-289.

85. **Johnsson, N., J. Vandekerckhove, J. Van-Damme, and K. Weber**. 1986. Binding sites for calcium, lipid, and p11 on the p36 substrate of retroviral tyrosine-specific kinase. FEBS Lett. **198**:361-364.

86. **Erikson, E., H.G. Tomasiewicz, and R.L. Erikson**. 1984. Biochemical characterization of a 34-kilodalton normal cellular substrate of pp60v-srcand an associated 6-kilodalton protein. Mol. Cell Biol. **4**:77-85.

87. **Glenney, J.R., Jr.** 1986. Phospholipid dependent Ca^{2+} binding by the 36-kDa tyrosine kinase substrate (calpactin) and its 33-kDa core. J. Biol. Chem. **261**:7247-7252.

88. **Johnsson, N., G. Marriott, and K. Weber**. 1988. p36, the major cytoplasmic substrate of src tyrosine protein kinase, binds to its p11 regulatory subunit via a short amino-terminal amphiphatic helix. EMBO J. **7**:2435-2442.

89. **Becker, T., K. Weber, and N. Johnsson**. 1990. Protein-protein recognition via short amphiphilic helices; a mutational analysis of the binding site of annexin II for p11. EMBO J. **9**:4207-4213.

90. **Kube, E., T. Becker, K. Weber, and V. Gerke**. 1992. Protein-protein interaction studied by site-directed mutagenesis. Characterization of the annexin II-binding site on p11, a member of the S100 protein family. J. Biol. Chem. **267**:14175-14182.

91. **Rety, S., J. Sopkova, M. Renouard, D. Osterloh, V. Gerke, S. Tabaries, F. Russo-Marie, and A. Lewit-Bentley**. 1999. The crystal structure of a complex of p11 with the annexin II N-terminal peptide. Nat. Struct. Biol **6**:89-95.

92. **Lewit-Bentley, A., S. Rety, S.J. Sopkova-de Oliveira, and V. Gerke**. 2000. S-100-annexin complexes: some insights from structural studies. Cell Biol. Int. **24**:799-802.

93. **Sopkova-de Oliveira, S.J., F.K. Oling, S. Rety, A. Brisson, J.C. Smith, and A. Lewit-Bentley**. 2000. S100 protein-annexin interactions: a model of the (ANx2-p11)(2) heterotetramer complex. Biochim. Biophys. Acta **1498**:181-191.

94. **Ayala-Sanmartin, J., J.P. Henry, and L.-A. Pradel**. 2001. Cholesterol regulates membrane binding and aggregation by annexin 2 at submicromolar Ca^{2+} concentrations. Biochim. Biophys. Acta. **1510**:18-28.

95. **Ayala-Sanmartin, J.** 2001. Cholesterol enhances phospholipid binding and aggregation of annexins by their core domain. Biochem. Biophys. Res. Comm. **283**:72-79.

96. **Powell, M.A. and Jr.J.R. Glenney**. 1987. Regulation of calpactin I phospholipid binding by calpactin I light chain binding and phosphorylation by p60v-src. Biochem. J. **247**:321-328.

97. **Drust, D.S. and C.E. Creutz**. 1988. Aggregation of chromaffin granules by calpactin at micromolar levels of calcium. Nature **331**:88-91.

98. **Johnstone, S.A., I. Hubaishy, and D.M. Waisman**. 1992. Phosphorylation of annexin II tetramer by protein kinase C inhibits aggregation of lipid vesicles by the protein. J. Biol. Chem. **267**:25976-25981.

99. **Liu, L., A.B. Fisher, and U.J. Zimmerman**. 1995. Lung annexin II promotes fusion of isolated lamellar bodies with liposomes. Biochim. Biophys. Acta. **1259**:166-172.

100. **Mayorga, L.S., W. Beron, M.N. Sarrouf, M.I. Colombo, C. Creutz, and P.D. Stahl**. 1994. Calcium-dependent fusion among endosomes. J. Biol. Chem. **269**:30927-30934.

101. **Filipenko, N.R. and D.M. Waisman** . 2001. The C-terminus of annexin II mediates binding to F-actin. J. Biol. Chem. **269**:30927-30934.

102. **Jones, P.G., G.J. Moore, and D.M. Waisman**. 1992. A nonapeptide to the putative F-actin binding site of annexin-II tetramer inhibits its calcium-dependent activation of actin filament bundling. J. Biol. Chem. **267**:13993-13997.

103. **Ma, A.S., M.E. Bystol, and A. Tranvan**. 1994. *In vitro* modulation of filament bundling in F-actin and keratins by annexin II and calcium. In Vitro Cell Dev. Biol. Animal 329-335.

104. **Ikebuchi, N.W. and D.M. Waisman**. 1990. Calcium-dependent regulation of actin filament bundling by lipocortin-85. J. Biol. Chem. **265**:3392-3400.

105. **Regnouf, F., A. Rendon, and L.A. Pradel**. 1991. Biochemical characterization of annexins I and II isolated from pig nervous tissue. J. Neurochem. **56**:1985-1996.

106. **Bellagamba, C., I. Hubaishy, J.D. Bjorge, S.L. Fitzpatrick, D.J. Fujita, and D.M. Waisman**. 1997. Tyrosine phosphorylation of annexin II tetramer is stimulated by membrane binding. J. Biol. Chem. **6**:3195-3199.

107. **Delouche, B., L.A. Pradel, and J.P. Henry**. 1997. Phosphorylation by protein kinase C of annexin 2 in chromaffin cells stimulated by nicotine. J. Neurochem. **68**:720-727.

108. **Brambilla, R., R. Zippel, E. Sturani, L. Morello, A. Peres, and L. Alberghina**. 1991. Characterization of the tyrosine phosphorylation of calpactin I (annexin II) induced by platelet-derived growth factor. Biochem. J. **278**:447-452.

109. **Hubaishy, I., P.G. Jones, J. Bjorhe, C. Bellagambe, S.L. Fitzpatrick, D.J. Fujita, and D.M. Waisman**. 1995. Modulation of annexin II tetramer by tyrosine phosphorylation. Biochem. **34**:14527-14534.

110. **Ayala-Sanmartin, J., P. Gouache, and J.P. Henry**. 2000. The N-terminal domain of annexin 2 regulates the Ca^{2+}-dependent membrane aggregation by the protein core domain: a site directed mutagenisis study. Biochem. **39**:15190-15198.

111. **Regnouf, F., I. Sagot, B. Delouche, G. Devilliers, J. Cartaud, J.-P. Henry, and L.-A. Pradel**. 1995. "In vitro" phosphorylation of annexin II tetramer by protein kinase C: Comparative properties of the unphosphoryated and phosphorylated annexin II on the aggregation

and fusion of chromaffin granule membranes. J. Biol. Chem. **270**:27143-27150.

112. **Pietrobon, D., F. Di Virgilio, and T. Pozzan**. 1990. Structural and functional aspects of calcium homeostasis in eukaryotic cells. Eur. J. Biochem. **193**:599-622.

113. **Courtneidge, S., R. Ralston, K. Alitalo, and J.M. Bishop**. 1983. Subcellular localization of an abundant substrate (p36) for tyrosine specific protein kinases. Mol. Cell Biol. **3**:340-350.

114. **Thiel, C., M. Osborn, and V. Gerke**. 1992. The tight association of the tyrosine kinase substrate annexin II with the submembranous cytoskeleton depends on intact p11- and Ca(2+)-binding sites. J. Cell Sci. **103**:733-742.

115. **Osborn, M., N. Johnsson, J. Wehland, and K. Weber**. 1988. The submembranous location of p11 and its interaction with the p36 substrate of pp60 src kinase in situ. Exp. Cell Res. **175**:81-96.

116. **Hajjar, K.A., C.A. Guevara, E. Lev, K. Dowling, and J. Chacko**. 1996. Interaction of the fibrinolytic receptor, annexin II, with the endothelial cell surface: Essential role of endonexin repeat 2. J. Biol. Chem. **271**:21652-21659.

117. **Yeatman, T.J., T.V. Updyke, M.A. Kaetzel, J.R. Dedman, and Nicolson.G.L.** 1993. Expression of annexins on the surface of non-metastatic and metastatic human and rodent tumor cells. Clin. Exp. Metastasis **11**:37-44.

118. **Wright, J.F., A. Kurosky, and S. Wasi**. 1994. An endothelial cell-surface form of annexin II binds human cytomegalovirus. Biochem. Biophys. Res. Comm. **198**:983-989.

119. **Hajjar, K.A., A.T. Jacovina, and J. Chacko**. 1994. An endothelial cell receptor for plasminogen/tissue plasminogen activator: Identity with annexin II. J. Biol. Chem. **269**:21191-21197.

120. **Kassam, G., K.-S. Choi, J. Ghuman, H.-M. Kang, S.L. Fitzpatrick, T. Zackson, S. Zackson, M. Toba, A. Shinomiya, and D.M. Waisman**. 1998. The role of annexin II tetramer in the activation of plasminogen. J. Biol. Chem. **273**:4790-4799.

121. **Siever, D.A. and H.P. Erickson**. 1997. Extracellular annexin II. Int. J. Biochem. Cell Biol. **29**:1219-1223.

122. **Jindal, H.K., W.G. Chaney, C.W. Anderson, R.G. Davis, and J.K. Vishwanatha**. 1991. The protein-tyrosine kinase substrate, calpactin

I heavy chain (p36), is part of the primer recognition protein complex that interacts with DNA polymerase alpha. J. Biol. Chem. **266**:5169-5176.

123. **Vishwanatha, J.K. and S. Kumble**. 1993. Involvement of annexin II in DNA replication: Evidence from cell free extracts of *Xenopus* eggs. J. Cell Sci. **105**:533-540.

124. **Hajjar, K.A. and S. Krishnan**. 1999. Annexin II: A mediator of the plasmin/plasminogen activator system. Trends in Cardiovas. Med. **9**:128-138.

125. **Raynor, C.M., J.F. Wright, D.M. Waisman, and E.L.G. Pryzdial**. 1999. Annexin II enhances cytomegalovirus binding and fusion to phospholipid membranes. Biochem. **38**:5089-5095.

126. **Mai, J., D.M. Waisman, and B.F. Sloane**. 2000. Cell surface complex of cathepsin B/annexin II tetramer in malignant progression. Biochim. Biophys. Acta. **1477**:215-230.

127. **Cines, D.B., E.S. Pollak, C.A. Buck, J. Loscalzo, G.A. Zimmerman, R.P. McEver, J.S. Pober, T.M. Wick, B.A. Konkle, B.S. Schwartz, E.S. Barnathan, K.R. McCrae, B.A. Hug, A.-M. Schmidt, and D.M. Stern**. 1998. Endothelial cells in physiology and in the pathophysiology of vascular disorders. Blood **91**:3527-3561.

128. **Hajjar, K.A. and N.M. Hamel**. 1990. Identification and characterization of human endothelial cell membrane binding sites for tissue plasminogen activator and urokinase. J. Biol. Chem. **265**:2908-2916.

129. **Cesarman, G.M., C.A. Guevara, and K.A. Hajjar**. 1994. An endothelial cell receptor for plasminogen/tissue plasminogen activator: Annexin II-mediated enhancement of tPA-dependent plasminogen activation. J. Biol. Chem. **269**:21198-21203.

130. **Hajjar, K.A., L. Mauri, A.T. Jacovina, F. Zhong, U.A. Mirza, J.C. Padovan, and B.T. Chait**. 1998. Tissue plasminogen activator binding to the annexin II tail domain. Direct modulation by homocysteine. J. Biol. Chem. **273**:9987-9993.

131. **Loscalzo, J.** 1996. The oxidant stress of hyperhomocysteinemia. J. Clin. Invest. **98**:5-7.

132. **Ling, Q. and K.A. Hajjar**. 2000. Inhibition of endothelial cell thromboresistence by homocysteine. J. Nutr. **130**:373S-376S.

133. **Kang H.M, K.S. Choi, G. Kassam, S.L. Fitzpatrick, M. Kwon, and D.M. Waisman**. 1999. Role of Annexin II Tetramer in Plasminogen Activation. Trends in Cardiovas. Med. **9**:92-102.

134. **Zolton, R.P. and W.H. Seegers**. 1974. Phospholipid requirements in thrombin formation. Thromb. Res. **4**:437-446.

135. **Rand, J.H.** 2000. The annexinopathies: a new category of diseases. Biochim. Biophys. Acta. **1498**:169-173.

136. **Menell, J.S., G.M. Cesarman, A.T. Jacovina, M.A. McLaughlin, E.A. Lev, and K.A. Hajjar**. 1999. Annexin II and bleeding in acute promyelocytic leukemia. New Eng. J. Med. **340**:994-1004.

137. **Falcone, D.J., W. Borth, K.M. Khan, and K.A. Hajjar**. 2001. Plasminogen-mediated matrix invasion and degradation by macrophages is dependent on surface expression of annexin II. Blood **97**:777-784.

138. **Ishii, H., M. Yoshida, M. Hiraoka, K.A. Hajjar, A. Tanaka, Y. Yasukochi, and F. Numano**. 2001. Recombinant annexin II modulates impaired fibrinolytic activity in vitro and in rat carotid artery. Circ. Res. **89**:1240-1245.

139. **Waitumbi, J.N., M.O. Opollo, R.O. Muga, A.O. Misore, and J.A. Stoute**. 2000. Red cell surface changes and erythrophagocytosis in children with severe *Plasmodium falciparum* anemia. Blood **95 (4)**:1481-1486.

140. **Choi, K.-S., J. Ghuman, G. Kassam, H.-M. Kang, S.L. Fitzpatrick, and D.M. Waisman**. 1998. Annexin II tetramer inhibits plasmin-dependent fibrinolysis. Biochem. **37**:648-655.

141. **Choi, K.-S., S.L. Fitzpatrick, N.R. Filipenko, D.K. Fogg, G. Kassam, A.M. Magliocco, and D.M. Waisman**. 2001. Regulation of plasmin-dependent fibrin clot lysis by annexin II heterotetramer. J. Biol. Chem. **276**:25212-25221.

142. **Wright, J.F., A. Kurosky, and S. Wasi**. 1994. An endothelial cell-surface form of annexin II binds human cytomegalovirus. Biochem. Biophys. Res. Comm. **198**:983-989.

143. **Nowlin, D.M., N.R. Cooper, and T. Compton**. 1991. Expression of a human cytomegalovirus receptor correlates with infectibility of cells. J. Virol. **65**:3114-3121.

144. **Wright, J.F., A. Kurosky, E.L.G. Pryzdial, and S. Wasi**. 1995. Host cellular protein annexin II is associated with cytomegalovirus particles isolated from cultured human fibroblasts. J. Virol. **69**:4784-4791.

145. **Pietropaolo, R.L. and T. Compton** . 1997. Direct interaction between human cytomegalovirus glycoprotein B and cellular annexin II. J. Virol. **71**:9803-9807.

146. **Reis, B., E. Bogner, M. Reschke, A. Richter, T. Mockenhaupt, and K. Radsak**. 1993. Stable Constitutive Expression of Glycoprotein-B (gpUL55) of Human Cytomegalovirus in Permissive Astrocytoma Cells. J. Gen. Virol. **74**:1371-1379.

147. **Derry, M.C., C.M. Restall, D.M. Waisman, and E.L. Pryzdial**. 2001. Annexin 2 tetramer enhances cytomegalovirus infection. J. Virol. **submitted**

148. **Wirl, G. and R. Schwartz-Albiez**. 1990. Collagen-binding proteins of mammary epithelial cells are related to Ca2(+)- and phospholipid-binding annexins. J. Cell Physiol. **144**:511-522.

149. **Cloutier, Y., F. Lagier, R. Lemieux, M.C. Blais, C. St-Arnaud, A. Cartier, and J.L. Malo**. 1989. New methodology for specific inhalation challenges with occupational agents in powder form. Eur. Respir. J. **2**:769-777.

150. **Vishwanatha, J.K., Y. Chiang, K.D. Kumble, P.M. Holingsworth, and P.M. Pour**. 1993. Enhanced expression of annexin II in human pancreatic carcinoma cells and primary pancreatic cancers. Carcinogenesis **14**:2575-2579.

151. **Kumble, K.D., M. Hirota, P.M. Pour, and J.K. Vishwanatha**. 1992. Enhanced levels of annexins in pancreatic cacinoma cells of Syrian hamsters and their intrapancreatic allografts. Cancer Res. **52**:163-167.

152. **Cole, S.P., M.J. Pinkoski, G. Bhardwaj, and R.G. Deeley**. 1992. Elevated expression of annexin II (lipocortin II, p36) in a multidrug resistant small cell lung cancer cell line. Br. J. Cancer **65**:498-502.

153. **Reeves, S.A., C. Chavez-Kappel, R. Davis, M. Rosenblum, and M.A. Israel**. 1992. Developmental regulation of annexin II (lipocortin 2) in human brain and expression in high grade glioma. Cancer Res. **52**:6871-6876.

154. **Frohlich, M., P. Mottë, K. Galvin, H. Takahashi, J. Wands, and M. Ozturk**. 1990. Enhanced expression of the protein kinase substrate p36 in human hepatocellular carcinoma. Mol. Cell Biol. **10**:3216-3223.

155. **Chiang, Y., R.G. Davis, and J.K. Vishwanatha**. 1996. Altered expression of annexin II in human B-cell lymphoma cell lines. Biochim. Biophys. Acta. **1313**:295-301.

156. **Fox, M.T., D.A. Prentice, and J.P. Hughes**. 1991. Increases in p11 and annexin II proteins correlate with differentiation in the PC12 pheochromocytoma. Biochem. Biophys. Res. Commun. **177**:1188-1193.

157. **Harder, T., C. Thiel, and V. Gerke**. 1993. Formation of the annexin II2p112 complex upon differentiation of F9 teratocarcinoma cells. J Cell Sci. **104**:1109-1117.

158. **Tressler, R.J., T.V. Updyke, T.J. Yeatman, and G.L. Nicolson**. 1993. extracellular annexin II is associated with divalent cation-dependent tumor cell-endothelial cell adhesion of metastatic RAW117 large-cell lymphoma cells. J. Cell Biochem. **53**:265-276.

159. **Mai, J., R.L. Finley, D.M. Waisman, and B.F. Sloane**. 2000. Human procapthepsin B interacts with the annexin II tetramer on the surface of tumor cells. J. Biol. Chem. **275**:12806-12812.

160. **Engelkamp, D., B.W. Schafer, M.G. Mattei, P. Erne, and C.W. Heizmann**. 1993. Six S100 genes are clustered on human chromosome 1q21: identification of two genes coding for the two previously unreported calcium binding proteins S100D and S100E. Proc.Natl.Acad.Sci.U.S.A. **9**:6547-6551.

161. **Cochrane, A.J., H.F. Lu, P.X. Li, R. Saxton, and D.R. Wen**. 1993. S-100 proteins remains a practical marker for melanocytic and other tumors. Melanoma Res. **3**:325-330.

162. **Davies, B.R., M.P. Davie, F.E. Gibbs, R. Barraclough, and P. Rudland**. 1993. Induction of the metastatic phenotype by transfection of a benign rat mammary epithelial cell line with the gene for p9Ka, a rat calcium binding protein, but not with oncogene EJ-ras-1. Oncogene **8**:999-1008.

163. **Schafer, B.W. and C.W. Heizmann**. 1996. The S100 Family of EF-hand calcium-binding proteins: functions and pathology. Trends Biochem. Sci. **21**:134-140.

164. **Mann, K.G. and R.L. Lundblad**. 1982. Biochemistry of thrombin, p. 112-126. In R.W. Colman, J. Hirsh, V.J. Marder, and E.W. Salzman (eds.), Hemostasis and thrombosis: Basic principles and clinical practice. J. B. Lippincott Company, Philadelphia.

165. **Jackson, C.M.** 1982. Mechanisms of protrhombin activation, p. 100-111. In R.W. Colman, J. Hirsh, V.J. Marder, and E.W. Salzman (eds.), Hemostasis and thrombosis: basic principles and clinical practice. J. B. Lippincott Company, Philadelphia.

166. **Brass, L.F. and M. Molino**. 1997. Protease-activated G protein-coupled receptors on human platelets and endothelial cells. Thrombosis & Haemostasis **78**:234-241.

167. **Lottenberg, R., J.A. Hall, J.W. Fenton, and C.M. Jackson**. 1982. The action of thrombin on peptide p-nitroaniline substrates: hydrolysis of Tos-Gly-Pro-Arg-pNA and D-Phe-Pip-Arg-pNA by human alpha and gamma and bovine alpha and beta-thrombins. Thromb. Res. **28**:313-332.

168. **Lundblad, R.L., M.E. Nesheim, D.L. Straight, S. Sailor, J. Bowie, J.W. Jenzano, J.D. Roberts, and K.G. Mann**. 1984. Bovine alpha- and beta-thrombin. Reduced fibrinogen-clotting activity of beta-thrombin is not a consequence of reduced affinity for fibrinogen. J. Biol. Chem. **259**:6991-6995.

169. **Takahashi, K., M. Aiken, J.W. Fenton, and D.A. Walz**. 1984. Thrombospondin fragmentation by alpha-thrombin and resistance to gamma-thrombin. Biochem. J. **224**:673-676.

170. **Jandl, J.H.** 1987. Hemostasis, p. 1213-1274. In J.H. Jandl (ed.), Blood: texbook of hematology. Little, Brown and Company, New York.

171. **Stubbs, M.T. and W. Bode**. 1995. The clot thickens: clues provided by thrombin structure. Trends Biochem. Sci. **20**:23-28.

172. **Zwaal, R.F. and A.J. Schroit**. 1997. Pathophysiologic implications of membrane phospholipid asymmetry in blood cells. Blood **89**:1121-1132.

173. **Bevers, E.M., P. Comfurius, D.W.C. Dekkers, M. Harmsma, and R.F. Zwaal**. 1998. [review] Transmembrane phospholipid distribution in blood cells: control mechanisms and pathological significance. Biol.Chem. **379**:973-986.

174. **Sutherland, M.R., C.M. Raynor, H. Leenknegt, J.F. Wright, and E.L.G. Pryzdial**. 1997. Coagulation initiated on herpesviruses. Proc.Natl.Acad.Sci.USA **94**:13510-13514.

175. **Sugama, Y. and A.B. Malik**. 1992. Thrombin Receptor-14 Amino Acid Peptide Mediates Endothelial Hyperadhesivity and Neutrophil Adhesion by P- Selectin Dependent Mechanism. Circ. Res **71**:1015-1019.

176. **Woolkalis, M.J., D.R. Manning, and L.F. Brass**. 1990. Opposite effects of thrombin on cAMP formation in human platelets and endothelial cells. J. Cell Biol. **111**:215a

177. **Tesfamariam, B., G.T. Allen, A. Normandin, and M.J. Antonaccio**. 1993. Involvement of the "tethered ligand" receptor in thrombin-induced endothelium-mediated relaxations. Am. J Physiol. **265**:H1744-H1749

178. **Schini, V.B., H. Hendrickson, D.M. Heublein, J.C.J. Burnett, and P.M. Vanhoutte**. 1989. Thrombin enhances the release of endothelin from cultured porcine endothelial cells. Eur. J. Pharmacol. **165**:333-334.

179. **Pollock, W.K., K.A. Wreggett, and R.F. Irvine**. 1988. Inositol phosphate production and Ca^{2+} mobilization in human umbilical vein endothelial cells stimulated by thrombin. Biochem. J. **256**:371-376.

180. **Magazine, H.I., J.M. King, and K.D. Srivastava**. 1996. Protease activated receptors modulate aortic vascular tone. Int. J. Cardiol. **53**:S75-S80

181. **Garcia, J.G.N., F.M. Pavalko, and C.E. Patterson**. 1995. Vascular endothelial cell activation and permeability responses to thrombin. Blood Coagulat. Fibrinol. **6**:609-626.

182. **Bartha, K., R. Muller-Peddinghaus, and L.A.A. van Rooijen**. 1989. Bradykinin and thrombin effects on polyphosphoinositide hydrolysis and prostacyclin production in endothelial cells. Biochem. J. **263**:149-155.

183. **Brock, T.A. and E.L. Capasso**. 1989. GTPγS increases thrombin-mediated inositol triphosphate accumulation in permeabilized human endothelial cells. Am. Rev. Respir. Dis. **140**:1121-1125.

184. **Hou, L., G.L. Howells, S. Kapas, and M.G. Macey**. 1998. The protease-activated receptors and their cellular expression and function in blood related cells. Br. J. Haematol. **101**:1-9.

185. **Vu, T.-K., D.T. Hung, V.I. Wheaton, and S.R. Coughlin**. 1991. Molecular cloning of a functional thrombin receptor reveals a novel proteolytic mechanism of receptor activation. Cell **64**:1057-1068.

186. **Rasmussen, U.B., V. Vouret-Craviari, S. Jallat, Y. Schlesinger, G. Pages, A. Pavirani, J.-P. Lecocq, and E. van Obberghen-Schilling**. 1991. cDNA clonning and expression of hamster α-thrombin receptor coupled to Ca^{2+} mobilization. FEBS Lett. **288**:123-128.

187. **Ishihara, H., A.J. Connolly, D. Zeng, M.L. Kahn, Y.W. Zheng, C. Timmons, T. Tram, and S.R. Coughlin**. 1997. Protease-activated

receptor 3 is a second thrombin receptor in humans. Nature **386**:502-506.

188. **Kahn, M.L., Y.W. Zhen, W. Huang, V. Bigornia, D. Zeng, S. Moff, R.V.J. Farese, C. Tam, and S.R. Coughlin**. 1998. A dual thrombin receptor for platelet activation. Science **394**:690-694.

189. **Xu, W.-F., H. Andersen, T.E. Whitmore, S.R. Presnell, D.P. Yee, A. Ching, T. Gilbert, E.W. Davie, and D.C. Foster**. 1998. Cloning and characterization of human protease-activated receptor 4. Proc.Natl.Acad.Sci.USA **95**:6642-6646.

190. **Lasne, D., J. Donato, H. Falet, and F. Rendu**. 1995. Different abilities of thrombin receptor activating peptide and thrombin to induce platelet calcium rise and full release. Thrombosis & Haemostasis **74**:1323-1328.

191. **Kahn, M.L., M. Nakanishi-Matsui, M.J. Shapiro, H. Ishihara, and S.R. Coughlin**. 1999. Protease-activated receptors 1 and 4 mediate activation of human platelets by thrombin. J. Clin. Invest. **103**:879-887.

192. **Liu, L., T.-K. Vu, C.T. Bemon, and S.R. Coughlin**. 1991. The region of the thrombin receptor resembling hirudin binds to thrombin and alters enzyme specificity. J. Biol. Chem. **266**:16977-16980.

193. **Garcia, J.G.N., C. Patterson, C. Bahler, J. Aschner, C.M. Hart, and D. English**. 1993. Thrombin receptor activating peptides induce Ca^{2+} mobilization , barrier dysfunction, prostaglandin synthesis, and platelet-derived growth factor synthesis in cultured endothelium. J. Cell Physiol. **156**:541-549.

194. **Muramatsu, I., A. Laniyonu, G.J. Moore, and M.D. Hollenberg**. 1992. Vascular actions of the thrombin receptor peptide. Can. J. Physiol. Pharmacol. **70**:996-1003.

195. **Tiruppathi, C., H. Lum, T.T. Andersen, J.W.I. Fenton, and A.B. Malik**. 1992. Thrombin receptor 14-amino acid peptide binds to endothelial cells and stimulates calcium transients. Am. J. Physiol. **263**:L595-L601

196. **McCarthy, S.A., I. Kuzu, K.C. Gatter, and R. Bicknell**. 1991. Heterogeneity of the endothelial cell and its role in organ preference of tumour metastasis. TiPS **12**:462-467.

197. **Gerritsen, M.E.** 1987. Functional heterogeneity of vascular endothelial cells. Biochemical Pharmacology **36**:2701-2711.

198. **Risau, W.** 1995. Differentiation of endothelium. FASEB J. **9**:926-933.

199. **Kvietys, P.R. and D.N. Granger**. 1997. Endothelial cell monolayers as a tool for studying microvascular pathophysiology. Am. J. Physiol. **273**:G1189-G1199

200. **Preissner, K.T.** 1990. Physiological role of vessel wall related antithrombotic mechanisms: Contribution of endogenous and exogenous heparin-like components to the anticoagulant potential of the endothelium. Haemostasis **20**:30-49.

201. **Plow, E.F., J. Felez, and L.A. Miles**. 1991. Cellular regulation of fibrinolysis. Thrombosis & Haemostasis **66**:32-36.

202. **Hajjar, K.A.** 1995. Cellular receptors in the regulation of plasmin generation. Thrombosis & Haemostasis **74**:294-301.

203. **Hajjar, K.A., N.M. Hamel, P.C. Harpel, and R.L. Nachman**. 1987. Binding of plasminogen to cultured human endothelial cells. J. Clin. Inv. **80**:1712-1719.

204. **Ganz, P.R., D. Dupuis, A.K. Dudani, and S. Hashemi**. 1991. Characterization of plasminogen binding to human capillary and arterial endothelial cells. Biochem. Cell Biol. **69**:442-448.

205. **Kassam, G., B.-H. Le, K.-S. Choi, H.-M. Kang, S.L. Fitzpatrick, P. Louie, and D.M. Waisman**. 1998. The p11 subunit of the annexin II Tetramer Plays a Key Role in the Stimulation of t-PA-Dependent Plasminogen Activation. Biochem. **37**:16958-16966.

206. **Miles, L.A., C.M. Dahlberg, J. Plescia, J. Felez, K. Kato, and E.F. Plow**. 1991. Role of cell-surface lysines in plasminogen binding to cells: Identification of alpha-enolase as a candidate plasminogen receptor. Biochem. **30**:1682-1691.

207. **Redlitz, A., B.J. Fowler, E.F. Plow, and L.A. Miles**. 1995. The role of an enolase-related molecule in plasminogen binding to cells. Eur.J Biochem. **227**:407-415.

208. **Dudani, A.K., C. Cummings, S. Hashemi, and P.R. Ganz**. 1993. Isolation of a novel 45 kDa plasminogen receptor from human endothelial cells. Thromb. Res **69**:185-196.

209. **Dudani, A.K., A. Pluskota, and P.R. Ganz**. 1994. Interaction of tissue plasminogen activator with the endothelial cell 45 kDa plasminogen receptor. Biochem. Cell Biol. **72**:126-131.

210. **Dudani, A.K. and P.R. Ganz**. 1996. Endothelial cells surface actin serves as a binding site for plasminogen, tissue plasminogen activator, and lipoprotein (a). Br. J. Haematol. **95**:168-178.

211. **Miles, L.A., C.M. Dahlberg, E. Levin, and E.F. Plow**. 1989. Gangliosides interact directly with plasminogen and urokinase and may mediate binding of these fibrinolytic components to cells. Biochem. **28**:9337-9343.

212. **Loyd, K.O. and K. Furukawa**. 1998. Biosynthesis and function of gangliosides- Recent advances. Glycoconjugate J. **15**:627-636.

213. **Felez, J., C.J. Chanquia, P. Fabregas, E.F. Plow, and L.A. Miles**. 1993. Competition between plasminogen and tissue plasminogen activator for cellular binding sites. Blood **82 (8)**:2433-2441.

214. **Fukao, H. and O. Matsuo**. 1998. Analysis of tissue-type plasminogen activator receptor (t-PAR) in human endothelial cells. Semin. Thromb. Haemost. **24**:269-273.

215. **Molino, M., M.J. Woolkalis, J. Reavy-Catewell, D. Pratico, P. Andrade-Gordon, E.S. Barnathan, and L.F. Brass**. 1997. Endothelial cell thrombin receptors and PAR-2: Two protease-activated receptors located in a single cellular environment. J. Biol. Chem. **272**:11133-11141.

216. **Cupit, L.D., V.A. Schmidt, and W.F. Bahou**. 1999. Proteolytically activated receptor-3. A member of an emerging gene family of protease receptors expressed on vascular endothelial cells and platelets. Trends Cardiovasc. Med. **9**:42-48.

217. **Hein, L., K. Ishii, S.R. Coughlin, and B.K. Kobilka**. 1994. Intracellular targeting and trafficking of thrombin receptors. A novel mechanism for resensitization of a G protein-coupled receptor. J. Biol. Chem. **269**:27719-27726.

218. **Horvat, R. and G.E. Palade**. 1995. The functional thrombin receptor is associated with plasmalemma and a large endosomal network in cultured human umbilical vein endothelial cells. J. Cell Sci. **108**:1155-1164.

219. **Camerer, E., J.A. Rottingen, E. Gjernes, K. Larsen, A.H. Skartlien, J.G. Iversen, and H. Prydz**. 1999. Coagulation factors VIIa and Xa induce cell signaling leading to up-regulation of the erg-1 gene. J. Biol. Chem. **274**:32225-32233.

220. **Bono, F., P. Schaeffer, J.P. Herault, C. Michaux, A.L. Nestor, J.C. Guillemot, and J.M. Herbert**. 2000. Factor Xa activated endothelial

celis by a receptor cascade between EPR-1 and PAR-2. Arterioscler. Thrombo. Vasc. Biol. **20**:E107-E112

221. **Kawabata, A., R. Kuroda, Y. Nakaya, K. Kawai, H. Nishikawa, and N. Kawao**. 2001. Factor xa-evoked re;axation in rat aorta: Involvement of PAR-2. Biochem. Biophys. Res. Comm. **282**:432-435.

222. **Riewald, M., V.V. Kravchenko, P.J. Petrovan, P.J. O'Brien, L.F. Brass, R.J. Ulevitch, and W. Ruf**. 2001. Gene induction by coagulation factor Xa is mediated by activation of protease activated receptor-1. Blood **97**:3109-3116.

223. **Camerer, E., W. Huang, and S.R. Coughlin**. 2000. Tissue factor- and factor Xa-dependent activation of protease activated receptor-2 by factor VIIa. Proc.Natl.Acad.Sci.U.S A. **97**:5255-5260.

224. **Horrevoets, A.J.G., H. Pannekoek, and M.E. Nesheim**. 1997. Production and characterization of recombinant human plasminogen(S741C-fluorescein): A novel approach to study zymogen activation without generation of active protease. J. Biol. Chem. **272**:2176-2182.

225. **Jaffe, E.A., R.I. Nachman, C.G. Becker, and C.R. Minick**. 1973. J Clin Invest. **52**:2745-2756.

226. **Verweij, C.L.** 1988. Biosynthesis of human von Willebrand factor. Haemostasis **18**:224-245.

227. **Gimbrone, M.A., R.S. Cotran, and J. Folkman**. 1974. Human vascular endothelial cells in culture. Growth and DNA synthesis. J. Cell Biol. **60**:673-684.

228. **Traverso, V., J.F. Morris, R.D. Flower, and J. Buckingham**. 1998. Lipocortin I (annexin I) in patches associated with the membrane of a lung adrenocarcinoma cell line and in the cytoplasm. J. Cell Sci. **111**:1405-1418.

229. **Albrecht, T., I. Boldogh, and M.P. Fons**. 1992. Receptor-initiated activation of cells and their oncogenes by herpes-family viruses. J. Invest. Dermatol. **98**:29S-35S.

230. **Winman, B.** 1980. On the reaction of plasmin or plasmin-streptokinase complex with aprotinin or alpha-2-antiplasmin. Thromb. Res. **17**:143-152.

231. **Ma, A.S.P., D.J. Bell, A.A. Mittal, and H. Harrison**. 1994. Immunocytochemical detection of extracellular annexin II in cultured human skin keratinocytes and isolation of annexin II isoforms enriched in the extracellular pool. J. Cell Sci. **107**:1973-1984.

232. **Damaj, M.I., S.P. Welch, and B.R. Martin**. 1994. Nicotine-induced antinociception in mice: Role of G-proteins and adenylate cyclase. Pharmacology, Biochemistry and Behavior **48**:37-42.

233. **Sagot, I., F. Regnouf, J.P. Henry, and L.A. Pradel**. 1997. Translocation of cytosolic annexin 2 to a Triton-insoluble membrane subdomain upon nicotine stimulation of chromaffin cultured cells. FEBS Lett. **410**:229-234.

234. **Stahlhut, M., K. Sandvig, and B. van Deurs**. 2000. Caveolae: Uniform structure with multiple functions in signaling, cell growth, and cancer. Expt. Cell Res. **261**:111-118.

235. **Kurchalia, T.V. and R.G. Parton**. 1999. Membrane microdomains and caveolae. Curr. Opin. Cell Biol. **11**:424-431.

236. **Harder, T. and V. Gerke**. 1994. The annexin IIp11(2) complex is the major protein component of the triton X-100-insoluble low-density fraction prepared from MDCK cells in the presence of Ca^{2+}. Biochim. Biophys. Acta **1223**:375-382.

237. **Stan, R.V., W.G. Roberts, D. Predescu, K. Ihida, L. Saucan, L. Ghitescu, and G.E. Palade**. 1997. Immunoisolation and partial characterization of endothelial plasmalemmal vesicles (caveolae). Mol. Biol. Cell **8**:595-605.

238. **van der Goot, F.G.** 1997. Separation of early steps in endocytic membrane transport. Electrophoresis **18**:2689-2693.

239. **Senda, T., W. Yu, T. Okabe, N. Sugimoto, and M. Matsuda**. 1998. Widespread association of annexin II with intracellular membrane systems and involvement of annexin II in granule-granule fusion in addition to granule-plasma membrane fusion in anterior pituitary cells. Histochem. J. **30**:331-338.

240. **Nilius, B., V. Gerke, J. Prenen, G. Szucs, S. Heinke, K. Weber, and g. Droogmans**. 1996. Annexin II modulates volume-activated chloride currents in vascular endothelial cells. J. Biol. Chem. **271**:30631-30636.

241. **Fukao, H., S. Ueshima, K. Okada, and O. Matsuo**. 2000. Binding of mutant tissue-type plasminogen activators to human endothelial cells and their extracellular matrix. Life Sci. **66 (25)**:2473-2487.

242. **Brooks, N.D., J.E. Grundy, N. Lavigne, M.C. Derry, C.M. Restall, C.R. Mackenzie, D.M. Waisman, and E.L.G. Pryzdial**. 2001. Calcium-dependent, phospholipid-independent binding of annexin II to annexin V. (UnPub)

243. **Daniel, T.O., V.C. Gibbs, D.F. Milfay, M.R. Gavaroy, and L.T. Williams**. 1986. Thrombin stimulates c-sis gene expression in microvascular endothelial cells. J. Biol. Chem. **261**:9579-9582.

244. **Chen, X.M., Q.N. He, W.H. Liu, Q.H. Xu, Y.Z. Ye, B. Fu, and L.F. Yu**. 2000. AP-1 mediated signal transduction in thrombin-induced regulation of PAI-1 expression in human mesangial cells. Chin. Med. J. **113**:514-519.

245. **Liu, W.H., X.M. Chen, and B. Fu**. 2000. Thrombin stimulates MMP-9 mRNA expression through AP-1 pathway in human mesangial cells. Acta Pharmacologica Sinica **21**:641-645.

246. **Anrather, D., M.T. Millan, A. Palmetshofer, S.C. Robson, C. Geczy, A.J. Ritchie, F.H. Bach, and B.M. Ewenstein**. 1997. Thrombin activates nuclear factor-κB and potentiates endothelial cell activation by TNF[1]. The Journal of Immunology **159**:5620-5628.

247. **Nakajima, T., I. Kitajima, H. Shin, I. Takasaki, K. Shigeta, K. Abeyama, Y. Yamashita, T. Tokioka, Y. Soejima, and I. Murayama**. 1994. Involvement of NF-kappa-B activation in thrombin-induced human vascular smooth muscle cell proliferation. Biochem. Biophys. Res. Comm. **204**:950-958.

248. **Stenina, O.I., E.J. Poptic, and P.E. Dicorleto**. 2000. Thrombin activate a Y box-binding protein (DNA-binding protein B) in endothelial cells. Journal of Clinical Investigation **106**:579-587.

249. **Quandt, K., K. Frech, H. Karas, E. Wingender, and T. Werner**. 1995. MatInd and MatInspector- New fast and versatile tools for detection of consensus matches in nucleotide sequence data. Nucleic Acids Res. **23**:4878-4884.

250. **Sower, L.E., D.A. Payne, R. Meyers, and D.H. Carney**. 1999. Thrombin peptide, TP508, induces differential gene expression in fibroblasts through a non-proteolytic activation pathway. Expt. Cell Res. **247**:422-431.

251. **Meyer, T.** 1991. Cell signaling by second messenger waves. Cell **64**:675-678.

252. **Barwise, J.L. and J.H. Walker**. 1996. Annexins II, IV, V and VI relocate in response to rises in intracellular calcium in human foreskin fibroblasts. J.Cell Sci. **109**:247-255.

253. **Blanchard, S., J.L. Barwise, V. Gerke, A. Goodall, P.F. Vaughn, and J.H. Walker**. 1996. Annexins in the human neuroblastoma SH-SY5Y: Demonstration of relocation of annexins II and V to membranes in

response to elevation of intracellular calcium by membrane depolarization and by calcium ionophore A23187. J. Neurochem. **67**:805-813.

254. **Trotter, P.J., M.A. Orchard, and J.H. Walker**. 1994. Biochim. Biophys. Acta **1222**:135-140.

255. **Compton, T., R.R. Nepomuceno, and D.M. Nowlin**. 1992. Human cytomegalovirus penetrates host cells by pH-independent fusion at the cell surface. Virology **191**:387-395.

256. **Compton, T., D.M. Nowlin, and N.R. Cooper**. 1993. Initiation of human cytomegalovirus infection requires initial interaction with cell surface heparan sulfate. Virology **193**:834-841.

257. **Albrecht, T., I. Boldogh, M. Fons, S. Abubakar, and C.Z. Deng**. 1990. Cell activation signals and the pathogenesis of human cytomegalovirus. Intervirology **31**:68-75.

258. **Boyle, K.A., R.L. Pietropaolo, and T. Compton**. 1999. Engagement of the cellular receptor for glycoprotein B of human cytomegalovirus activates the interferon-responsive pathway. Molecular & Cellular Biology **19**:3607-3613.

259. **Valyi-Nagy, T., Z. Bandi, I. Boldogh, and T. Albrecht**. 1988. Hydrolysis of inositol lipids: An early signal of human cytomegalovirus infection. Arch. Virol. **101**:199-207.

260. **Nokta, M., D. Eaton, O.S. Steinsland, and T. Albrecht**. 1987. Ca(2+) responses in cytomegalovirus-infected fibroblasts of human origin. Virology **157**:259-267.

261. **Nokta, M., M.P. Fons, D.C. Eaton, and T. Albrecht**. 1988. Cytomegalovirus: sodium entry and development of cytomegaly in human fibroblasts. Virology **164**:411-419.

262. **Abubakar, S., I. Boldogh, and T. Albrecht**. 1990. Human cytomegalovirus stimulates arachidonic acid metabolism through pathways that are affected by inhibitors of phospholipase A2 and protein kinase C. Biochem. Biophys. Res Comm. **166**:953-959.

263. **Boldogh, I., M.P. Fons, and T. Albrecht**. 1993. Increased levels of sequence specific DNA-binding proteins in human cytomegalovirus-infected cells. Biochem. Biophys. Res. Comm. **197**:1505-1510.

264. **Shibutani, T., T.M. Johnson, Z.X. Yu, V.J. Ferrans, J. Moss, and S.E. Epstein**. 1997. Pertussis toxin-sensitive G proteins as mediators of

the signal transduction pathways activated by cytomegalovirus infection of smooth muscle cells. J. Clin. Invest. **100**:2054-2061.

265. **Carlquist, J.F., L. Edelman, D.W. Bennion, and J.L. Anderson**. 1999. Cytomegalovirus induction of interleukin-6 in lung fibroblasts occurs independently of active infection and involves a G protein and the transcription factor NF-kappaB. J. Inf. Dis. **179**:1094-1100.

266. **Simmen, K.A., J. Singh, B.G.M. Luukkonen, M. Lopper, N.E. Miller, M.R. Jackson, Compton T., and K. Früh**. 2001. Global modulation of cellular transcription by human cytomegalovirus is initiated by viral glycoprotein B. Proc.Natl.Acad.Sci.USA **98**:7140-7145.

267. **Wohl, R.C. and K.C. Robbins**. 1982. Methods for studying fibrinolytic pathway components in human plasma. Thromb. Res. **27**:523-535.

268. **Castellino, F.J. and J.R. Powell** . 1981. Human plasminogen. Meth.Enz. **80**:365-378.

269. **Suenson, E., P. Bjerrum, A. Holm, M. Meldal, J. Selmer, and L.C. Petersen**. 1990. The role of fragment X polymers in the fibrin enhancement of tissue plasminogen activator-catalyzed plasmin formation. J. Biol. Chem. **265**:22228-22237.

270. **Nesheim, M., J.C. Fredenburgh, and G.R. Larsen**. 1990. The dissociation constants and stoichiometries of the interaction of Lys-plasminogen and chloromethylketone derivatives of tissue plasminogen activator and the variant delta-FEIX with intact fibrin. J. Biol. Chem. **265**:21541-21548.

271. **Hoylaerts, M., D.C. Rijken, H.R. Lijnen, and D. Collen**. 1982. Kinetics of the activation of plasminogen by human tissue plasminogen activator: Role of fibrin. J. Biol. Chem. **257 (6)**:2912-2919.

272. **Wohl, R.C., L. Summaria, and K.C. Robbins**. 1980. Kinetics of activation of human plasminogen by different activator species at pH 7.4 and 37 degrees C. J. Biol. Chem. **255**:2005-2013.

273. **Fredenburgh, J.C. and M.E. Nesheim**. 1992. Lys-plasminogen is a significant intermediate in the activation of Glu-plasminogen during fibrinolysis *in vitro*. J. Biol. Chem. **267 (36)**:26150-26156.

274. **Gong, Y., S.-O. Kim, J. Felez, D.K. Grella, F.J. Castellino, and L.A. Miles**. 2001. Conversion of Glu-Plasminogen to Lys-Plasminogen is Necessary for Optimal Stimulation of Plasminogen Activation on the Endothelial Cell Surface. J. Biol. Chem.

7. CURRICULUM VITAE

Name: **Peterson, Erica Ann**

Education:

1999-2002: Masters of Science, Biochemistry program, University of Ottawa

1995-1999: Honors B.Sc. (Magna Cum Laude) in Biochemistry, University of Ottawa.

1991-1995: Baccalauréat Générale, Lycée Français Paul Claudel.

Research Experience:

2000– 2002: Canadian Blood Services, Ottawa
Title: Technical assistant
Project Title: A Novel C2 Domain-Containing Protein, P110, is Blood Specific and Binds to Anionic Phospholipid in the Presence of Calcium.
Supervisors: Abed Zeibdawi and Dr. Ed Pryzdial

1999–2002: Canadian Blood Services, Ottawa
Title: Graduate Research Trainee (M.Sc. student)
Project Title: Thrombin Induces Cell Surface Expression of the Plasminogen Receptor Annexin II: A Novel Link Between Coagulation and Fibrinolysis.
Supervisor: Dr. Ed Pryzdial

1998-1999: Canadian blood services, Ottawa
Title: Undergraduate Research Trainee
Project Title: Effect of Thrombin or Cytomegalovirus on Cellular Annexin II Distribution.
Supervisor: Dr. Ed Pryzdial

Scholarships/Awards:

1999-2000:Admissions Scholarship, University of Ottawa

1997-1998: Dean's List, University of Ottawa

1998-1999: Dean's List, University of Ottawa

Papers in Preparation:

1. **Peterson, E.A.**, Sutherland, M.R., Nesheim, M.E., and Pryzdial, E.L.G. "Thrombin induces cell surface exposure of the plasminogen receptor, annexin II: A novel link between coagulation and fibrinolysis"

To be submitted to *Blood* (2002).

2. Zeibdawi, A., **Peterson, E.A.**, Lemieux, R., Aye, M.T., Giulivi, A., and Pryzdial, E.L.G. "P135, a Novel Human Protein Containing Synaptotagmin-Like C2 Domains is Restricted to Blood Cells and Highly Expressed in Leukemic Cells."

To be submitted to *Blood* (2002).

Conference Presentations:

1. **Erica Peterson**, Michael Sutherland, and Ed Pryzdial. Effect of Thrombin on Cellular Annexin II Distribution. Canadian Federation of Biological Sciences, 43rd Annual Meeting, June 22nd –25th 2000.

2. **Erica Peterson**, Michael Sutherland, and Ed Pryzdial. Effect of Thrombin on Cellular Annexin II Distribution. Canadian Federation of Biological Sciences, 44th Annual Meeting, June 20th –24th 2001.

3. Abed Zeibdawi, **Erica Peterson**, Real Lemieux, Maung Aye, Antonio Giulivi, and Ed Pryzdial. A Novel C2 Domain-Containing Protein, P110, is Blood Specific and Bonds to Anionic Phospholipid in the Presence of Calcium. Canadian Federation of Biological Sciences, 44th Annual Meeting, June 20th –24th 2001.

8. STATEMENT OF CONTRIBUTION OF COLLABORATORS

I have taken charge of all the experimental results presented in this thesis, including experimental design, performance of the experimental procedures, and interpretation and analysis of the data.

I would like to acknowledge the following people for their participation in my research project:

-Dr. David Waisman (University of Calgary) for supplying purified A2, p11 and A2t used as positive controls for western blotting (Sections 3.2 and 3.3) and for providing us with the anti-p11 antibody utilized in the plasminogen binding experiments (Section 3.6.2).

-Dr. Michael Nesheim (Queens University) for providing the biotin- and fluorescein-labeled plasminogen used in plasminogen binding experiments (Sections 3.6.1.1 and 3.6.1.2).